Designing Localization Algorithms for Wireless Sensor Networks: A Geometric Approach

Thesis submitted in partial fulfillment of
the requirements for the degree of
Doctor of Philosophy

by

Kaushik Mondal
(Roll No. 09612305)

Under the Supervision of
Dr. Partha Sarathi Mandal

to the

Department of Mathematics
Indian Institute of Technology Guwahati
Guwahati - 781039, India

December 2014

CERTIFICATE

This is to certify that this thesis entitled "**Designing Localization Algorithms for Wireless Sensor Networks: A Geometric Approach**" being submitted by Mr. Kaushik Mondal to the Department of Mathematics, Indian Institute of Technology Guwahati, is a record of bona fide research work under my supervision and is worthy of consideration for the award of the degree of Doctor of Philosophy of the Institute.

The results contained in this thesis have not been submitted in part or full to any other university or institute for the award of any degree or diploma.

Place: IIT Guwahati
Date:

Dr. Partha Sarathi Mandal
Department of Mathematics
Indian Institute of Technology Guwahati
Guwahati-781039, Assam, India

ACKNOWLEDGEMENTS

First I want to acknowledge my father. Like him, I wanted to study Mathematics, do PhD from an IIT and be a teacher. I feel I am in the right way. From my childhood, my mother always taught me to be a good person at first which I will continue to try for rest of my life. I convey my deepest gratitude to my parents for all their encouragements, supports and inspirations not only during my PhD but throughout my life. I am also grateful to my brother who is very close to my heart and understands me so well. My love and blessings are always with him.

I met with Rima, my wife, in our graduating days and she became a part of my life thereafter. She always encouraged me for higher studies knowing that we may have to stay apart for a considerable amount of time. In between we got married and we have a little son. She managed everything single handedly and never complained. I do not have enough words to express my love for her.

I consider myself lucky to have Dr. Partha Sarathi Mandal as my supervisor. The day, I met him first in his office, I can remember, he advised me to consult him without any hesitation if I face any problem in this new place. From that very day I started to feel that I have a guardian here as well. As days went by, love and respect continued to grow. Manytimes, I felt that I was talking with my friend while discussing with him. Still, after spending five and half years, I fear him more than a student fears a teacher. Apart from academic lessons, I have learnt a lot from him which helped me to grow up in many ways. I cannot remember the day when I first met "boudi": (Dr. Debarati Mitra, Sir's wife). I found another very nice and down to earth person in her. You always find her with a broad smile in her face. After a year of my joining, Barun, a good and responsible guy, joined as a scholar under sir. I, Barun, sir and boudi often went out for dinner in the city or had lunch at sir's apartment as all of us are fond of good food. It gave me a feeling of having a small family away from home. I enjoyed those days very much during this memorable journey.

I remain grateful to sir for taking me as a PhD student knowing that I did not have any knowledge in the field of Computer Science having done my bachelor and master degree in Mathematics. He introduced me with the field of Computer Science, particularly with Distributed Computing. Whenever I had problems, he gave me ample time to clear

my doubts. His proper guidance and invaluable advises towards my work helped me immensely.

I want to thank Prof. Sukumar Nandi, Prof. Diganta Goswami and Dr. Kalpesh Kapoor for their valuable inputs towards my work. I thank Prof. Bhabani K. Sinha, Prof. Krishnendu Mukhopadhyaya of Indian Statistical Institute and Dr. Arindam Karmakar of Tezpur University for giving their valuable suggestions for my work from their busy schedules. All the comments, suggestions helped me a lot.

My sincere thanks goes to all my teachers of Visva Bharati University, specially Dr. Anjan Kumar Bhuniya who often spent his valuable time for my study even outside office hours. I extend my thanks to Anjan sir, Goutam sir, Srikanth sir, Rajen sir, Vinay sir, Siddhartha sir, Pratyush sir and Sriparna madam who did not let me feel that even I have not done any course under them. I express my sincere thanks to Sridhar da, Santanu da, Phatik da and Pran da for helping me out in official and system related matters.

I cherished my stay in the institute largely due to my friends. I thank Arnab, Avijit da, Mandar, Debopam, Kalyan, Kartoon, Manna, Murali, Santu, Abhisek, Anirban, Purnendu da, Sahu da, Niladri da and many others for their encouragement and delightful company. I thank Sandip for his help during my course work. I am specially thankful to Himadri for his help in various matters. The list would be never ending. We read together during course work, he helped me to learn writing codes, fixed the problems each time I encountered with my laptop and thousands more.

I am deeply indebted to my school and university friends Sukanta, Saptarshi, Pratyush, Falguni, Avijit, Rajib, Nikhil da, Sudipto da, Samiran da, Ramkrishna da, Biplab da and others who always inspired me for research work.

The development of this dissertation would not have been possible without the financial support from the Council of Scientific and Industrial Research (CSIR), Government of India. I would also like to thank the Indian Institute of Technology Guwahati for providing me a good academic environment and financial support during the last few months of my research work.

Place: IIT Guwahati

Date: Kaushik Mondal

ABSTRACT

Localization is one of the most important issues in wireless sensor networks. Localization problems are more challenging when line-of-sight signals between anchors and sensors are not available. We approach geometrically towards localization of static sensors based on non-line-of-sight signals. Two range-based deterministic algorithms are proposed for localization using static anchors. The first algorithm assumes presence of line-of-sight and one-bound signals. Then we relax the assumption and propose another algorithm which localizes sensors based on receiving unknown-bound signals.

Usually, large number of static anchors are required to localize all sensors in a network. Measurement errors are unavoidable in range-based localization algorithms. To overcome these problems, range-free localization algorithms using mobile anchors are proposed in literature, where a mobile anchor localizes all static sensors traveling through the sensor network. There are two different aspects of the existing algorithms. One aspect is to improve localization accuracy whereas the other tries to reduce path lengths of mobile anchors. The challenge is to design a movement strategy for mobile anchors which reduces path length while meeting the requirements of a range-free technique that yields better positioning accuracy. We propose a distributed range-free path planning algorithm for mobile anchors to localize sensors in arbitrary connected network. Another path planning algorithm for mobile anchors is proposed to localize sensors in a rectangular region with known boundary. The algorithms are designed in such a way that sensors can use an existing range-free algorithm for better positioning accuracy. Both these algorithms guarantee full localization.

In mobile wireless sensor networks, mobile sensors are needed to localize frequently unlike the static sensors. Mobility of the sensors incur additional challenges for localization. We propose a localization algorithm for mobile sensors assuming sensors do not change direction during localization. An upper bound on localization error is ensured by this algorithm. Then we relax the assumption and propose another algorithm which localizes in presence of obstacles. Both algorithms are range-free, distributed and deterministic. Each of our proposed algorithms in this thesis are compared with recent works to show better performance.

Contents

Chapter 1

Introduction

A sensor is an autonomous device consisting of a small processor, a transceiver, a memory unit, a power source and sensing units. It has a communication range to communicate with neighboring sensors which are located within its communication circle. Once sensors are deployed over a region of interest, they form a network. Sensors monitor physical or environmental conditions like light, temperature, humidity, etc, [39] and cooperatively send data through the network to a sink. Estimating position of a sensor in wireless sensor networks (WSNs) is very crucial for many real-life applications since finding location of data source in very important. Knowledge about position of sensors is the basic requirement for geometric routing and many position-based applications such as surveillance environment monitoring, industrial monitoring, structural monitoring, real time tracking, habitat monitoring [11, 21, 28] etc. The goal of localization is to estimate position of each sensor as accurately as possible, depending on the requirements of underlying applications. Although GPS is one of the widely used technique for location discovery in outdoor networks [31], from the point of view of accuracy, cost and energy preservation, it is not always practical to equip each sensor with a GPS receiver. A sensor with its known position is termed as *anchor*. Anchor broadcasts signals with its own position which are received by sensors to estimate their position. Direct signals are termed as line-of-sight (LOS) signals [4, 6, 10, 15, 20, 27, 35, 70], whereas non-line-of-sight (NLOS) signals [14, 22, 43, 61, 66, 67, 68, 77, 82, 83] reflect and/or scatter by various obstacles before reaching to the destination sensors. Signal which reflects once before reaching to

a sensor is defined as *one-bound* signal [68]. Similarly, multiple time reflected signals are called as *multiple-bound*. Information from the received signals and known positions of the anchors are used to localize rest of the sensors in a WSN. There exist many localization algorithms [4, 6, 10, 15, 20, 46, 56, 62, 68, 75, 84, 92] by which sensors can compute their positions. Generally localization algorithms are classified into two categories: range-based [68] and range-free [75, 84]. Range-based algorithms need to estimate distance or angle information for positioning sensors, while range-free techniques rely on connectivity information between anchors and sensors. Usually range-based techniques give better accuracy whereas range-free techniques are simpler and cost effective. Range-based techniques use received signal strength indicator (RSSI) [20], time of arrival (TOA) [92], time difference of arrival (TDOA) [26, 85] to measure distances and angle of arrival (AOA) [56, 86] to measure angles. In TOA technique, time synchronization between anchor and sensor is required to compute distance between them. But time synchronization in WSN is not very easy to implement. To avoid time synchronization, round trip delay method is used [71, 72]. Friis transmission equation [49] is used to measure distance between anchor and sensor in RSSI method. TOA technique provides better distance estimations than RSSI technique. Time difference of arrival is calculated in TDOA method for distance calculation. Using AOA technique, a sensor calculates the angle of arrival of signal from an anchor by using directional antennas or digital compass [56]. Range measurement errors and absence of LOS signals affect localization accuracy in range-based techniques. In range-free techniques, usually anchors broadcast beacon periodically with fixed time period. Ideally communication area of any anchor is a circular disk in two dimension plane with range of the anchor as its radius. However in practice, radio propagation is usually not homogenous in all directions because of the presence of multi-path fading and different path losses depending on the direction of propagation, which is termed as radio propagation irregularity [78]. Due to irregular radio propagation, signal does not reach up to the boundary of the circular disk at every direction which affects localization accuracy. So accurate localization is a challenging problem.

Usually to localize a static sensor, three reference points are required. So for a large network, several number of static anchors are needed for localization. This motivates researchers to use mobile anchor so that it can move around the network while serving

as reference points to the sensors [46, 75, 84]. By using a mobile anchor, we can save large number of anchors with deployment cost in the expense of the mobility of the mobile anchor. So, path planning of the mobile anchor has become an important issue in the area of localization. The path planning problem [13, 34, 36, 37, 47, 48, 59] can be divided in two different types depending on the knowledge of the underlying topology formed by the sensors and the area of sensor deployment. For the first type, information like connectivity is used whereas boundary information of the network is known in the second type. The objectives of path planning are reducing path length, providing good localization accuracy and full localization.

Mobile wireless sensor networks (MWSNs) is a recent development of WSNs where sensors have mobility depending on the applications. There are lots of applications [24] of MWSNs in service industry, house keeping, wildlife tracking, pollution monitoring, photon detection, shooter detection etc. In MWSN, mobile sensors are more powerful in terms of energy because they need to localize themselves frequently than static sensors where localizing a static sensor once is sufficient. Now a days, advanced mobile sensors who can control their movement, for example, mobile actuated sensor [18, 23], are motivating researchers to find accurate localization methods. Generally there are three phases in a localization method, (1) coordination, (2) measurement or data gathering and (3) computation. In MWSN, mobile sensors are used to record time stamps of events like receiving beacons in the coordination phase. This technique is used in many localization schemes [40]. Measurement phase is different for range-based and range-free algorithms. Range-based algorithms [41, 54] depends on distant and angle measurements and generally produce better results than range-free. In this phase sensors gather information like hop count [55] in range-free algorithms. In the computation phase, approximate position of the sensors are determined using the gathered information. Dead reckoning' [33, 89] is a technique used in this phase for mobile sensor localization. In this technique the sensor calculates current position using previous position, moving speed and time difference between current time and the time when the position of the sensor was last updated. Mobile sensor localization methods can be centralized [40, 41] as well as distributed [69]. Since mobility requires rapid and continuous localization, distributed algorithms are more effective than the centralized algorithms. Based on mobility of anchors and sensors, it is

possible to classify localization algorithms into four categories: (1) static sensors using static anchors, (2) mobile sensors using static anchors, (3) static sensors using mobile anchors and (4) mobile sensors using mobile anchors. In this thesis, we look upon first three categories of localization problems stated above.

1.1 Scope of the Thesis

In this thesis, we approach towards different kind of localization problems geometrically. We propose range-based localization techniques for static sensors using static anchors in absence of LOS signals under different assumptions. Then we propose range-free localization techniques for mobile sensors using static anchors under different assumptions in presence of obstacles. Finally, we look upon path planning problem for mobile anchor towards range-free localization. Two range-free path planning algorithms are proposed for mobile anchor to localize static sensors under different scenario. In this section we briefly describe the problems with results of this thesis.

1.1.1 Localization in Presence of One-bound NLOS Signal

In chapter 3, we propose range-based localization algorithm for static sensors in presence of one-bound NLOS signals using static anchors. We use round trip delay method during TOA technique for distance estimation and AOA technique for angle measurement. We prove that in presence of measurement errors, the sensor in question lies within a convex hull. Simulation results show that positioning accuracy of our scheme in presence of measurement errors is better than the existing localization algorithm [14]. Considering only two NLOS signals from an anchor, when the maximum error in distance measurement is 1 meter, we achieve about 40% reduction in the root mean square error (RMSE) in positioning compared to the semi-definite programming (SDP) scheme [14], which uses at least eight NLOS signals to localize a sensor. If we use more than two signals then positioning error decreases. For robust localization anchor needs three reply signals from a sensor via different paths in absence of measurement errors. Since only one anchor is sufficient, this gives us an advantage particularly in dealing with the sparse networks.

1.1.2 Analysis of Multiple-Bound Signals towards Localization

Practically, a signal may reflect more than once before reaching to a sensor. In chapter 4, we analyze multiple-bound signals to use unknown-bound NLOS signals for localization of static sensors using static anchors based on range estimations. To the best of our knowledge, there is no geometrical algorithms present in literature taking care of multiple-bound signals to localize static sensors. This motivates us to approach geometrically towards NLOS localization of static sensors. We use RSS technique in addition to TOA and AOA to handle multiple-bound signals. If signal traverses d distance from an anchor before reaching the sensor then possible locations of the sensor are always within a circle of radius d centering at the anchor. Now using information of a received multiple-bound signal, we are able compute a circle with radius less than d, where the sensor is bound to reside. We propose a technique to localize sensor when it receives multiple-bound signals and the number of bounds are unknown. In this case, only assumption is that the maximum possible number of bounds in the system is known. Simulation results show improvement over trilateration when sensor receives three unknown-bound signals from different anchors.

1.1.3 Mobile Sensor Localization using Static Anchor under Constrained Motion

In chapter 5, we propose range-free localization algorithms for mobile sensors using static anchors where mobile sensors do not change direction of movement during localization. Under this assumption, our proposed algorithm LWCD localizes sensors within any predefined error bound ϵ when it passes through communication circles of two different anchors. As it passes through more communication circles, positioning error can be further reduced. Simulation results of LWCD show around 75% improvement of the positioning error over the existing algorithm [90] in presence of radio irregularity. When mobile sensor passes through three and five more communication circles, 40% and 55% further reduction in error has been shown respectively. According to our model, obstacles may lie in between anchor and sensors to block communication. In presence of obstacles our proposed algorithm LWCDPO can localize mobile sensors within same error bound as LWCD.

1.1.4 Mobile Sensor Localization in Presence of Obstacles

In chapter 6, we propose range-free localization algorithm for mobile sensors using static anchors where mobile sensors change direction during localization. Obstacles may present any where in the network. Simulation results show 67% and 63% improvement of the positioning error over the existing algorithm [90] corresponding to two different selection criteria in presence of radio irregularity. We propose a novel technique for obstacle detection and proposed another algorithm LPO which localizes sensors in presence of obstacles with change of direction. It achieves 52% and 49% improvements corresponding to two different selection criteria in terms of localization accuracy compared to [90] in presence of radio irregularity.

1.1.5 Path Planning for Mobile Anchor in Connected Networks

In chapter 7, we consider path planning problem for mobile anchors in any arbitrary connected network to localize static sensors. We propose a distributed range-free movement strategy to localize all sensors within $r/2$ error-bound in a connected network, where r is the transmission range of the sensors and the mobile anchor. To the best of our knowledge, this is the first work where localization and path planning are done using connectivity of the network without any range estimation. Simulation results show improvement over existing work [48] in terms of both path length and localization accuracy.

1.1.6 Path Planning for Mobile Anchor in Rectangular Regions

In chapter 8, we propose path planning for mobile anchors in any rectangular region with known boundary to localize static sensors. Theoretically we show that the length of the path traversed by the anchor is lesser in the proposed hexagonal movement strategy compared to other existing path planning methods [25, 34, 37, 59] for covering a rectangular region. Simulation results support all theoretical results for path planning with localization accuracy. Results show 7.35% to 27.74% improvement of our scheme over different schemes in terms of path length while covering a bounded rectangular region.

Chapter 2

Review of Related Works

2.1 Introduction

Localization is one of the most important issues in WSNs and it is an widely studied research area. Many localization algorithms [4, 6, 10, 15, 20, 46, 56, 62, 75, 84, 92] are there in literature. Localization algorithms can be classified in different categories depending on range estimation, mobility of sensors and anchors etc. Based on range estimation, there are two categories; range-based [12, 15, 20, 27, 64, 70, 79, 80] and range-free [9, 30, 44, 55, 60, 81, 84]. Positioning using range-based algorithms are more accurate than range-free ones. Usually for range estimation, TOA [20, 71], TDOA [15, 26], AOA [22, 54] and RSSI [16] are used. To improve accuracy in range estimations, better range estimation tools are designed. Few of the recent developments are listed below. Zhang et al. [91] proposed a distributed angle estimation method for localization with multipath fading. Oberholzer et al. proposed ultrasonic-based ranging platform, called SpiderBat [56] which is the first ultrasonic-based sensor platform that can measure absolute angles between sensors within an error of 5 degree. It is possible to estimate sensor's position with a precision of the order of a few centimeters with the help of measured angles. Srirangarajan et al. [74] proposed a TOA based ranging technique which gives sub meter accuracy in distance measurement. Here accuracy does not depend on the distance between the transmitter and the receiver. Sinha et al. [72] used round trip delay method for distance measurement using electromagnetic signal and showed that there is an error of 3 meter while measuring

a distance equal to 1.5 kilometer. On the other hand, range-free techniques rely on connectivity information, hop-count etc. Hence range-free techniques are cost effective as they do not need special hardware like range-based schemes. Localization algorithms are divided into four categories based on mobility of anchors and sensors; (1) static sensors using static anchors, (2) mobile sensors using static anchors, (3) static sensors using mobile anchors and (4) mobile sensors using mobile anchors. According to this classification, we present our literature study.

2.2 Static Sensor Localization using Static Anchor

Trilateration [70] is used for sensor localization when the distances between a sensor and at least three anchors are known. It finds the intersection point of the three circles centered at the anchors as the position of the sensor. Error in distance measurement leads to an intersection area of those three circles instead of a point in the method of trilateration. When the number of anchors are more than three, then multilateration is used for positioning. Multilateration provides better accuracy than trilateration as possible area of presence is less due to more number of reference points. Minimum mean square error method (MMSE) [92] is used in multilateration which attempts to detect the position of a sensor by minimizing the error using an objective function. In triangulation technique, measured angles are used for positioning instead of distances. Patil et al. [62] used circular triangulation. A time-based positioning scheme (TPS) [15] for outdoor is proposed, which uses TDOA to detect location of the sensors. TPS is good in terms of computation overhead and scalability. Bulusu et al. [9] proposed a localization algorithm based on computing centroid of the proximate reference points using radio frequency communications. Localization techniques proposed by AbdelSalam et al. [2, 3] used AOA, RSSI technique and centroid method for localizing sensors using a single anchor. Ortiz et al. [35] used trigonometric figures for sensor localization in a probabilistic model and showed improvements over [9] in terms of positional accuracy. Sometimes sensors may be under the control of some adversaries or some attackers. In that case after calculating the position, verification is also required to ensure correct position of the sensor before using the position for some applications. This is known as secure localization. Capkun

et al. proposed verifiable multilateration [10] for secure positioning using set of verifiers. Delat et al. proposed a deterministic secure localization algorithm [20] based on RSSI and TDOA techniques. Authors proved that six and four verifiers are sufficient to detect a faking sensor using TDOA and RSSI technique respectively and hence provide stronger results than [10]. In range-free techniques [6], information like hop counts, connectivity are used. Sub-area localization (SAL) [4] is a range-free technique, where the central server finds the correct sub-area and sets the center of mass of the sub-area as the sensor's position.

Localization becomes more challenging under NLOS scenario i.e., when LOS path is not available. Ebrahimian and Scholtz [22] proposed a source localization scheme using reflection, where direct and reflected signals are used. Here the sensors are equipped with unidirectional antenna. Pahlavan et al. [61] proposed indoor geo-location in the absence of direct path by mitigating NLOS ranging errors. Considering NLOS ranging errors, Sinha et al. [73] proposed a technique which finds an area where a sensor is bound to reside. Technique for refinement of area of presence of sensors is also given in their scheme. Chen et al. [14] proposed a probabilistic NLOS sensor localization scheme based on semi definite programming where NLOS localization problem is approximated by a convex optimization problem using the SDP relaxation technique. In this paper authors considered different cases depending on the prior knowledge of probabilities and distributions of NLOS errors. We are intended to approach geometrically towards NLOS localization problem in this thesis.

2.3 Static Sensor Localization using Mobile Anchor

Now we look at an overview of the existing static sensor localization schemes using mobile anchor. A sphere-based localization algorithm [42] is proposed, which solves multiple linear equations to estimate positions of sensors. A novel flying landmark localization algorithm [60] is proposed, where anchor broadcasts its location information as it flies through the sensing space. Then each unknown node in the sensing space estimates its own location based on the basic geometry principles. Zhang et al. [92] proposed a secure localization algorithm for static anchors. Chia-Ho-Ou et al. [17] proposed a localization

scheme using mobile anchors with directional antenna. Ssu et al. [75] proposed a localization scheme, where the sensor's position is estimated as the intersection of perpendicular bisector of two computed chords. However this scheme suffers from short chord length problem. Our proposed range-free deterministic localization algorithms for mobile sensors are motivated by the strategy of beacon point selection used in [75]. Xiao et al. [84] improved over that scheme using pre-arrival and post-departure points along with the beacon points to localize a sensor. Later Lee et al. [46] used beacon distance more effectively as another geometric constraint and proposed a more accurate localization scheme. In all the three schemes [46, 75, 84], since static sensors receive beacons from mobile anchors, sensors know the co-ordinates of the beacon points. Hence chord formed by two beacon points is unique [75]. Similarly unique circular lamina with known equations of the circles can be formed using a beacon point in [46]. All these schemes are range-free and provides good positioning accuracy. To reduce energy consumption, it is also very important to propose suitable movement strategy for mobile anchor so that path length can be reduced. Below we discuss existing path planning algorithms for mobile anchor.

We can view the path planning problem in two different ways depending on the knowledge of the area of sensor deployment and the underlying topology formed by the sensors. Topology-based path planning, can be viewed as a graph traversal problem. Sensors have information about their neighbors which they send to the mobile anchor for determining the path. Li et al. [47] proposed two algorithms named breadth first and backtracking greedy algorithms. Li et al. [48] proposed a depth first traversal scheme $DREAMS$ to localize the sensors. Both these works need range estimations. In $DREAMS$, mobile anchor first visits a sensor using random movement before performing depth-first traversal on the network. An already visited localized sensor provides information to the anchor about it's next destination. Algorithm stops when anchor returns to the first sensor. During depth-first traversal, anchor performs distance-based heuristic movement using received signal strength from sensors. Kim et al. [36] proposed a path planning for randomly deployed sensors using trilateration method for localization. An already localized sensor becomes a reference point to help other sensors to find their position which reduces path length but localization error may propagate. Chang et al. [13] proposed another path planning algorithm of the mobile anchor, where localization are done using the scheme

proposed by Galstyan et al. [1] and mobile sensor calculates its trajectory by moving around already localized sensors. Our aim is to propose a path planning algorithm which can decide its trajectory without using any range estimation in a connected network. Using connectivity of the network, we discover neighbors of a sensor as well as localize it by the scheme [46] using our proposed path planning algorithm.

Assuming known boundaries of a network, *Scan*, *Doublescan* and *Hilbert* schemes are proposed by Koutsonikolas et al. [37]. They used the localization scheme [52]. *Scan* covers the whole area uniformly where the mobile anchor travels in line segments along X-axis (or Y-axis) keeping a fixed distance between two line segments. In *Doublescan*, anchor moves along both X-axis and Y-axis, which improves localization accuracy in the expense of traveled distance. *Hilbert* reduces both error and path length with compare to the other two. Huang et al. [34] proposed two path planning schemes namely *Circles* and *S-curves*. The authors propose a Gaussian-Markov algorithm [38] to optimize the path length of mobile anchor. But Gaussian-Markov algorithm can not improve over the above mentioned algorithms. Based on trilateration, Han et al. [25] proposed a path planning scheme for a mobile anchor. Using RSSI technique, sensor measures distances from three different non collinear points and finds its position. Chia-Ho-Ou et al. [59] proposed a movement strategy of the anchor which helps sensors to localize with good accuracy by reducing the short chord length problem of the scheme [75]. Another path planning $MAALRH$ [29] is proposed, but it produces largest path length compared to other strategies while covering a rectangular region including the corner points using a boundary compensation method named $MAALRH\_BCM$. Our aim is to propose a path planning which minimizes the path length compared to the existing works in literature and guarantee positioning of each sensor using scheme proposed by Lee et al. [46].

2.4 Mobile Sensor Localization

Algorithms for localizing static sensors can be applied for localizing mobile sensors, but computation cost is more since repeated run of the algorithms is needed as the mobile sensors change their position frequently. Tilak et al. [76] experimented how frequently localization algorithms for static sensors need to be executed to localize mobile sensors

with an acceptable accuracy and energy consumption. Navstar global positioning system [31] is the mostly used technique for localizing mobile sensors. Kostas et al. proposed a range-based algorithm [8] for navigation of mobile robots. Datta et al. [19] proposed an algorithm which can be used for both static and mobile sensor networks, where sensors constructs polygon of presence and shrinks it using received information, while mobile sensors dilate it before sending to its neighbors. Yu et al. [88] proposed an range based mobile sensor localization algorithm, assuming that the mobile sensors are not always moving in the network. A time based self-organizing localization algorithm [53] is proposed, where trilateration is used for localization. Han et al. [27] propose anchor's position selection algorithm based on triangulation which shows that the unknown sensor's localization error is the least when three anchors form an equilateral triangle. In [32], authors proposed ultrasonic-based localization system for mobile robot. Their proposed algorithm provides sufficient accuracy in the positioning of a robot based on ultrasonic reflection. An algorithm proposed [87], where mobile sensors predict their positions using recorded beacon information by guessing a mobility pattern under a statistical model. Hu et al. [33] adapted sequential Monte Carlo Localization (MCL) to localize mobile sensors. It assumes that all the mobile sensors know their maximum speed. Also sampling efficiency of MCL is low. Number of anchors should be high to achieve good localization accuracy in this algorithm. Uchiyama et al. [77] proposed urban pedestrians localization (UPL) algorithm for positioning mobile users in urban area. In this work authors consider known positions of the obstacles and calculate the area of presence of mobile users with certain degree of accuracy. UPL provides better localization accuracy compared to MCL [33]. Alikhani et al. [5] proposed iCCA-MAP algorithm and compared it with MCL. Later Baggio et al. [7] proposed Monte Carlo localization Boxed (MCB), which improved on MCL by using bounding box (called anchor box here). Sampling efficiency was improved using bounding box by reducing the scope of the presence of the sensor. Zhang et al. [90] proposed Weighted Monte Carlo Localization (WMCL), which improved over MCB by reducing the size of bounding box constructed in MCB. This work is based on sequential Monte Carlo Localization [33]. WMCL uses two-hop beacon neighbors negative effects along with estimated position information of sensor's neighbors to further reduce the size of the sensors bounding box. Hence WMCL has higher sampling efficiency than

MCB as well as MCL. WMCL also improves the localization accuracy by using estimated position information of sensors. But WMCL has large communication cost. WMCL-A and WMCL-B [90] reduce communication cost. However, average errors of WMCL-A and WMCL-B are relatively high than WMCL. A range-free algorithm for mobile sensor localization is proposed in [58] depending on beacon point selection. The idea of modifying beacon point positions is good but in practice marking beacon points suffers from mobility of both sensors and anchors. Localization schemes in [50, 57] localizes mobile sensors based on recorded historical information by predicting coordinates of the mobile sensor. There are also some range-free algorithms for localizing static sensors using mobile anchors. Chia-Ho-Ou et al. [17] proposed a localization scheme using mobile anchors with directional antenna. Authors proposed algorithms based on maximum likelihood estimator in [57, 80] to locate mobile sensors. Venkatesh et al. proposed an algorithm [79] based on constrained least square estimator for localization of mobile sensors. In [12], authors used residual test to discard NLOS signals before localize mobile sensors. Schemes based on statistical models are usually computationally complex. In [45], authors proposed an indoor mobile sensor localization algorithm based on RSSI measurement using past signal strength measurements. Miao et al. [51] proposed range-based geometric localization algorithm considering NLOS signals. Seow et al. [68] proposed a localization algorithm in presence of multiple-bound signals in the network. A statistical proximity test is used to discard multiple-bound signals with a high degree of accuracy. Remaining LOS and one-bound signals are used for sensor localization. Error can be accumulated in [68] since the discarding technique relays on statistical proximity test. Our aim is to propose a range-free localization algorithm for mobile sensors using static anchor.

Chapter 3

Localization in Presence of One-bound NLOS Signal

3.1 Introduction

In presence of obstacles, LOS signals may get blocked. Then localization under NLOS condition becomes quite challenging due to absence of LOS signals. In literature, there are different NLOS mitigation and localization methods using statistical techniques. Our aim is to localize sensors geometrically under NLOS condition using TOA and AOA ranging techniques. In absence of LOS signal, reflected signals may reach to the sensors. It is difficult to figure out how many times a signal reflects before reaching to a sensor. So under NLOS condition, it is challenging to propose localization technique relying on geometry as structure of the signal propagation path is difficult to obtain. In this chapter we propose a localization algorithm imposing constraint on number of reflections/bounds, which helps to view the problem as a geometric problem. Theoretically, in absence of measurement errors, accurate positioning is possible for one-bound signal. Area of presence of sensors is computed in presence of measurement errors.

3.1.1 Our contribution

In this chapter we propose a deterministic algorithm that calculates position of a sensor using received beacons from an anchor. If a sensor unwillingly measures incorrect AOA of

a received signal and replies back with an unexpected delay then anchor can detect that wrong angle information and time delay during localization. For robust localization anchor needs three reply signals from a sensor via different paths in absence of measurement errors. According to our model, each beacon is reflected only once before reaching the destination sensor and maximum possible angle and distance measurement errors are known. Our scheme gives accurate positioning if there is no range measurement errors, whereas considering measurement errors, positioning can only be done approximately. Simulation results show that positioning accuracy of our scheme in presence of measurement errors is better than the existing localization algorithm [14]. For the sake of comparison, we introduce Gaussian noise with mean = 0 and standard deviation = 4 meter along with measurement errors. Simulation results show that considering only two NLOS signals from an anchor, when the maximum error in distance measurement is 1 meter, about 40% reduction in the root mean square error (RMSE) in positioning is achieved compared to the semi-definite programming (SDP) scheme proposed in [14], which uses at least eight NLOS signals to localize a sensor. If more than two signals are used then positioning error decreases. For example, if there are eight NLOS signals and the maximum error in distance measurement is 6 meter, then the RMSE in positioning is reduced by about 74%.

Another good feature of our proposed approach is that in most of the earlier works [4, 6, 10, 15, 20, 62, 92], usually three anchors are used to locate a sensor. But in our approach, only one anchor is sufficient to calculate the position of a sensor. This gives us an advantage particularly in dealing with the sparse networks, by having only a single anchor, which can locate all other sensors in its range.

The rest of the chapter is organized as follows. The basic idea on which our proposed approach is developed, are explained in section 3.2. Section 3.3 discusses about the positioning in presence of distance and angle measurement errors. In section 3.4, we present the system model and our proposed algorithm. The simulation results of our algorithm considering errors in measurements are presented in section 3.5, along with performance comparison with existing approach. In section 3.6, we show how the proposed approach can be extended to localization in three dimension. Section 3.7 discusses about how the anchor can detect wrong angle information or error in round trip delay while

localizing a sensor, assuming no errors in measurements. We conclude in section 3.8.

3.2 Basic Idea

Sensor with unique *id* are deployed on a two dimensional plane. There are some reflectors and anchors in the same plane. The position of a sensor is calculated based on a chosen coordinate system. The positions of the anchors are known and those can be identified uniquely by their positions. An anchor broadcasts beacon along with its position. A sensor may receive the beacon directly (LOS communication) or after a reflection from some reflector. We assume that there can be at most one reflection in the path from any anchor to another sensor. One sensor may, however, receive more than one beacons from different anchors. After receiving a beacon from an anchor, a sensor transmits back the signal in the same direction from which it received the beacon (the angle of arrival with respect to the common coordinate system being measured by AOA technique). After receiving those beacons, the anchors also use TOA and AOA techniques to calculate the round-trip time of arrival and angle of arrival with respect to the same coordinates system for the same sensor. We show later that with the help of those angles of arrival and the distances calculated from the TOA technique, it is possible for the anchors to find the exact position of a sensor.

The connection between the geometry of Fig. 3.1 used in the following Lemma 3.2.1 and our localization problem is the following: S is considered as an anchor as well as its position, P is the point of reflection on a reflector and Q is considered as a sensor as well as its position, which is to be computed. The sensor Q receives the beacon from S through the path SQ via P, after one reflection at P. We now state the following result:

Lemma 3.2.1. *Consider a fixed point S on a straight line l with gradient m_l. Let L be the set of all parallel straight lines with gradient m_L such that $m_l \neq m_L$. Let P_i be the point of intersections of l with a line $\ell_i \in L$, for $i = 1, 2, \cdots$ (Ref. Fig. 3.1). Let Q_is be the points on ℓ_i such that $SP_i + P_iQ_i = d$, for $i = 1, 2, \cdots$, where d is a fixed distance. Then all the Q_is must lie on a straight line.*

Proof. Without loss of generality, let the fixed point S on the straight line l be the origin

of the coordinate system, having the coordinates (0,0). As shown in Fig. 3.1, P is the point of intersection of l with some straight line $\ell \in L$. Let Q be the point on ℓ such that $SP + PQ = d$. We show that the locus of Q is a straight line.

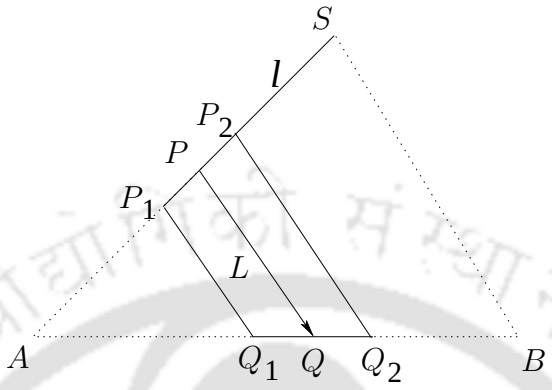

Figure 3.1: Showing one *fixed_distance_line*, Q_1Q_2

Noting that the equation of the straight line l is $y = m_l x$, let the coordinates of the point P be equal to $(c, m_l c)$, for some $c \neq 0$ and those of $Q = (\alpha, \beta)$. Hence, the gradient of PQ is $m_L = \frac{\beta - m_l c}{\alpha - c}$, which implies that $\beta = \alpha m_L + c(m_l - m_L)$. Now, $SP = \pm c\sqrt{1+m_l^2}$, $PQ = \pm(\alpha - c)\sqrt{1+m_L^2}$, the positive or negative signs are chosen depending on the values of c and $(\alpha - c)$. Then from $SP + PQ = d$ and $\beta = \alpha m_L + c(m_l - m_L)$, we get $\beta = \alpha\left[\frac{m_l\sqrt{1+m_L^2} - m_L\sqrt{1+m_l^2}}{\sqrt{1+m_L^2} - \sqrt{1+m_l^2}}\right] \pm \frac{d(m_l - m_L)}{\sqrt{1+m_L^2} - \sqrt{1+m_l^2}}$ or $\beta = \alpha\left[\frac{m_l\sqrt{1+m_L^2} + m_L\sqrt{1+m_l^2}}{\sqrt{1+m_L^2} + \sqrt{1+m_l^2}}\right] \pm \frac{d(m_l - m_L)}{\sqrt{1+m_L^2} + \sqrt{1+m_l^2}}$, which implies that the locus of Q is a straight line. □

Let the coordinates of the point P_1 in Fig. 3.1 be $(c', m_l c')$, for some $c' \neq 0$ and those of Q_1 be equal to (α', β'). Then using $SP_1 + P_1Q_1 = d$ and $m_L = \frac{\beta' - m_l c'}{\alpha' - c'}$, we get $\alpha' = c' \pm \frac{d \pm c'\sqrt{1+m_l^2}}{\sqrt{1+m_L^2}}$ and the corresponding $\beta' = m_l c' \pm m_L \frac{d \pm c'\sqrt{1+m_l^2}}{\sqrt{1+m_L^2}}$. Similarly, let the coordinates of the point P_2 in Fig. 3.1 be $(k, m_l k)$, for some k such that $c' \neq k \neq 0$ and those of $Q_2 = (\alpha'', \beta'')$. Then using $SP_2 + P_2Q_2 = d$ and $m_L = \frac{\beta'' - m_l k}{\alpha'' - k}$, we get, $\alpha'' = k \pm \frac{d \pm k\sqrt{1+m_l^2}}{\sqrt{1+m_L^2}}$ and the corresponding $\beta'' = m_l k \pm m_L \frac{d \pm k\sqrt{1+m_l^2}}{\sqrt{1+m_L^2})}$.

Considering all combinations of α', β' calculated above, we get four possible positions Q_1', Q_1'', Q_1''' and Q_1'''' for Q_1, as shown in Fig. 3.2, with the above computed values of the coordinates of Q_1. Similarly, there are four possible positions Q_2', Q_2'', Q_2''' and Q_2'''' for Q_2. Each such possible position of Q_1 corresponds to one possible position of Q_2 and we get

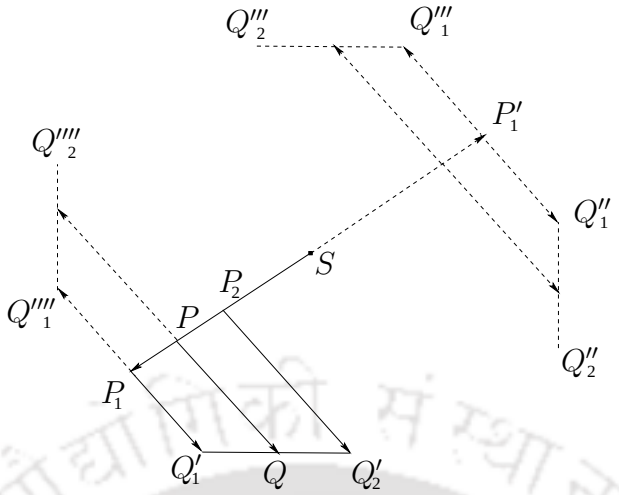

Figure 3.2: Showing four possible *fixed_distance_lines*, $Q'_1Q'_2$, $Q''_1Q''_2$, $Q'''_1Q'''_2$, $Q''''_1Q''''_2$.

four lines $Q'_1Q'_2$, $Q''_1Q''_2$, $Q'''_1Q'''_2$ and $Q''''_1Q''''_2$, as shown in Fig. 3.2. From the computed coordinate values of Q_1 and Q_2, the gradient of the line joining Q_1 and Q_2 is either $M' = \frac{m_l\sqrt{1+m_L^2}-m_L\sqrt{1+m_l^2}}{\sqrt{1+m_L^2}-\sqrt{1+m_l^2}}$ or $M'' = \frac{m_l\sqrt{1+m_L^2}+m_L\sqrt{1+m_l^2}}{\sqrt{1+m_L^2}+\sqrt{1+m_l^2}}$. Also, we see that $M'M'' = -1$

Thus, among the four lines $Q'_1Q'_2$, $Q''_1Q''_2$, $Q'''_1Q'''_2$ and $Q''''_1Q''''_2$, as shown in Fig. 3.2, the non-intersecting lines are parallel to each other, i.e., $Q'_1Q'_2 \parallel Q'''_1Q'''_2$ and $Q''_1Q''_2 \parallel Q''''_1Q''''_2$ and the intersecting lines are perpendicular to each other, i.e., $Q'_1Q'_2 \perp Q''_1Q''_2$, $Q''_1Q''_2 \perp Q'''_1Q'''_2$, $Q'''_1Q'''_2 \perp Q''''_1Q''''_2$, and $Q''''_1Q''''_2 \perp Q'_1Q'_2$.

Definition 3.2.2. The locus of Q is a straight line, which we define as the $fixed\_distance\_line_{S,m_l,m_L,d}$ corresponding to the point S on the straight line l with gradient m_l, the gradient m_L of the set L of parallel lines and the fixed distance d.

We denote $fixed\_distance\_line_{S,m_l,m_L,d}$ by $FDL_{S,m_l,m_L,d}$. However, when the values of the subscripts S, m_l, m_L and d are apparent from the context, we would, for simplicity, denote it only by FDL, by dropping the subscripts. The straight lines $Q'_1Q'_2$, $Q''_1Q''_2$, $Q'''_1Q'''_2$ and $Q''''_1Q''''_2$, as shown in Fig. 3.2, are four possible $FDL_{S,m_l,m_L,d}$. From the above discussions, the following result is obtained.

Lemma 3.2.3. *Among the four $FDL_{S,m_l,m_L,d}$, the intersecting lines are perpendicular to each other, and the non-intersecting lines are parallel to each other.*

Lemma 3.2.4. *A bisector of one of the angles between the straight lines l and any line belonging to L is parallel to the $FDL_{S,m_l,m_L,d}$.*

Proof. It follows that gradients of the angular bisectors of the angles between l and any line $\in L$ are $\frac{(m_l\sqrt{1+m_L^2}-m_L\sqrt{1+m_l^2})}{(\sqrt{1+m_L^2}-\sqrt{1+m_l^2})}$ and $\frac{(m_l\sqrt{1+m_L^2}+m_L\sqrt{1+m_l^2})}{(\sqrt{1+m_L^2}+\sqrt{1+m_l^2})}$. According to Lemma 3.2.1, these are possible gradients of the $FDL_{S,m_l,m_L,d}$. □

Lemma 3.2.5. *The position of a sensor cannot be uniquely identified if and only if the sensor receives two beacons from the same anchor which are reflected from two parallel reflectors.*

Proof. First, we examine the characteristics of a pair of beacons, received by a sensor from an anchor. As shown in the Fig. 3.3, S is the anchor, Q is the actual position of the sensor. Q receives beacons from S through P_1 and P_2, where P_1 and P_2 are the two points of reflection. Let $\angle P_1QX' = \theta_1$, $\angle P_2QX' = \theta_2$, (all the angles are measured counterclockwise with respect to the positive X-axis), $SP_1 + P_1Q = d_1$ and $SP_2 + P_2Q = d_2$. By virtue of TOA and AOA measurements, all of these parameters, i.e., θ_1, θ_2, d_1 and d_2 are known to S (the exact details of finding the values of these four parameters are explained later in this section).

In Fig. 3.3, we show another arbitrarily chosen point P_1' on the line SP_1 of gradient, say, m_l and another point Q' such that $\angle P_1'Q'X'' = \theta_1$ and $SP_1' + P_1'Q' = d_1$. This implies that the point Q' is on the FDL_{S,m_l,m_L,d_1} where m_L is the gradient of the line P_1Q. That means, line QQ' itself is the FDL_{S,m_l,m_L,d_1}.

Similarly, if we find another point P_2' on the line SP_2 having gradient, say, m_l' such that $\angle P_2'Q'X'' = \theta_2$ and $SP_2' + P_2'Q' = d_2$, then the line QQ' will also be the FDL_{S,m_l',m_L',d_2}, where m_L' is the gradient of the line P_2Q. Now we have problems in uniquely identifying the position of the sensor from the signals reflected from P_1 and P_2, as the solutions for the possible position of Q in this case are infinitely many (corresponding to the line QQ'). We note that under such a situation, according to Lemma 3.2.4, QQ' is parallel to the bisectors of both the angles $\angle SP_1Q$ and $\angle SP_2Q$. Hence, the two reflectors are parallel to each other.

Conversely, assume that there are two parallel reflectors. Two beacons from an anchor reflected from those two parallel reflectors reach a sensor. Hence, the bisectors of the

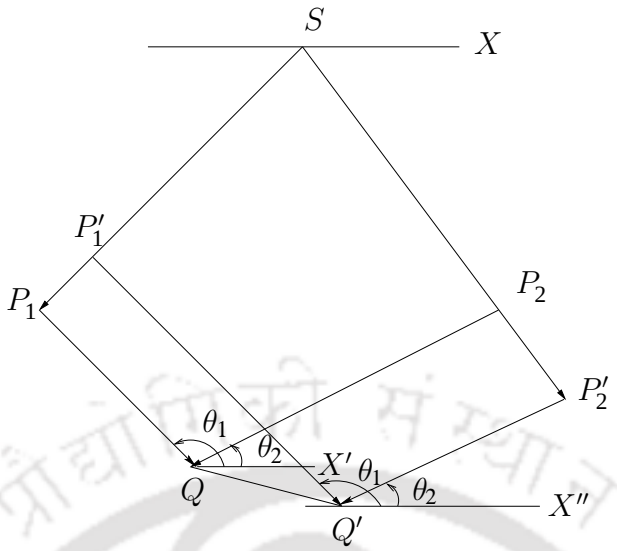

Figure 3.3: Showing infinite many solutions for the position of a sensor along the line QQ'

angles formed at the points of reflections are parallel. According to Lemma 3.2.4, the *FDLs* corresponding to these two reflected paths have the same gradient, i.e., the possible solutions for the position of the sensor are on a line. □

Whenever a sensor Q receives a beacon from the anchor S, it measures the angle of arrival, say θ of the received signal, with respect to the positive X-axis (measured in the counterclockwise direction) and immediately sends back a signal along the same angle θ which is received by S. Through this signal, S also receives the information about this angle θ from Q. The anchor S, on receiving this signal back from Q, measures the round-trip delay of this signal from S to Q and back to S, from which S can compute the distance between S and Q along this path of signal propagation. S also measures the angle of arrival, say δ while receiving the signal from Q, with respect to the positive X-axis (measured in the counterclockwise direction). We now have the following result.

Theorem 3.2.6. *A sensor finds its position correctly if it receives either i) the direct (LOS) signal from an anchor, or ii) two reflected signals from an anchor with the corresponding reflectors not being parallel to each other.*

Proof. Without loss of generality, let S be the origin of the coordinate system. Let the position of the sensor Q be (α, β). We need to compute α and β.

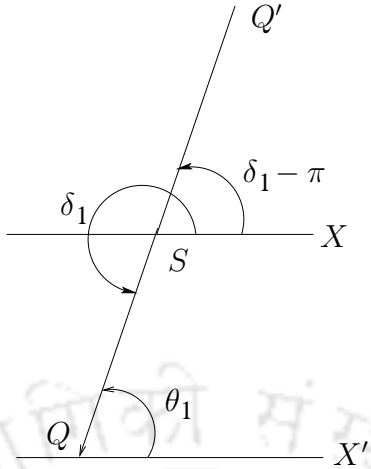

Figure 3.4: An example showing another possible position Q' of the sensor Q.

Case 1: Q receives a direct signal from S.

Fig. 3.4 shows a path through which Q receives the beacon from the anchor S directly. By virtue of the actions taken by Q and S as discussed above, S knows the distances $SQ = d$ and also the angles $\angle SQX' = \theta_1$ and $\angle XSQ = \delta_1$ as shown in Fig. 3.4. If S finds that $\theta_1 = \delta_1 \pm \pi$, then S identifies that the signal path SQ is a direct one (LOS) and then it calculates the position of Q as follows.

The equation of the straight line SQ is $y = m_1 x$, where $\tan \delta_1 = m_1$. Hence, $\beta = m_1 \alpha$. Since $SQ = d$, we have $\alpha^2(1+m_1^2) = d^2$, from which we get $\alpha = \pm \frac{d}{\sqrt{1+m_1^2}}$. The coordinates $\left(\frac{d}{\sqrt{1+m_1^2}} , \frac{m_1 d}{\sqrt{1+m_1^2}} \right)$ and $\left(\frac{-d}{\sqrt{1+m_1^2}} , \frac{-m_1 d}{\sqrt{1+m_1^2}} \right)$ are the two possible positions of Q as shown in Fig. 3.4. S then verifies which of the above two computed coordinate values of Q corresponds to the required relationship between δ_1 and θ_1, and selects that one as the final position of Q.

According to Fig. 3.4, if $\theta_1 = \delta_1 - \pi$ holds, then Q is the position of the sensor else if $\theta_1 = \delta_1 + \pi$ holds, then Q' is the position of the sensor.

Case 2: Q receives two reflected signals from S.

S can identify this case if $\theta_1 \neq \delta_1 \pm \pi$ and $\theta_2 \neq \delta_2 \pm \pi$. The situation can be illustrated by Fig. 3.5, where we assume that P' and P'' are the two points of reflection on the reflecting surfaces. By virtue of the actions taken by S and Q discussed above for each of the two reflected signals, S knows the angles $\angle XSP' = \delta_1$, $\angle P'QX' = \theta_1$, $\angle XSP'' = \delta_2$,

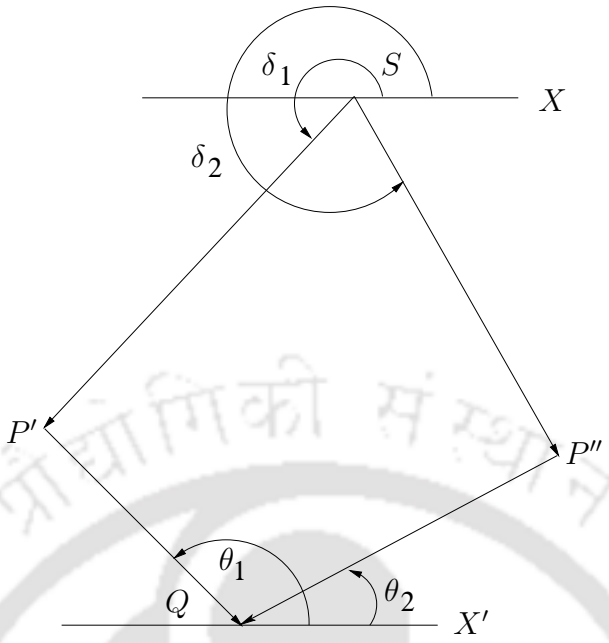

Figure 3.5: An example showing both reflected beacons received by a sensor Q.

and $\angle P''QX' = \theta_2$, as well as the distances $SP' + P'Q = d_1$, and $SP'' + P''Q = d_2$. Let $\tan\delta_1 = m_1$ and $\tan\delta_2 = m_2$. Then the equations of SP' and SP'' are $y = m_1x$ and $y = m_2x$, respectively. Similarly, let $\tan\theta_1 = m_3$ and $\tan\theta_2 = m_4$. Then the equations of $P'Q$ and $P''Q$ are $y-\beta = m_3(x-\alpha)$ and $y-\beta = m_4(x-\alpha)$, respectively. Now S computes the coordinates of the point P' in terms of α, β as the intersection point of the straight lines SP' and $P'Q$. Similarly, the coordinates of P'' are computed by S as the intersection point of the lines SP'' and $P''Q$. Thus, the coordinates of $P' = \left(\frac{\beta-m_3\alpha}{m_1-m_3}\ ,\ \frac{m_1(\beta-m_3\alpha)}{m_1-m_3}\right)$, and those of $P'' = \left(\frac{\beta-m_4\alpha}{m_2-m_4}\ ,\ \frac{m_2(\beta-m_4\alpha)}{m_2-m_4}\right)$. Then S solves the following two equations:

$$SP' + P'Q = d_1 \text{ and } \mathrm{SP''} + \mathrm{P''Q} = \mathrm{d_2} \tag{3.2.1}$$

which actually means solving the following two second degree equations:

$$\alpha^2 + \beta^2 + 2\left(d_1\sqrt{1+m_1^2} - (\alpha + m_1\beta)\right)\frac{(\beta - m_3\alpha)}{(m_1 - m_3)} - d_1^2 = 0$$
$$\alpha^2 + \beta^2 + 2\left(d_2\sqrt{1+m_2^2} - (\alpha + m_2\beta)\right)\frac{(\beta - m_4\alpha)}{(m_2 - m_4)} - d_2^2 = 0$$

These two equations give four solutions as the possible position of the sensor, which are actually the four intersection points of the eight *FDLs* corresponding to these two reflected paths. In Fig. 3.6, the four possible positions of the sensor are shown as Q, Q', Q_1 and Q'_1, resulting from the solutions. All these four points satisfy equation 3.2.1, but only one of these satisfies the angle constraints (namely, two angles made by the beacons at S and two angles at Q). Corresponding to the line joining S and one reflection point, say P as shown in Fig. 3.6, two of the solution points are on one side of this line and the remaining two are on the other side. The ambiguity about the actual solution point can be resolved as follows.

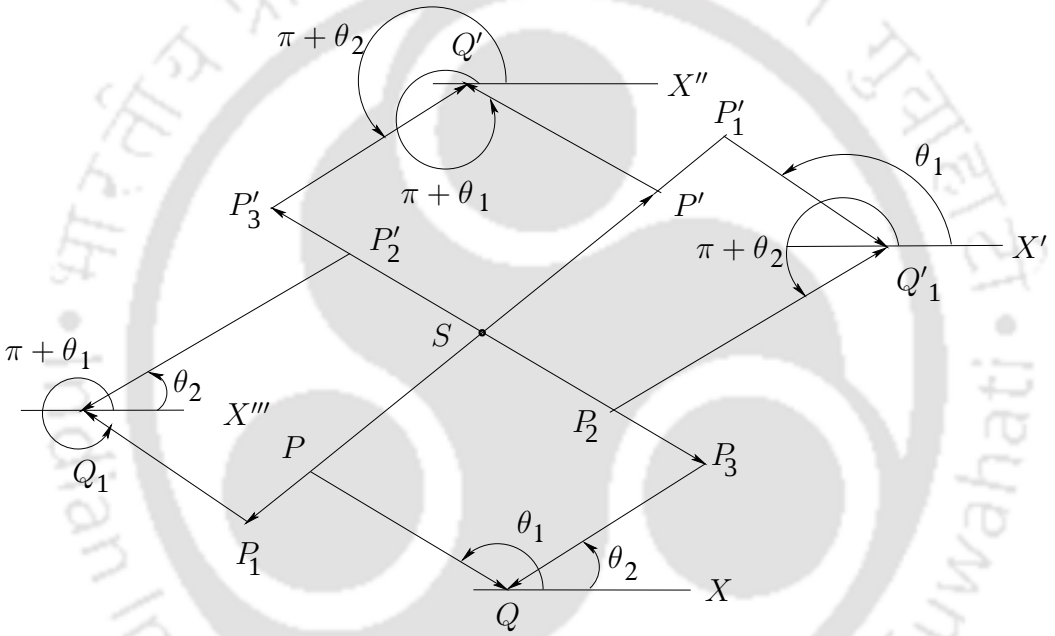

Figure 3.6: An example showing four possible positions Q, Q', Q_1, Q'_1 of a sensor Q.

Corresponding to each of the four solution points obtained by solving equation 3.2.1, the values of α and β are substituted back in equation $y - \beta = m_3(x - \alpha)$ and $y - \beta = m_4(x - \alpha)$. The first one of these two equations and $y = m_1 x$ are solved to get the coordinates of one reflection point, say P' (see Fig. 3.5), while the second one and $y = m_2 x$ are solved to find the coordinates of the other reflection point, say P'' in Fig. 3.5. The angles made by the lines $SP', SP'', P'Q$ and $P''Q$ are computed and compared with the actually measured angles $\delta_1, \delta_2, \theta_1$, and θ_2, respectively.

All possible positions, Q, Q', Q_1 and Q'_1 of a sensor are associated with a four-tuple

$(\delta', \delta'', \theta', \theta'')$, where $\delta', \delta'', \theta', \theta''$ are the angles made at S and at the sensor respectively by both the signals with respect to the positive X-axis. According to Fig. 3.6, the correct position of the sensor is either $Q(\delta_1, \delta_2, \theta_1, \theta_2)$ or $Q'(\delta_1 - \pi, \delta_2 - \pi, \theta_1 + \pi, \theta_2 + \pi)$ or $Q_1(\delta_1, \delta_2 - \pi, \theta_1 + \pi, \theta_2)$ or $Q_1'(\delta_1 - \pi, \delta_2, \theta_1, \theta_2 + \pi)$. As anchor S has the information about all the four angles made by the signals, it can choose the correct position of the sensor by matching those known angles with the four-tuples of those four possible positions. □

3.3 Positioning in Presence of Errors in Measurement

In a practical situation, there are some errors in measuring angles and distances using AOA and TOA techniques. Let $\Delta\alpha$ and $\Delta\beta$ be the possible errors in finding the coordinates α and β respectively of a sensor resulting due to such errors in measurement. To obtain the expressions for these errors $\Delta\alpha$ and $\Delta\beta$ in terms of the errors Δm and Δd in measuring the gradient m and distance d respectively, we use the results in Lemma 3.2.1 to evaluate α and β, instead of the two quadratic equations as in equation 3.2.1. From Lemma 3.2.1, the locus of the sensor Q is the line AB which intersects with the two straight lines of gradients m_1 and m_3 passing through the anchor S at the points A and B respectively. Exact coordinates of A and B are calculated using angles measured by AOA technique. We thus get two equations as given in equation 3.3.1 solving which the values of α and β can be obtained.

$$\left.\begin{array}{l} \left(\sqrt{1+m_1^2} - \sqrt{1+m_3^2}\right)\beta - \left(m_3\sqrt{1+m_1^2} - m_1\sqrt{1+m_3^2}\right)\alpha + d_1(m_3 - m_1) = 0 \\ \left(\sqrt{1+m_2^2} - \sqrt{1+m_4^2}\right)\beta - \left(m_4\sqrt{1+m_2^2} - m_2\sqrt{1+m_4^2}\right)\alpha + d_2(m_4 - m_2) = 0 \end{array}\right\} \quad (3.3.1)$$

To find the effect of errors in measuring angles and distances, first differentiate the above two equations in equation 3.3.1 with respect to m_1, m_2, m_3, m_4, d_1, d_2. Then to maximize the errors $\Delta\alpha$ and $\Delta\beta$ due to the error in measuring the angles, put $\Delta m_1 = -\Delta m_3 = \Delta m$ and $\Delta m_2 = -\Delta m_4 = \Delta m$. Also, we assume that $\Delta d_i = \Delta d$ for $i = 1, 2$. Differentiating the first equation in equation 3.3.1, we get the following:

$$p\Delta\alpha + q\Delta\beta = r\Delta m + s\Delta d \quad (3.3.2)$$

where, $p = m_1\sqrt{1+m_3^2} - m_3\sqrt{1+m_1^2}$, $q = \sqrt{1+m_1^2} - \sqrt{1+m_3^2}$,
$r = \left(\frac{m_1}{\sqrt{1+m_1^2}} - \frac{m_3}{\sqrt{1+m_3^2}}\right)\beta - \left(\frac{m_1 m_3}{\sqrt{1+m_1^2}} + \frac{m_1 m_3}{sqrt1+m_3^2} - \sqrt{1+m_1^2} - \sqrt{1+m_3^2}\right)\alpha$ and
$s = m_3 - m_1$.

Similarly differentiating the second equation in equation 3.3.1, we get

$$p'\Delta\alpha + q'\Delta\beta = r'\Delta m + s'\Delta d \tag{3.3.3}$$

where, $p' = m_2\sqrt{1+m_4^2} - m_4\sqrt{1+m_2^2}$, $q' = \sqrt{1+m_2^2} - \sqrt{1+m_4^2}$,
$r' = \left(\frac{m_2}{\sqrt{1+m_2^2}} - \frac{m_4}{\sqrt{1+m_4^2}}\right)\beta - \left(\frac{m_2 m_4}{\sqrt{1+m_2^2}} + \frac{m_2 m_4}{sqrt1+m_4^2} - \sqrt{1+m_2^2} - \sqrt{1+m_4^2}\right)\alpha$ and
$s' = m_4 - m_2$.

Solving equation 3.3.2 and equation 3.3.3 for $\Delta\alpha$ and $\Delta\beta$, we get the following:

$$\begin{pmatrix} \Delta\alpha \\ \Delta\beta \end{pmatrix} = \frac{1}{pq' - qp'} \begin{pmatrix} q' & -q \\ -p' & p \end{pmatrix} \begin{pmatrix} r & s \\ r' & s' \end{pmatrix} \begin{pmatrix} \Delta m \\ \Delta d \end{pmatrix} \tag{3.3.4}$$

From the above equation 3.3.4, one can calculate maximum positioning error $\Delta\alpha$ and $\Delta\beta$ using multi-variable optimization technique.

Again, through a different approach, however, for each received signal, erroneous measurements of angles and distances lead us to an area instead of a line segment, where the sensor is bound to reside. To find that area, we state the following theorem which is based on the assumption that the values of the maximum possible errors in measuring distances and angles are a priori known to the anchor. This assumption is justified because of the results reported in [56, 63].

Theorem 3.3.1. *On a two-dimensional plane, in presence of errors in measuring the angles and distances, the anchor can locate any sensor within a convex hull containing the sensor, if the values of the maximum possible errors in measuring distances and angles are known.*

Proof. Let the maximum possible errors in angle measurement and distance measurement be ϕ and w, respectively. In Fig. 3.7, the line QX' is drawn parallel to the line SX. Let the error-free angles at the anchor S and the sensor Q corresponding to a one-bound signal be $\delta(= \angle XSP)$ and $\theta(= \angle PQX')$ respectively. Due to the measurement error,

δ and θ may be measured as δ' $(= \angle XSP')$ and θ' $(= \angle P'Q'X'')$ respectively, where $\delta' \in [\delta - \phi, \delta + \phi]$ and $\theta' \in [\theta - \phi, \theta + \phi]$. So, for computing the position of the sensor Q, the anchor has to consider the range $[\delta' - \phi, \delta' + \phi]$ and $[\theta' - \phi, \theta' + \phi]$, which contains the actual angle of arrivals δ and θ at S and Q respectively. The anchor measures the distance from S to Q' via P' instead of S to Q via P along the signal path due to error *i.e.*, measures d' instead of d, where $d' \in [d - w, d + w]$. Similarly, the anchor has to consider the range of distance $[d' - w, d' + w]$ which contains the actual distance d.

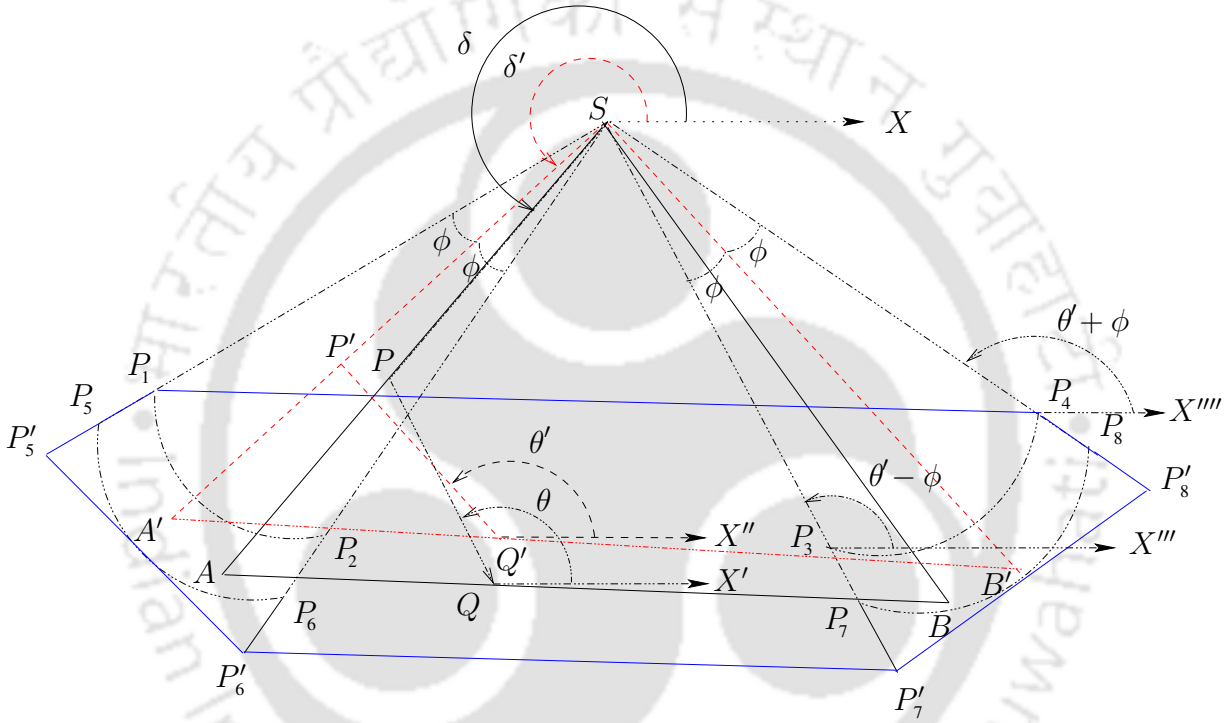

Figure 3.7: An example showing the convex hull $P_1P_4P'_8P'_7P'_6P'_5P_1$ corresponding to the measured one-bound signal path SQ' via P', instead of the actual signal propagation path SQ via P. The sensor Q must lie within this convex hull

According to Lemma 3.2.1, if the sensor Q receives a one-bound signal SQ via P as shown in Fig. 3.1 and Fig. 3.7 where δ and θ are the angles made by SP and PQ with the positive X-axis at S and at Q respectively, then AB is the line of presence of the sensor Q. But, due to the erroneous angle and distance measurements δ', θ' and d', $A'B'$ would be calculated instead of AB.

According to Fig. 3.7, $\angle XSP_1 = \delta' - \phi$, $\angle XSP_2 = \delta' + \phi$. Also, assuming that P_3X''' and P_4X'''' are two lines in the direction of positive X-axis, $\angle SP_3X''' = \theta' - \phi$,

$\angle SP_4X'''' = \theta' + \phi$. Each point on arc P_1P_2 and arc P_3P_4 is at a distance $d' - w$ from the anchor S. Using the Lemma 3.2.1, the sensor Q may lie on any one of the line segments joining any two points from arc P_1P_2 and arc P_3P_4. Similarly, the anchor computes the arcs P_5P_6 and P_7P_8 considering distance $d' + w$ and all possible angles. The sensor may lie on any one of the line segments joining any two points from arc P_5P_6 and arc P_7P_8 for $d' + w$.

Considering all possible distances in $[d' - w, d' + w]$, we can say that the sensor Q definitely lies on any line joining any two points from region R_1 and region R_2 such that both of them are at same distance from S, where R_1 is bounded by arc P_1P_2, line segment P_2P_6, arc P_6P_5, line segment P_5P_1 and R_2 is bounded by arc P_3P_4, line segment P_4P_8, arc P_8P_7, line segment P_7P_3 respectively. Let us draw two tangents at the middle points of the arcs P_5P_6 and P_7P_8 respectively which meet the lines SP_1, SP_2, SP_3 and SP_4 to generate the points of intersections P_5', P_6', P_7', P_8', as shown in Fig. 3.7. From the figure, it follows that the sensor Q lies within the convex hull generated by the points $P_1, P_2, P_5', P_6', P_3, P_4, P_7', P_8'$, because the points P_5', P_6', P_7', P_8' have been generated in such a way that the convex hull contains all the points on the circular arcs P_5P_6 and P_7P_8. □

If the received signal obeys the angular constraint ($\theta' = \delta' \pm \pi$) of being an LOS signal, then also by the same method as discussed above, we can find a convex hull where the sensor definitely lies. The sensor must lie within the intersection area of convex hulls generated from multiple received signals. As intersection area of convex hulls is also a convex hull. The center of mass of the intersection area is finally taken as the approximate position of the sensor.

3.4 Proposed Localization Algorithm

3.4.1 System model

We assume that all anchors are equipped with an omnidirectional antenna for sending a beacon and also a directional antenna for the measurement of angle of arrival of a signal from other sensors. An anchor sends its own position as *id* with the beacon signal. We further assume that other sensors are equipped with directional antennas for the

measurement of angle of arrival of the beacon signal from an anchor. An anchor is said to be a *neighbor* of another anchor if it is located within twice the transmission range of the second anchor. Anchors are synchronized with some global clock (possibly through GPS) such that at a time only one anchor sends a beacon to avoid collision with the beacons from neighboring anchors. This ensures that a receiving sensor receives only one beacon at a time from a particular anchor. A sensor receives the beacon from the anchor by using a directional antenna so that it can also measure the angle of arrival of the beacon signal. Because of this directional antenna, the sensor does not experience a collision even when it receives more than one beacon from an anchor coming through different paths at different angles. After receiving a beacon, a sensor transmits back a signal to the anchor, in the same direction in which it has received the beacon from the anchor. This signal carries the *id* of the sensor and the angle of arrival (AOA) of the beacon in the format, <*id*, AOA>. After receiving the reply, the anchor measures the traveled distance by calculating round trip delay. This method is used to avoid time synchronization between the sensor and the anchor.

3.4.2 The algorithm

Algorithm 1 FINDPOSITION(ϕ, w)

1: Anchor S sends a beacon with <anchor_id> using omnidirectional antenna.
2: **for** each sensor Q who hears the beacon **do**
3: Q measures the angles of arrival (θ_i) of all received beacon(s), $i = 1, 2, \cdots$, and transmits back <sensor_id, θ_i > to S via the same path(s).
4: **end for**
5: S measures the angles of arrival (δ_i) while receiving all replies and computes the corresponding distances (d_i) traveled by the beacon by measuring the TOA.
6: Using known values of ϕ and w, S finds convex hulls corresponding to each received signals as described in section 3.3. Same procedure generates line segments instead of convex hulls if $\phi = 0$ and $w = 0$.
7: S returns intersection of the line segments if $\phi = 0$ and $w = 0$; otherwise it returns the position of the center of mass of the intersection of all the convex hulls, as the position of Q.

Based on above discussion, the Algorithm 1 (FINDPOSITION) is proposed considering maximum angle measurement error ϕ and distance measurement error w as described in

section 3.3. It finds the position of a sensor Q using the received beacon signals from an anchor S. Algorithm returns approximate position as the center of mass of the intersection of the generated convex hulls as in Theorem 3.3.1. In presence of measurement errors, parallel reflectors do not have any impact on the localization method opposed to the Lemma 3.2.5 proved in case of errorless range estimations. But if there is no measurement errors in the environment, i.e. $\phi = 0$ and $w = 0$, then a line segment is generated instead of a convex hull corresponding to each signal. In this case accurate position is calculated as the intersection of two *FDLs* according to the Theorem 3.2.6.

3.5 Simulation

In the simulation of our proposed Algorithm 1: FindPosition, we consider presence of errors in both angle and distance measurements. Simulation is done on a MATLAB platform considering random errors in TOA and AOA measurements within some given maximum values. Sensors and anchors are placed randomly in a 10 meter by 10 meter square area on a two dimensional plane. Communication range of the anchors are 25 meter. One-bound signals are generated randomly such that the traveled distance of any signal obeys the communication range of the anchors. Since we generate one-bound signals by choosing reflectors randomly, LOS paths may also be encountered, i.e., the signal paths can be be one-bound as well as LOS. According to SpiderBat [56] and Cricket compass [63], we consider that the measured angles are within ± 5 degree of the actual angle, i.e., the value of ϕ is taken as 5 degree, which is the maximum measurement error in AOA technique. In [56], authors showed that using ultrasonic signal, distance measurement can be performed within an error of few millimeter when the range is around 15 meter. With reference to both [56] and [72], where round trip delay is used, we consider a maximum error of 0.02 meter in distance measurement for a communication range of 25 meter. Though known values of maximum possible measurement errors are used for simulation, yet for some unknown environment, it is possible to estimate the maximum possible errors. It can be done either theoretically using environmental parameters or practically by experiments.

In Table 3.1, we show sample outputs of ten different runs out of large number of

Table 3.1: Positioning errors (E_{psn}) (in meter) due to measurement errors for a particular sensor position

for signal one				**for signal two**				Computed position	Actual position	E_{psn}
Reflecting pt.	E_{δ_1}	E_{θ_1}	E_{d_1}	Reflecting pt.	E_{δ_2}	E_{θ_2}	E_{d_2}			
(8.1,9.0)	3.73	1.32	.016	(0.9,2.7)	0.46	4.64	.018	(7.87,3.42)	(7,4)	1.04
(6.5,0.3)	3.49	1.78	.017	(7.5,7.4)	1.07	3.28	.006	(7.09,4.17)	(7,4)	0.19
(4.3,3.8)	2.65	3.13	.011	(4.8,4.4)	1.46	2.54	.008	(7.50,2.32)	(7,4)	1.75
(2.7,6.7)	1.55	3.81	.013	(4.9,9.5)	1.59	2.76	.003	(6.88,2.80)	(7,4)	1.20
(7.5,2.5)	0.05	3.90	.008	(9.5,5.4)	3.61	2.42	.014	(7.66,3.62)	(7,4)	0.76
(8.4,2.5)	3.14	4.29	.010	(3.4,1.9)	2.48	0.26	.004	(7.02,3.95)	(7,4)	0.05
(0.7,0.5)	0.30	4.34	.011	(1.2,5.6)	0.30	1.62	.019	(6.64,4.57)	(7,4)	0.67
(1.6,7.9)	1.88	3.34	.001	(6.0,2.6)	1.54	2.48	.007	(6.28,4.84)	(7,4)	1.10
(4.5,0.8)	2.71	3.47	.016	(8.2,5.3)	4.96	0.57	.016	(6.59,4.80)	(7,4)	0.89
(1.0,9.6)	4.95	3.17	.011	(8.6,0.8)	1.00	3.00	.009	(8.60,2.82)	(7,4)	1.98

runs of our simulation for a particular sensor position (7,4) which receive two signals from an anchor placed at the origin (0,0). In Table 3.2, sample outputs of our simulation are shown for ten different randomly selected positions of sensors which receive two signals from an anchor placed at the origin (0,0). Measurement errors for both the signals are shown in Table 3.1 and in Table 3.2. To calculate positioning error as shown on Table3.1 and 3.2, signals are randomly generated by generating random reflecting points. In the tables, errors in angle measurements are shown as $E_{\delta_i} = |\delta_i - \delta_i'|$ and $E_{\theta_i} = |\theta_i - \theta_i'|$, for $i = 1, 2$, while the errors in distance measurement are shown as $E_{d_i} = |d_i - d_i'|$, $i = 1, 2$, for both the signals. The positioning errors (E_{psn}) as shown in the tables are computed as the Euclidean distances between the actual positions and the computed positions. In the tables, all angle differences are shown in degree, distance measurement errors and positioning errors are given in meter. We take average over such 1000 runs as shown in Table 3.1 and 3.2 to find average error of our algorithm shown in the first column of Table 3.3 for two received signals against each of the randomly selected anchor points.

From our simulation results, it can be observed that with the increasing number of received signals, the average positioning error decreases. This happens since the anchor computes the center of mass of the area of intersection of convex hulls generated from these received signals. The intersection area decreases as shown in Fig. 3.8 with the increasing

Table 3.2: Positioning errors (E_{psn}) (in meter) due to measurement errors for different sensor positions

for signal one				**for signal two**				Computed position	Actual position	E_{psn}
Reflecting pt.	E_{δ_1}	E_{θ_1}	E_{d_1}	Reflecting pt.	E_{δ_2}	E_{θ_2}	E_{d_2}			
(8.4,4.4)	1.43	4.27	.003	(5.5,8.5)	2.17	4.80	.010	(1.82,6.21)	(1.52,6.92)	0.77
(5.4.1.9)	1.83	2.33	.005	(4.2,1.7)	1.81	0.91	.011	(1.34,3.93)	(2.52,3.71)	1.20
(5.0.3.0)	0.11	4.63	.010	(7.8,1.6)	3.19	1.26	.017	(4.70,8.54)	(4.90.8.33)	0.29
(0.2,3.8)	3.11	4.91	.008	(2.3,4.3)	3.90	2.21	.019	(3.89,3.32)	(3.04,4.42)	1.39
(8.8,2.0)	4.29	2.72	.017	(0.6,7.1)	3.87	1.30	.007	(2.05,4.52)	(2.27,4.82)	0.37
(2.4,0.2)	2.98	0.95	.002	(8.9,9.1)	0.30	1.17	.003	(7.44,6.66)	(7.55,6.42)	0.26
(4.1,9.5)	1.93	4.92	.002	(9.5,7.9)	0.99	2.61	.010	(0.24,0.26)	(0.07,1.08)	0.83
(0.3,8.6)	0.88	0.81	.016	(3.0,6.2)	0.92	3.95	.010	(6.68,7.51)	(6.12,8.04)	0.77
(0.6,3.7)	2.63	1.87	.015	(4.5,0.6)	0.88	0.16	.019	(7.31,3.79)	(6.66,4.77)	1.17
(4.2,1.1)	3.62	2.19	.019	(4.3,6.7)	1.61	2.39	.015	(7.96,3.30)	(8.06,3.46)	0.19

Table 3.3: Average positioning errors (in meter) with varying positions of anchors and sensors

No of received signals→ Anchor Position (↓)	2	3	4	5	6	7	8	9	10	11	12
(0,0)	1.37	0.69	0.51	0.42	0.37	0.34	0.31	0.29	0.28	0.26	0.23
(3,9)	1.12	0.56	0.43	0.37	0.31	0.29	0.27	0.26	0.24	0.24	0.21
(5,6)	0.99	0.53	0.39	0.35	0.33	0.30	0.29	0.27	0.26	0.23	0.19
(3,2)	1.21	0.62	0.42	0.36	0.34	0.28	0.27	0.27	0.24	0.23	0.22
(8,8)	1.19	0.59	0.39	0.35	0.31	0.29	0.27	0.25	0.25	0.22	0.20
(4,4)	1.04	0.52	0.38	0.34	0.30	0.27	0.27	0.26	0.23	0.22	0.21
(7,6)	1.14	0.54	0.39	0.33	0.31	0.29	0.28	0.26	0.26	0.23	0.21
(1,3)	1.22	0.61	0.37	0.31	0.30	0.29	0.27	0.24	0.22	0.22	0.20
(4,9)	1.06	0.56	0.39	0.36	0.33	0.29	0.28	0.26	0.23	0.22	0.19
(7,5)	0.97	0.46	0.34	0.28	0.25	0.24	0.24	0.23	0.22	0.20	0.18
(6,2)	1.05	0.58	0.41	0.39	0.36	0.34	0.28	0.26	0.24	0.23	0.21
(2,4)	1.15	0.57	0.38	0.34	0.30	0.29	0.29	0.26	0.24	0.22	0.21
(6,6)	0.98	0.44	0.32	0.29	0.27	0.24	0.23	0.23	0.21	0.20	0.18
(1,9)	1.21	0.64	0.43	0.37	0.32	0.30	0.28	0.26	0.24	0.23	0.22
(8,8)	1.11	0.56	0.38	0.34	0.32	0.31	0.31	0.30	0.27	0.24	0.23
(2,5)	1.14	0.55	0.38	0.34	0.31	0.30	0.29	0.28	0.25	0.25	0.23
(5,3)	1.01	0.49	0.36	0.33	0.29	0.28	0.25	0.25	0.24	0.21	0.20
(9,5)	1.22	0.62	0.41	0.37	0.35	0.31	0.30	0.27	0.24	0.24	0.22
(5,1)	1.18	0.63	0.39	0.36	0.33	0.30	0.28	0.27	0.25	0.23	0.22
(4,5)	0.96	0.46	0.35	0.32	0.30	0.28	0.25	0.24	0.22	0.21	0.18

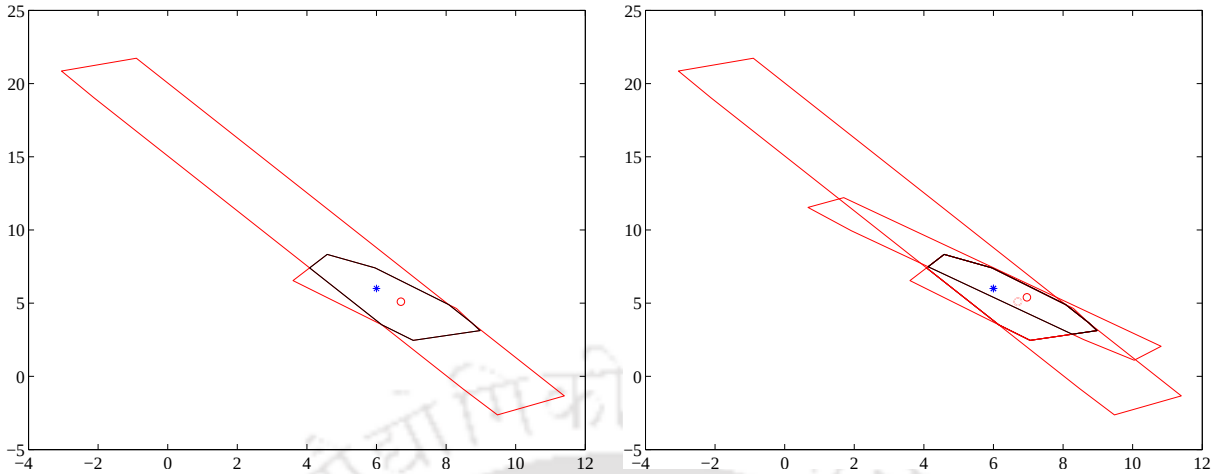

(a) Intersection of two convex hulls

(b) Intersection of three convex hulls

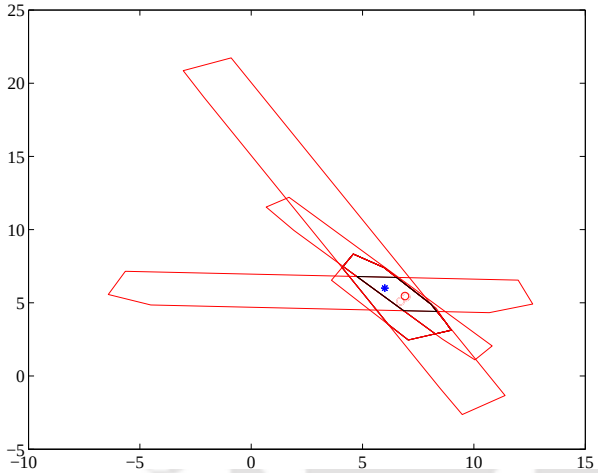

(c) Intersection of four convex hulls

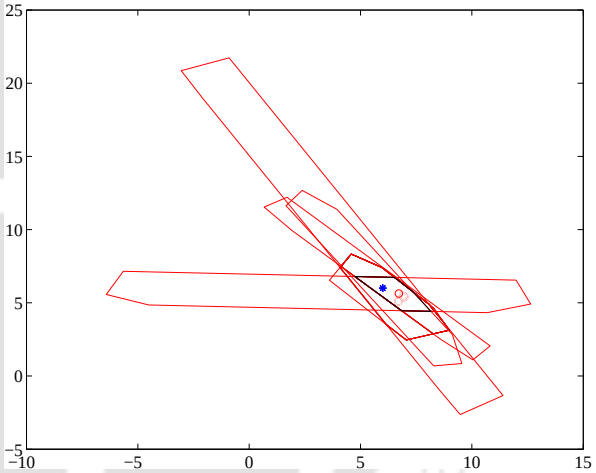

(d) Intersection of five convex hulls

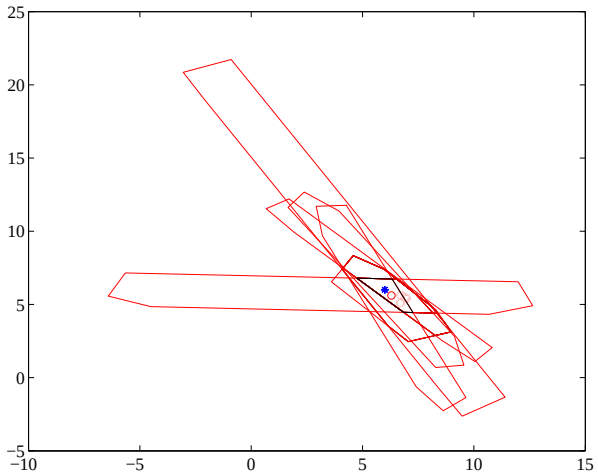

(e) Intersection of six convex hulls

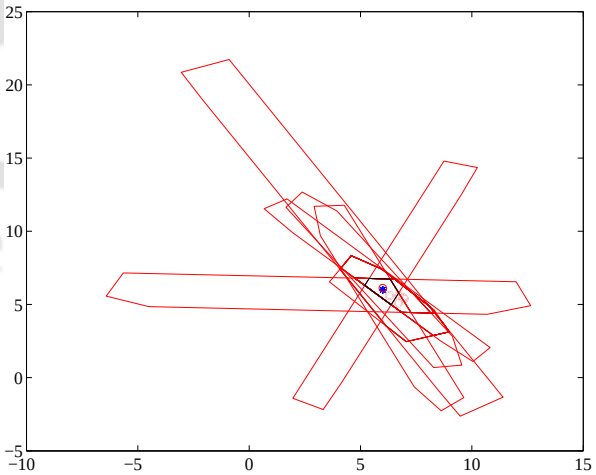

(f) Intersection of seven convex hulls

Figure 3.8: Error decreases as the intersection area reduces with the increasing number of convex hulls for different received signals

Table 3.4: Mean and standard deviation of positioning errors (in meter) corresponding to Table 3.3

No of received signals→	2	3	4	5	6	7	8	9	10	11	12
Mean	1.11	0.56	0.39	0.34	0.31	0.29	0.27	0.26	0.24	0.22	0.20
Standard deviation	.104	.063	.038	.031	.027	.024	.020	.017	.017	.014	.016

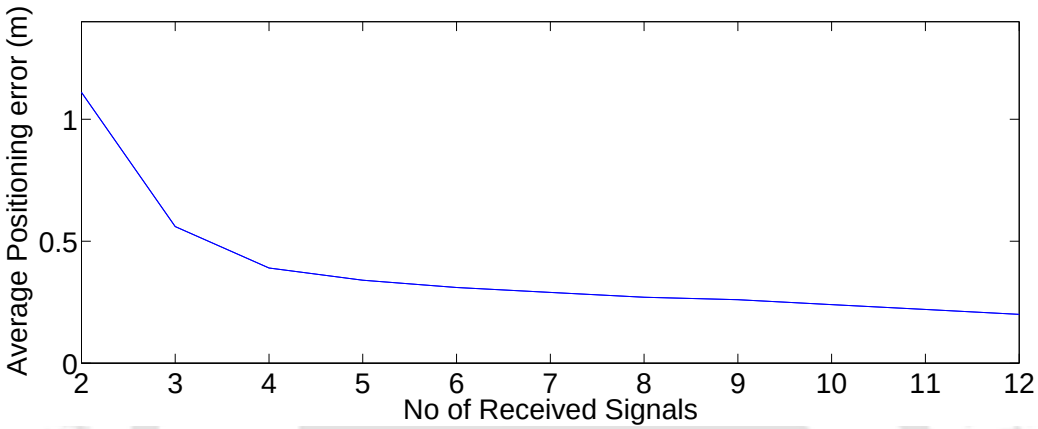

Figure 3.9: Average error for different number of received signals

number of convex hulls. Fig. 3.8 shows how intersection area as well as positioning error decreases as number of signals i.e., convex hulls increases. The computed position is marked as 'red circle', while the actual position of the sensor is marked as 'blue star' in these figures.

Simulation is performed considering 2 to 12 received signals from an anchor to find the effect of increased number of convex hulls on the average positioning error as shown in each row of Table 3.3. Different rows of Table 3.3 shows the result for different randomly selected anchor positions. To calculate each entry of the average positioning error in this table, the simulation has been run 1000 times (100 times each for 10 different sensor positions) where in each case signals are generated randomly by choosing random reflectors. Each row of Table 3.3 shows average positioning errors for different number of received signals from particular anchor. Table 3.3 shows that average errors are similar for any number of received signal for different anchor positions. Table 3.4 shows values of mean positioning errors and standard deviations considering all anchors corresponding to each

column of Table 3.3. Graphical representation of this data is shown in Fig. 3.9, which shows that average positioning error decreases at a very fast rate when the number of signals increases from two to six and after that it decreases slowly.

3.5.1 Comparison with existing works

We compare our proposed algorithm with the NLOS sensor localization scheme proposed in [14]. In that paper, authors shown the RMSE in positioning varying the mean NLOS measurement error (λ) from 1 meter to 6 meter with fixed measurement noise, which follows Gaussian distribution with mean = 0 and standard deviation = 4 meter. The RMSE varied from 3.78 meter to 4.20 meter when the probability of NLOS propagation is unknown. To built same set up for comparison with [14] through simulation, we place 18 anchors randomly on a 40 meter by 40 meter two dimensional square area and generate sensor positions randomly inside the square. We consider the values of maximum distance error, $w = 1$ meter to $w = 6$ meter, maximum angle measurement error $\phi = 5$ degree and introduce Gaussian noise with mean = 0 and standard deviation = 4 meter.

Table 3.5: Comparison of RMSE (in meter) in presence of Gaussian noise with mean = 0 and standard deviation = 4 meter with the SDP scheme

	Proposed Algorithm							SDP [14]
No. of received signal $\rightarrow$ Max distance error in meter $(w)(\downarrow)$	2	3	4	5	6	7	8	≥ 8
1	2.28	1.51	1.24	1.03	0.91	0.81	0.74	3.78
2	2.44	1.69	1.39	1.14	1.01	0.92	0.88	3.75
3	2.63	1.86	1.47	1.21	1.08	0.99	0.90	3.78
4	2.77	1.95	1.48	1.27	1.14	1.03	1.04	3.78
5	2.88	1.92	1.53	1.29	1.16	1.05	1.06	3.96
6	3.04	2.06	1.62	1.38	1.20	1.12	1.09	4.20

Table 3.5 shows RMSE for different values of maximum distance measurement error and for different numbers of received signals. Each average value of the RMSE is computed for 1000 runs. All error values are in meter in Table 3.5. Table 3.5 shows that considering only two NLOS signals from an anchor, when the maximum errors in distance measurement are 1 meter and 6 meter, we achieve about 40% and 28% reduction respectively in RMSE compared to the SDP scheme proposed in [14], which shows at least eight

NLOS signals to localize a sensor (as illustrated in their numerical results). If the number of received signals is increased, our method gives even more accurate results. For example, if there are eight NLOS signals and the maximum errors in distance measurement are 1 meter and 6 meter, then the RMSE in positioning is reduced by about 81% and 74% respectively. For better understanding, graphical representation of these data are shown in Fig. 3.10.

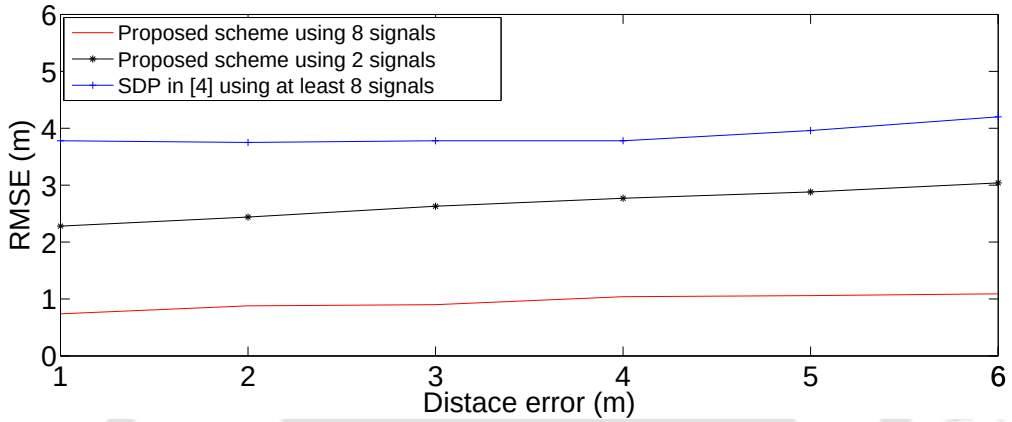

Figure 3.10: Graphical representation of Table3.5

3.6 Localization in Three Dimension

Suppose the sensors and the anchors are deployed in a three dimensional space where location of the anchors are known with respect to a common coordinate system. In that case if we consider a one-bound signal from an anchor to the sensor, whose position is to be calculated then the anchor, the sensor and the reflecting point lie on a plane. But these planes may be different for different one-bound signals received by the sensor. The locus of the sensor for a one-bound signal is again a straight line in absence of measurement errors as it was in the two dimensional case (Ref. Lemma 3.2.1). To find the equation of the straight line AB (see Fig. 3.1), the anchor measures the angles made by the line segment SP with X, Y, and Z axes and the sensor under consideration measures the angles made by the line segment PQ with X, Y, and Z axes to get the direction cosines of both the line segments SP and PQ.

Let (a_1, b_1, c_1) and (a_2, b_2, c_2) be the direction cosines of SP and PQ respectively. Also let the distance traveled by the signal be d i.e., $SP + PQ = d$. Then the coordinates of A and B are (da_1, db_1, dc_1) and (da_2, db_2, dc_2) respectively considering the anchor S is located at the origin. There are two possible positions for both A and B since we can move d distance along the lines with known direction cosines in both directions from S. We have to choose the correct coordinates of A and B using the known angles. So the equation of the line on which Q lies is given by,

$$\frac{x - da_1}{d(a_2 - a_1)} = \frac{y - db_1}{d(b_2 - b_1)} = \frac{z - dc_1}{d(c_2 - c_1)} \tag{3.6.1}$$

Now consider another signal which traveled d' distance. Let the direction cosines of the line segments of this signal be (a'_1, b'_1, c'_1) and (a'_2, b'_2, c'_2). Then in a similar manner, we get another equation of a straight line on which Q lies. In this case the equation becomes

$$\frac{x - d'a'_1}{d'(a'_2 - a'_1)} = \frac{y - d'b'_1}{d'(b'_2 - b'_1)} = \frac{z - d'c'_1}{d'(c'_2 - c'_1)} \tag{3.6.2}$$

To get the actual position of Q, we need to find the intersection point of these two straight lines represented by equation 3.6.1 and equation 3.6.2. The point of intersection is

$$\{k'd'(a'_2 - a'_1) + d'a'_1,\ k'd'(b'_2 - b'_1) + d'b'_1,\ k'd'(c'_2 - c'_1) + d'c'_1\},$$
$$\text{where } k' = \frac{dd'(b'_2a_2 + a'_1b_1 - b'_2a_1 - b_2a'_1) + d^2(a_1b_2 - b_1a_2)}{d'((a'_2 - a'_1)(b_2 - b_1) - (a_2 - a_1)(b'_2 - b'_1))}$$

If the equation of the two straight lines are same then S can not find the actual position since there are infinitely many possible positions of Q along the straight line. The following result is very much similar to the one we have for avoiding the situation of having infinitely many solutions in two dimension.

Theorem 3.6.1. *The position of a sensor can be uniquely identified by the above method, if and only if the sensor receives two beacons from the anchor where the reflecting planes are not parallel to each other.*

Proof. We can say from Lemma 3.2.4 that the straight line 3.6.1 (corresponding to equa-

tion 3.6.1) is parallel to the bisector of the angle $\angle SPQ$ (see Fig. 3.1) which is perpendicular to the reflecting plane. Similarly, the straight line 3.6.2 (corresponding to equation 3.6.2) is also perpendicular to the other reflecting plane from where the corresponding signal is received.

First assume that the reflecting planes are not parallel. Then the straight lines 3.6.1 and 3.6.2 are also not parallel. So, these straight lines intersect at Q. Conversely, assume that we can uniquely compute the position of Q. That means, the straight lines 3.6.1 and 3.6.2 intersect, i.e., the slopes of the straight lines 3.6.1 and 3.6.2 are different. Hence, the planes which are perpendicular to the straight lines 3.6.1 and 3.6.2 are not parallel, i.e., the reflecting surfaces are not parallel to each other. □

3.7 Robust Localization in NLOS

In this section we show that our proposed localization technique is robust if wrong position information get assigned to some sensors by accident. Consequently, anchor receives wrong angle and distance information from those sensors. Here wrong position information means wrong angle information somehow sent by the sensor to the anchor as well as the unwilling occurrence of time delay at the sensor while replying the signal back. Distance measurement errors generate due to unwilling delay introduced by the sensor while replying back the received signal as anchor uses round trip delay to calculate distance. We show below that in absence of measurement errors, an anchor can detect such kind of errors generated at the sensor.

Theorem 3.7.1. *In absence of errors in measurement, three signals are sufficient for the anchor to detect inconsistent angle of arrival and/or distance information sent by the sensor.*

Proof. Suppose a sensor Q receives three reflected signals from an anchor S via P', P'', and P''' as shown in Fig. 3.11. First consider the signals SQ via P' and SQ via P''. Let S receives wrong information θ_1' and θ_2' instead of θ_1 and θ_2 and calculates wrong traveled distance due to delay in reply at Q. S calculates two *FDLs* which intersect at Q', say, as shown in Fig. 3.11. S can misinterpret Q' as the correct position of Q if it would

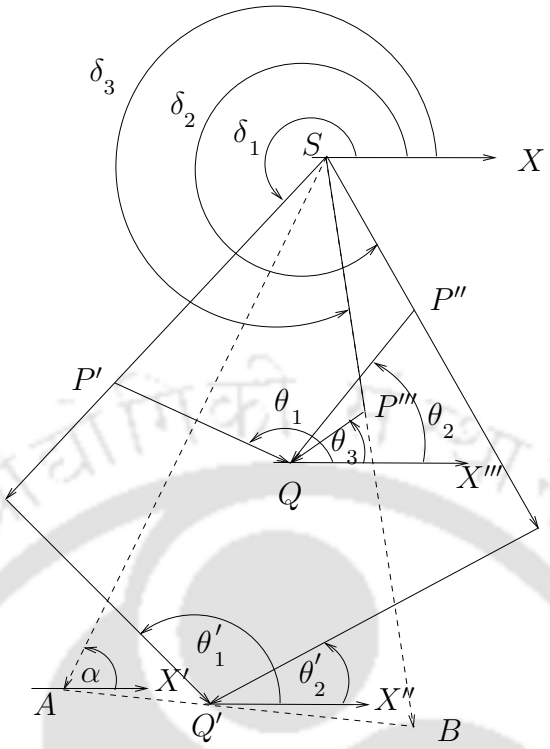

Figure 3.11: Q' is a wrong position of Q based on received one-bound signals (SQ reflected at P' and SQ reflected at P'')

have received only these two reply signals. Now consider the third signal i.e., the signals SQ via P'''. We discuss about the possible values of θ'_3 and the replying delay at Q so that the *FDL* for SQ via P''' also passes through Q'. If it happens, S can not detect the inconsistency. First, the calculated distance should be at least equal to SQ', which may happen if there is an appropriate time delay at Q. Let d'_3 be the wrongly calculated traveled distance for the third signal such that $d'_3 \geq SQ'$. So, one end point of the *FDL* for SQ via P''' is fixed as S calculates it using the values d'_3 and δ_3. Let this point be B, as shown in Fig. 3.11. The other end point A, of this *FDL* depends on the wrongly sent value θ'_3 by Q. But only for a particular position of A, Q' lies on the line segment AB. That is only for a particular value of θ'_3, Q' lies on the line segment AB. Let $\theta'_3 = \alpha$ be that particular value for this instance as shown in Fig. 3.11. θ'_3 can take any value among the infinite possible values 0 to 360 degree as there is no control of the sensor over θ'_3. Probability of choosing the value α among infinitely many possible values ranging from 0 to 360 degree is equal to zero. So, passing of three *FDLs* through a single point

is an impossible event if arbitrarily wrong information are accumulated at S. Hence, in absence of errors in measurement, three signals are sufficient for S to detect inconsistent information. □

3.8 Conclusions

In this work, we have proposed a deterministic algorithm to find the position of a sensor based on receiving at least two reflected signals without having any knowledge about the positions of those reflectors. If sensor receives signals from different anchors then communication between the anchors are required. Simulation results in presence of measurement errors show better positioning accuracy of proposed scheme compared to [14]. The positioning error does not increase significantly with significant increment of distance measurement error. Strong point of our approach is that our algorithm works in a sparse network since only two reflected signals from an anchor are sufficient for finding the position of a sensor. We have also shown that with accurate range measurements the anchor can detect some erroneous situations like wrong angle information and error in round trip delay while localizing the sensor. However, further studies are needed for detecting such situations in presence of errors in measurements.

Chapter 4

Analysis of Multiple-Bound Signals towards Localization

4.1 Introduction

In this chapter we generalize the localization problem of the previous chapter by allowing multiple reflections of a signal before reaching to a sensor. We first solve it for two-bound signals and then generalize it for multiple-bound signals. An area of presence is found for a sensor which receives a signal reflected more than once. Since it is not possible to know number of reflections of a received signal, we propose solution for unknown-bound signal. Theoretically, we prove that it is possible to localize sensor which receives unknown-bound signals, within an area, assuming that we know the maximum possible number of bounds in the environment. Comparison with trilateration shows improvement when sensor receives three unknown-bound signals from different anchors.

4.1.1 Our contribution

In this chapter we analyze multiple-bound signals so that sensor can use received signals irrespective of the number of reflections. If signal traverses d distance from an anchor before reaching the sensor then the possible location of the sensor is always within a circle of radius d centering at the anchor. Now using information of a received unknown-bound signal, we are able compute a circle with radius less than d, where the sensor is

bound to reside. We also propose a technique to localize sensor when it receives multiple-bound signals and the number of bounds are unknown. In this case, assumption is that the maximum possible number of bounds in the system is known. To the best of our knowledge there is no work in literature considering multiple-bound (reflected more than once) signals to locate the position of a sensor deterministically. Simulation results show that on an average 35% improvement in terms of area of presence and 40% improvement in terms of average error over trilateration using three two-bound signals, whereas on an average, 10% improvement in terms of area of presence and 4% improvement in terms of average error over trilateration when a sensor receives three unknown-bound signals from different anchors.

The organization of the remaining part of this chapter is as follows. Basic idea is explained in section 4.2. Analysis of two-bound signal is given in section 4.3. Analysis of multiple-bound signal is discussed in section 4.4. In section 4.5, area of presence of a sensor which received an unknown-bound signal is computed. Proposed localization algorithm is presented in section 4.6. Comparison with simulation results are shown in section 4.7. Finally, we conclude in section 4.8.

4.2 Basic Idea

According to the algorithm proposed in the previous chapter, position of a sensor is calculated based on TOA and AOA measurement techniques under the model which allows up to one-bound signals. Using AOA technique, receiving angles of arrival θ at the sensor and δ at the anchor are measured, whereas the path length d traveled by the signal is measured by TOA technique. Following theorem shows that in presence of multiple-bound (more than one-bound) signal, AOA and TOA measurements are not sufficient to localize a sensor.

Theorem 4.2.1. *(Impossibility) Under the model which allows multiple-bound signal, TOA and AOA measurements are insufficient to locate a sensor in a specific position with multiple-bound signals.*

Proof. We prove it for a two-bound signal. Let a sensor Q receives two-bound signal from

an anchor S. Now, we show that for any position of Q within the circle of radius d centering at S, there exist reflecting points P and P' satisfying TOA and AOA measurements. Let Q' be an arbitrary position of Q. Total distance d is calculated by the anchor S using TOA technique, which is actually the sum of the three distances, say, d_1, d_2, d_3, where d_1, d_2, d_3 are the distances from anchor S to first reflecting point P, first reflecting point to second reflecting point P' and second reflecting point to the sensor Q' respectively. Let two angles δ and θ are calculated using AOA technique at S and Q' respectively with the positive direction of X-axis in the counter clockwise direction as shown in Fig. 4.1.

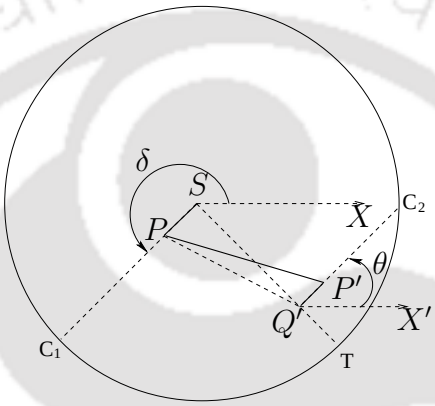

Figure 4.1: Showing a two-bound signal from S to Q'

Since the sensor receives a two-bound signal, so Q' should satisfy $SQ' = D < d = ST$ as shown in Fig. 4.1. SC_1 and $Q'C_2$ are two straight lines such that $\angle XSC_1 = \delta$ and $\angle C_2Q'X' = \theta$, where X, X' are the direction of the positive X-axis. We have to find two points P, P' on SC_1 and $Q'C_2$ respectively such that $SP + PP' + P'Q' = d$. Using property of continuity of a real line, existence of P, P' can be easily shown. Hence it is possible to locate Q only somewhere within the circle of radius d; no further accuracy is possible. □

So for further reduction of possible area of presence of the sensor which receives a two-bound signal, another ranging technique is required. We use RSSI technique for that purpose. Communication model between anchor and sensors is explained below.

Communication model: Sensors with unique ids are deployed in a two dimensional plane, where reflectors and anchors are also located. The anchors are uniquely identified

by their known positions in a common coordinate system. An anchor uses ultrasonic and electromagnetic signals to broadcast beacons along with its position. Signal strength of the electromagnetic signal for sending beacons is denoted by S_s. A sensor receives LOS signal if there are no obstacles or reflectors on the direct path, otherwise the sensor may receive NLOS signal after one/multiple reflections. On receiving beacons, a sensor measures (i) receiving angle of arrival θ of a ultrasonic signal with the positive X-axis using directional antenna and (ii) receiving signal strength S_r of the electromagnetic signal. Then it transmits back the ultrasonic signal with the angle information θ, received signal strength S_r along the same path using its directional antenna. Anchor measures the angle of arrival δ of the beacon using directional antenna while receiving from the sensor. It calculates the distance d traversed by the beacon using round trip delay of arrival of the ultrasonic signal using TOA technique.

Now we discuss how RSSI technique provides another constraint to compute the sensor's position. In case of LOS signal the Friis transmission equation [49] given below is used for RSSI technique:

$$S_r = S_s \left(\frac{\lambda}{4\pi d}\right)^n, \tag{4.2.1}$$

where S_s is the sending signal strength, S_r is the receiving signal strength, d is the distance between sender and receiver and n is the path loss exponent, in case of multi-path effect $n \in [2, 6]$. In this work, we take n is equal to 2. But our algorithm will work for any specific n depending on the environment where the sensors are deployed. So, the equation for LOS signal is,

$$S_r = S_s \frac{c}{d^2}, \tag{4.2.2}$$

where $c = \left(\frac{\lambda}{4\pi}\right)^2$ is a known constant. In case of one-bound signal as shown in Fig. 4.2, the signal travels from S to Q via the reflecting point P where $SP = d_1$ and $PQ = d_2$. We apply the Friis transmission equation on the path SP, then $S'_r = S_s \frac{c}{d_1^2}$ if S'_r is the signal strength at P. Let h percentage of the signal strength be decreased after reflection at P. Then Friis transmission equation for the remaining path PQ is $S_r = \frac{100-h}{100} S'_r \frac{c}{d_2^2} =$

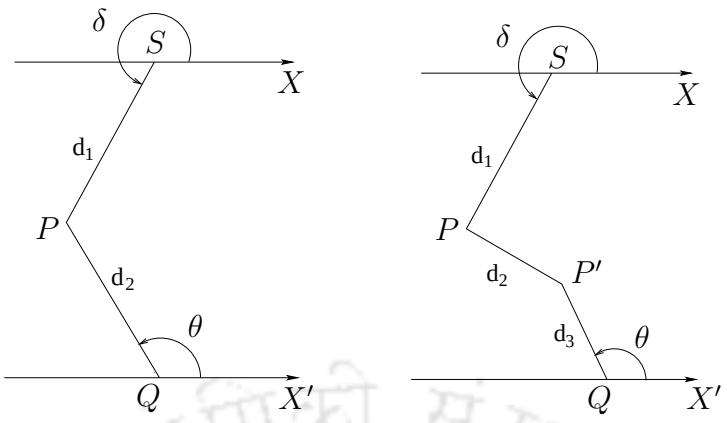

(a) one-bound signal (b) Two-bound signal

Figure 4.2: Figures showing one-bound and two-bound signals reach to Q

$\frac{100-h}{100} S_s \frac{c^2}{d_1^2 d_2^2}$, where S_r is the receiving signal strength at Q.

Similarly, the Friis transmission equation in case of a two-bound signal is given below.

$$S_r = S_s \frac{c''^3}{d_1^2 d_2^2 d_3^2} \quad \text{where } c'' = c\left(\frac{100-h}{100}\right)^{\frac{2}{3}}, \tag{4.2.3}$$

where $\sum_{i\in\{1,2,3\}} d_i = d$.

The value of $d_1 \times d_2 \times d_3$ of a two-bound signal is calculated from equation 4.2.3. In the following analysis we explain how to find location of a sensor Q with two-bound signal.

4.3 Analysis of Two-Bound Signal

Let sensor Q receives a two-bound signal from anchor S and d be the total distance traveled by the signal which is measured using TOA technique, then,

$$d = d_1 + d_2 + d_3 \tag{4.3.1}$$

Combining equation 4.3.1 and equation 4.2.3,

$$d = d_1 + d_2 + d_3 \text{ and } d_1 d_2 d_3 = \sqrt{c''^3 \frac{S_s}{S_r}} \quad (= k, say) \tag{4.3.2}$$

There is a possibility of infinitely many solutions of d_1, d_2, d_3 for the above two equations,

which indicates that the possible solution of Q is not unique. The possible solution space of Q always lies within a circle of radius d with the center at the anchor S. Our objective is to reduce the solution space as much as possible compared to the circle with radius d centering at the anchor. Equation 4.3.2 can be viewed as follows.

$$d_1 d_2 (d - d_1 - d_2) = k \text{ where } d_1, d_2 > 0 \tag{4.3.3}$$

Equation 4.3.3 represents a curve Γ in a two-dimensional plane with the variables d_1, d_2. Each point (d_1, d_2) on Γ corresponds to a solution of the equation 4.3.3. Only the positive values of d_1 and d_2 are considered as they represent distances. As the equation is symmetric with respect to d_1 and d_2, if (a, b) is a solution then (b, a) is also a solution and vice versa. For any given point (d_1, d_2) on Γ, now we analyze the possible positions of sensor Q.

A point (d_1, d_2) on Γ implies an instance of the two-bound signal is made of three parts with lengths d_1, d_2 and $d - d_1 - d_2$. Fig. 4.3 shows such a signal. According to Fig. 4.3, sensor Q receives a two-bound signal of length d via reflecting points P, P' such that $\angle XSP = \delta$, $\angle P'QX' = \theta$, $SP = d_1$, $PP' = d_3$ and $P'Q = d_2$, where $d_3 = d - d_1 - d_2$ as d_3 is substituted with the given d_1 and d_2. Since the angle $\angle SPP'$ is unknown, locus of P' is the circle with radius $d - d_1 - d_2$ centering at P. Q is at a distance d_2 from P' maintaining the angle constraint θ, so each point on the locus of P' corresponds to a possible position of Q. That is, locus of Q is also a circle generated by shifting the locus of P' by d_2 distance maintaining θ. Basically the center P of locus of P' moves d_2 satisfying θ and reaches to a point P'' in Fig. 4.3, which is the center of locus of Q.

We find the center P'' of the circle on which Q lies, by moving d_1 at an angle δ and then by moving d_2 at an angle θ. Q lies on the circle with radius $d - d_1 - d_2$ centering at P''. So, for a particular solution of equation 4.3.3, say, $\bar{d_1}$ and $\bar{d_2}$, Q lies on the circle with radius $d - \bar{d_1} - \bar{d_2}$ and center at $\left(\pm\frac{\bar{d_1}}{\sqrt{(1+m_1^2)}} \pm \frac{\bar{d_2}}{\sqrt{(1+m_2^2)}}, \pm\frac{m_1\bar{d_1}}{\sqrt{(1+m_1^2)}} \pm \frac{m_2\bar{d_2}}{\sqrt{(1+m_2^2)}} \right)$ as shown in Fig. 4.3, where, $PP'' = P'Q$, $P''Q = PP'$ and $\tan\delta = m_1$, $\tan\theta = m_2$. We can choose signs according the known angles.

Based on the above discussion, according to every point (d_1, d_2) on the curve Γ, we can find the center $(T_1(d_1, d_2), T_2(d_1, d_2))$ of the corresponding circle as shown in Fig. 4.3

using the following linear transformations:

$$T_1(d_1, d_2) = \pm\frac{d_1}{\sqrt{(1+m_1^2)}} \pm \frac{d_2}{\sqrt{(1+m_2^2)}}$$
$$T_2(d_1, d_2) = \pm\frac{m_1 d_1}{\sqrt{(1+m_1^2)}} \pm \frac{m_2 d_2}{\sqrt{(1+m_2^2)}} \tag{4.3.4}$$

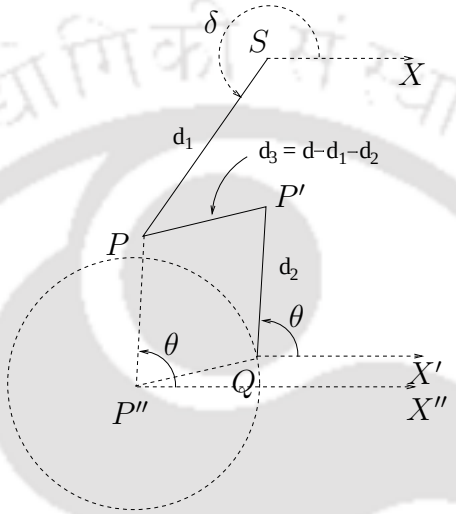

Figure 4.3: The circle on which the sensor lies in case of the two-bound signals

Γ is a continuous curve and the transformations of equation 4.3.4 are linear, so it maps Γ to another continuous curve $T(\Gamma)$. $T(\Gamma)$ is the locus of the centers of all the circles on which the sensor Q may lie. Now look on the range of the radius of the circles. For the maximum range, we need to find the $\max(d - d_1 - d_2)$ among every point (d_1, d_2) on the curve (equation 4.3.3), which is same as to find the $\min(d_1 + d_2)$. Similarly, we can find the circle of minimum radius by finding $\min(d - d_1 - d_2)$.

We can find the points (d_1', d_2') and (d_1'', d_2'') corresponding to the minimum and maximum values of $(d_1 + d_2)$ for all (d_1, d_2) on the curve (equation 4.3.3), using Lagrange method of several variables or using some numerical scheme. Now the radius of the circles are varying from $(d - d_1'' - d_2'')$ to $(d - d_1' - d_2')$ continuously over a continuous curve. The area covered by the circumferences of the all circles is the area where Q lies. The following Theorem 4.3.1 helps to find the area.

Theorem 4.3.1. *Let* $C = (T_1(d_1, d_2), T_2(d_1, d_2))$ *and* $C' = (T_1(d_1', d_2'), T_2(d_1', d_2'))$ *be two*

points corresponding to points (d_1, d_2) *and* (d_1', d_2') *respectively from equation 4.3.3. Then the circle with center* C *is contained in the circle with center* C' *if* $d_1 > d_1', d_2 > d_2'$.

Proof. First we have to find the center corresponding to (d_1, d_2) and (d_1', d_2'). There are several cases.

Case 1: If $\delta \in \left(0, \frac{\pi}{2}\right) \cup \left(3\frac{\pi}{2}, 2\pi\right)$ and $\theta \in \left(0, \frac{\pi}{2}\right) \cup \left(3\frac{\pi}{2}, 2\pi\right)$ then

$$((T_1(d_1, d_2), T_2(d_1, d_2)) = \left(\frac{d_1}{\sqrt{(1+m_1^2)}} - \frac{d_2}{\sqrt{(1+m_2^2)}}, \frac{m_1 d_1}{\sqrt{(1+m_1^2)}} - \frac{m_2 d_2}{\sqrt{(1+m_2^2)}}\right) \text{ and}$$

$$((T_1(d_1', d_2'), T_2(d_1', d_2')) = \left(\frac{d_1'}{\sqrt{(1+m_1^2)}} - \frac{d_2'}{\sqrt{(1+m_2^2)}}, \frac{m_1 d_1'}{\sqrt{(1+m_1^2)}} - \frac{m_2 d_2'}{\sqrt{(1+m_2^2)}}\right).$$

Let $C_r = d - d_1 - d_2$ and $C_r' = d - d_1' - d_2'$ be the radius of the circles with centers C and C' respectively. $(CC')^2 \leq (d_1 - d_1')^2 + (d_2 - d_2')^2 + 2(d_1 - d_1')(d_2 - d_2')$ if $\left|\frac{(1+m_1 m_2)}{\sqrt{(1+m_1^2)(1+m_2^2)}}\right| < 1$ and $(d_1 - d_1')(d_2 - d_2') > 0$.

Assume that for some values of m_1 and m_2, $\left(\frac{(1+m_1 m_2)}{\sqrt{(1+m_1^2)(1+m_2^2)}}\right)^2 > 1$ holds. That implies $(m_1 - m_2)^2 < 0$, which is a contradiction. So, $(CC')^2 \leq \{(d_1 + d_2) - (d_1' + d_2')\}^2$ if $(d_1 - d_1')(d_2 - d_2') > 0$. Implies, $CC' + C_r \leq C_r'$ if $d_1 > d_1', d_2 > d_2'$. Therefore, the circle with center at C is contained in the circle with center at C' as shown in Fig. 4.4, where $C_r' = C'G'$ and $C_r = CG$ are the radius of the circles with center at C', C respectively.

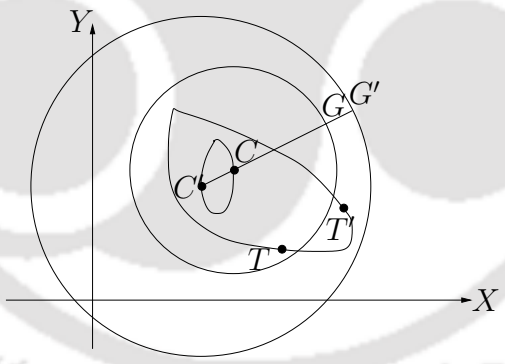

Figure 4.4: Figure showing circle with center at C is lying within the circle with center at C', T and T' are the points on the curve (equation 4.3.3) and C and C' are the corresponding centers from equation 4.3.4

Case 2: $\delta \in \left(0, \frac{\pi}{2}\right) \cup \left(3\frac{\pi}{2}, 2\pi\right)$ and $\theta \in \left(\frac{\pi}{2}, 3\frac{\pi}{2}\right)$

$$((T_1(d_1, d_2), T_2(d_1, d_2)) = \left(\frac{d_1}{\sqrt{(1+m_1^2)}} + \frac{d_2}{\sqrt{(1+m_2^2)}}, \frac{m_1 d_1}{\sqrt{(1+m_1^2)}} + \frac{m_2 d_2}{\sqrt{(1+m_2^2)}}\right) \text{ and}$$

$$((T_1(d_1', d_2'), T_2(d_1', d_2')) = \left(\frac{d_1'}{\sqrt{(1+m_1^2)}} + \frac{d_2'}{\sqrt{(1+m_2^2)}}, \frac{m_1 d_1'}{\sqrt{(1+m_1^2)}} + \frac{m_2 d_2'}{\sqrt{(1+m_2^2)}}\right).$$

$(CC')^2 = (d_1 - d_1')^2 + (d_2 - d_2')^2 - \frac{2(d_1-d_1')(d_2-d_2')(1+m_1m_2)}{\sqrt{(1+m_1^2)(1+m_2^2)}}$

$\leq (d_1 - d_1')^2 + (d_2 - d_2')^2 + 2(d_1 - d_1')(d_2 - d_2')$ if $(d_1 - d_1')(d_2 - d_2') > 0$.

That implies, $CC' + C_r \leq C_r'$ if $d_1 > d_1', d_2 > d_2'$.

Case 3: $\delta \in \left(\frac{\pi}{2}, 3\frac{\pi}{2}\right)$ and $\theta \in \left(0, \frac{\pi}{2}\right) \cup \left(3\frac{\pi}{2}, 2\pi\right)$

$((T_1(d_1, d_2), T_2(d_1, d_2)) = \left(\frac{-d_1}{\sqrt{(1+m_1^2)}} - \frac{d_2}{\sqrt{(1+m_2^2)}}, \frac{-m_1 d_1}{\sqrt{(1+m_1^2)}} - \frac{m_2 d_2}{\sqrt{(1+m_2^2)}}\right)$ and

$((T_1(d_1', d_2'), T_2(d_1', d_2')) = \left(\frac{-d_1'}{\sqrt{(1+m_1^2)}} - \frac{d_2'}{\sqrt{(1+m_2^2)}}, \frac{-m_1 d_1'}{\sqrt{(1+m_1^2)}} - \frac{m_2 d_2'}{\sqrt{(1+m_2^2)}}\right)$.

This is same as Case 2.

Case 4: $\delta \in \left(\frac{\pi}{2}, 3\frac{\pi}{2}\right)$ and $\theta \in \left(\frac{\pi}{2}, 3\frac{\pi}{2}\right)$

$((T_1(d_1, d_2), T_2(d_1, d_2)) = \left(\frac{-d_1}{\sqrt{(1+m_1^2)}} + \frac{d_2}{\sqrt{(1+m_2^2)}}, \frac{-m_1 d_1}{\sqrt{(1+m_1^2)}} + \frac{m_2 d_2}{\sqrt{(1+m_2^2)}}\right)$ and

$((T_1(d_1', d_2'), T_2(d_1', d_2')) = \left(\frac{-d_1'}{\sqrt{(1+m_1^2)}} + \frac{d_2'}{\sqrt{(1+m_2^2)}}, \frac{-m_1 d_1'}{\sqrt{(1+m_1^2)}} + \frac{m_2 d_2'}{\sqrt{(1+m_2^2)}}\right)$.

This is same as Case 1. □

4.3.1 Area of presence for a two-Bound signal

The above result of Theorem 4.3.1 is used to cover all possible circles on which Q may lie. Using Lagrange multiplier for several variable or using some numerical techniques, we can find $y_m = min\{y\}$ and $x_m = min\{x\}$ on equation 4.3.3. Note that the values of x_m and y_m are same due to the symmetric nature of the curve (equation 4.3.3). Now, by the above Theorem 4.3.1, the circle with center at $(T_1(x_m, y_m), T_2(x_m, y_m))$ and radius $d - x_m - y_m$ includes all the circles (where Q may lie) corresponding to all other points on equation 4.3.3. So, the area bounded by the circle with center at $C = (T_1(x_m, y_m), T_2(x_m, y_m))$ and radius $R = d - x_m - y_m$ is the possible location of Q. We call this circle as *minimum enclosing circle*.

We can further reduce possible area of Q by choosing appropriate numbers of overlapping circles such that the area of the union of the circles is less compare to the circle with center at C and radius R. Let, cover the area by three circles. How to chose three circles (for example, in general p circles) instead of one circle for reducing the area is given below and corresponding illustration is given in Fig. 4.5. Let $C_1 = (T_1(x_1, y_1), T_2(x_1, y_1))$,

$C_2 = (T_1(x_2, y_2), T_2(x_2, y_2))$ and $C_3 = (T_1(x_3, y_3), T_2(x_3, y_3))$ be centers and R_1, R_2 and R_3 be the radiuses of the three circles. Now find three set of center and radius for the circles. For which we can compute x_0 from equation 4.3.3 corresponding to y_m and the interval, $\frac{x_0 - x_m}{3} = u$ (say). Now $x_1 = x_0 - u$, $y_1 = y_m$ and $R_1 = d - x_1 - y_1$ specify the first circle. For second circle, compute $y_2 = y$ corresponding to x_1 from equation 4.3.3 and $x_2 = x_1 - u$ and radius $R_2 = d - x_2 - y_2$. Like second circle for the third circle, compute $y_3 = y$ corresponding to x_2 from equation 4.3.3 and $x_3 = x_2 - u$ which is same as x_m and radius $R_3 = d - x_3 - y_3$.

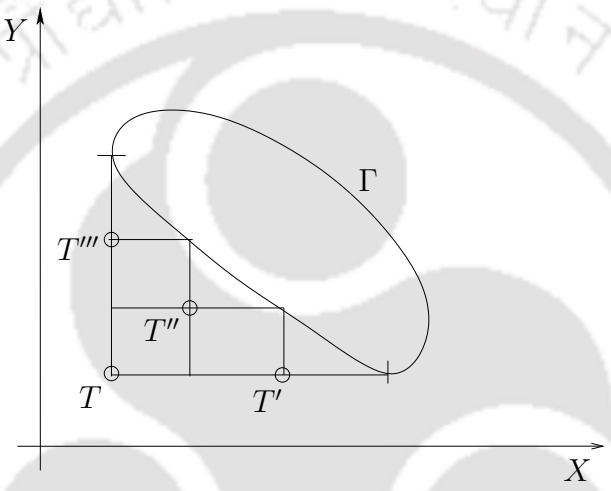

Figure 4.5: Figure showing points $T = (x_m, y_m)$, $T' = (x_1, y_1)$, $T'' = (x_2, y_2)$, $T''' = (x_3, y_3)$ for the curve Γ (equation 4.3.3) and corresponding to the circles with center at C, C_1, C_2 and C_3 respectively

With reference to Fig. 4.5 we can say that the three circles corresponding to the points T', T'' and T''' also covers all the circles as the circle corresponding to T does. For any $p \neq 1$, we get lesser area than $p = 1$. It happens since the radius of the circle is the largest when $p = 1$. Since the radius of the circles decreases as p increases, the efficiency increases with p. Simulation studies give this result for $p = 1, 2, 3$. If Q receives multiple number of two-bound signal from S then S finds the intersection of the areas calculated using each of the two-bound signal as the possible position of the sensor in question. Then center of gravity of the intersected area can be considered as the approximate position of the sensor Q.

4.4 Analysis of Multiple-Bound Signal

In this section we analyze area of presence of a sensor which receives a multi-bound signal. From now onward the notation $d_{i,n}$ is used as distance between $(i-1)$th and ith reflecting points for an n-bound signal, where $1 < i < n+1$. Distance between anchor and the first reflecting point is $d_{1,n}$. Distance between the n-th reflecting point and the sensor is $d_{n+1,n}$. The minimum possible value of $d_{i,n}$ for $1 \leq i \leq n+1$ is denoted by $d_{min,n}$. Let $d_{1,n}, d_{2,n}, \cdots d_{n+1,n}$ be a known instance of distances for a n-bound signal. By AOA technique, angles δ and θ made by the signal at S and Q with positive X-axis are also known. As we did in case of two-bound signal, similarly move $d_{1,n}$ and $d_{n+1,n}$ distance starting from S maintaining known angle constraints and reach at a point L. Now draw a circle of radius $d_{2,n} + d_{3,n} + \cdots + d_{n,n}$ centering at L, then the sensor must lie within that circle. Since the angles made by the reflectors in between are not known, we consider $d_{2,n} + d_{3,n} + \cdots + d_{n,n}$ as the radius of the circle within which the sensor must lie. In Fig. 4.6 an example for a three-bound signal is shown. We move SP and $P''Q$ respectively from S maintaining known angles δ and θ made by the signal at S and Q with positive X-axis. Since $\angle PP'P''$ is not known, we consider the circle centering at P''' with radius $PP' + P'P''$. The sensor must lie within this circle.

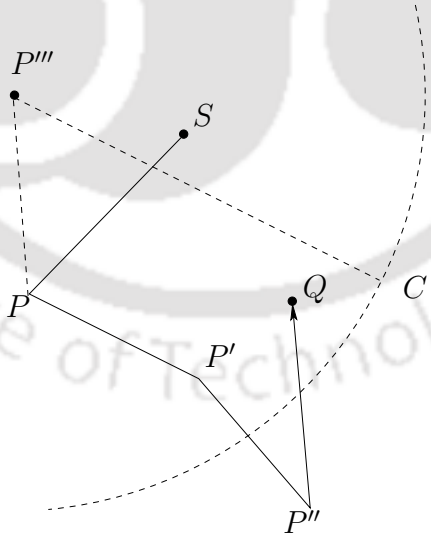

Figure 4.6: Showing the circle within which sensor must lie for a known instance of a three-bound signal

In case of two-bound signal, for known values of $d_{1,2}, d_{2,2}, d_{3,2}$, δ and θ, we got a circle on which the sensor must lie. But in case of n-bound signal, we get the area within a circle if $d_{1,n}, d_{2,n}, \cdots, d_{n+1,n}$, δ and θ are known. For a received signal strength S_r there are infinitely many combination of $d_{1,2}, d_{2,2}, d_{3,2}$. Union of those infinitely many circles is the area within which the sensor is bound to reside as described in section 4.3.1. Similarly, in case of n-bound signal, there are infinitely many possible values of $d_{1,n}, d_{2,n}, \cdots, d_{n+1,n}$. Each possible instance corresponds to a circle. Anchor have to find the union of all such infinitely many circles to find the possible area of presence of a sensor which received a n-bound signal. We proceed in the same way as we did for a two-bound signal to get a circle within which the sensor must lie. Using the value of received signal strength S_r, the value of $d_{1,2}d_{2,2}d_{3,2}$ which was denoted by k can be calculated for a two-bound signal from equation 4.3.2. From now onwards we use k_n for $d_{1,n}d_{2,n}\cdots d_{n+1,n}$ of a n-bound signal. The generalized version of equation equation 4.3.2 for finding k_n of a n-bound signal is given below:

$$\begin{aligned} S_r &= S_s \frac{c^{n+1}\left(\frac{100-h}{100}\right)^n}{d_{1,n}^2 d_{2,n}^2 \cdots d_{n+1,n}^2} \\ d_{1,n}d_{2,n}\cdots d_{n+1,n} &= \sqrt{c^{n+1}\left(\frac{100-h}{100}\right)^n \frac{S_s}{S_r}} = k_n \end{aligned} \tag{4.4.1}$$

We find $d_{min,n}$ satisfying $d_{1,n}d_{2,n}\cdots d_{n,n}(d - d_{1,n} - d_{2,n} - \cdots - d_{n,n}) = k_n$, where d is measured using TOA for the received n-bound signal. If we move $d_{min,n}$ and $d_{min,n}$ distance starting from S maintaining known angle constraints and draw a circle of radius $d - 2d_{min,n}$, then the sensor must lie within that circle. Following Theorem 4.4.1 illustrates what would happen if a sensor is localized after receiving a n-bound and a p-bound signal such that $k_p = k_n$.

Theorem 4.4.1. *If $d_{min,n} < d_{min,p}$ then the minimum enclosing circle of the p-bound signal is contained within the minimum enclosing circle of the n-bound signal, otherwise minimum enclosing circle of the p-bound signal contains the minimum enclosing circle of the n-bound signal, where both signal traveled d distance.*

Proof. In Fig. 4.7, $SP = PP' = d_{min,p}$ and $P'C = d - 2d_{min,p}$ such that the circle centering at P' is the possible area of presence for a p-bound signal with d, k_p, δ and

θ. Let $d_{min,n} < d_{min,p}$. In Fig. 4.7, $SL = LL' = d_{min,n}$. Now, $L'C = L'P' + P'C < L'T + TP' + P'C = (d_{min,p} - d_{min,n}) + (d_{min,p} - d_{min,n}) + (d - 2d_{min,p}) = d - 2d_{min,n} = L'C'$. So, the circle centering at L' with radius $d - 2d_{min,n}$ contains the point C, which is the furthest point from L' among the points on the circle centering at P'. Hence, the circle of the n-bound signal contains that of p-bound signal. Now, let $d_{min,n} \geq d_{min,p}$. Following similar logic, the minimum enclosing circle of the p-bound signal contains that of n-bound signal. □

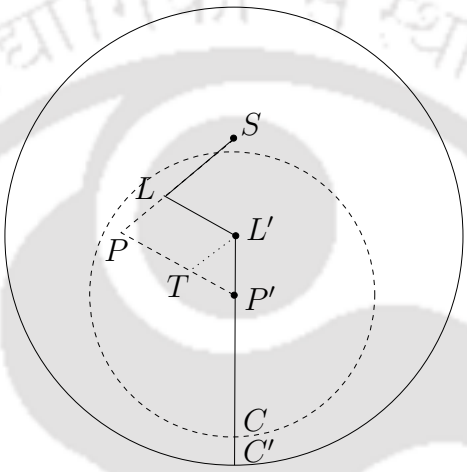

Figure 4.7: Showing possible area of presence for a p-bound signal and of a n-bound signal

Lemma 4.4.2. *Maximum possible value of k_{n-1} is equal to $\left(\frac{d}{n}\right)^n$ where $d_{1,n-1}\ d_{2,n-1} \cdots d_{n-1,n-1}\ (d - d_{1,n-1} - \cdots - d_{n-1,n-1}) = k_{n-1}$ and $d_i > 0$ for all $i = 1$ to $n - 1$.*

Proof. Consider the function $f = d_{1,n-1}d_{2,n-1}...d_{n-1,n-1}(d - d_{1,n-1} - d_{2,n-1} - \cdots - d_{n-1,n-1})$. We have to find the values of $d_{i,n-1}$, for which f attains maximum. $f'(d_{i,n-1}) = 0$ implies $d = d_{i,n-1} + (d_{1,n-1} + d_{2,n-1} + \cdots + d_{n-1,n-1})$ for all i, which implies $d_{i,n-1} = \frac{d}{n}$ for all i. $f''(d_{i,n-1}) < 0$ implies f attains maximum when $d_{i,n-1} = \frac{d}{n}$ and hence the maximum value of k_{n-1} is $\left(\frac{d}{n}\right)^n$. □

Lemma 4.4.3. *If $d_{min,n-1} = d_{i,n-1}$ for some i in the equation $d_{1,n-1} \cdots d_{n-1,n-1}(d - d_{1,n-1} - \cdots - d_{n-1,n-1}) = k_{n-1}$, then $d_{j,n-1} = \frac{d - d_{min,n-1}}{n-1}$ for all $j \neq i$.*

Proof. Without loss of generality let $d_{1,n-1} = d_{min,n-1}$. So, $d_{2,n-1} \cdots d_{n-1,n-1}d_{n,n-1} = \frac{k_{n-1}}{d_{min,n-1}}$. Now consider $g = d_{2,n-1} \cdots d_{n-1,n-1}d_{n,n-1}$, where $d_{2,n-1} + \cdots + d_{n-1,n-1} + d_{n,n-1} =$

$d - d_{min,n-1}$. Using Lemma 4.4.2, we can say, g attains maximum when $d_{2,n-1} = d_{3,n-1} = \cdots = d_{n-1,n-1} = d_{n,n-1} = \frac{d-d_{min,n-1}}{n-1}$ and maximum value of $g = \left[\frac{d-d_{min,n-1}}{n-1}\right]^{n-1}$. Clearly $d_{min,n-1} \in \left(0, \frac{d}{n}\right]$. So, $\left[\frac{d-d_{min,n-1}}{n-1}\right]^{n-1} \geq \frac{k_{n-1}}{d_{min,n-1}}$. Consider function $h(c) = c\left[\frac{d-c}{n-1}\right]^{n-1}$. $h'(c) \geq 0$ implies h is increasing $\in \left(0, \frac{d}{n}\right]$. If $d_{min,n-1}\left[\frac{d-d_{min,n-1}}{n-1}\right]^{n-1} = k_{n-1}$, then the lemma is proved. Else if $d_{min,n-1}\left[\frac{d-d_{min,n-1}}{n-1}\right]^{n-1} > k_{n-1}$, then the property of function h implies that $d_{min,n-1}$ can not be the minimum, which is a contradiction. Hence proved.

□

Lemma 4.4.4. *There may not exist a p-bound signal with same d and k_n of a n-bound signal and vice versa.*

Proof. If p is such that $k_n > \left(\frac{d}{p+1}\right)^{p+1}$, then using Lemma 4.4.2, we can say that for those values of d and k_n a p-bound signal can not exist. The other part is similar. □

For example we can find d and k_2 corresponding to a two-bound signal, such that a three-bound signal cannot exist. Such values of d must satisfy the inequality $\left(\frac{d}{3}\right)^3 > \left(\frac{d}{4}\right)^4$, which implies $d < \frac{256}{27} = 9.48$. So, for $d < 9.48$ and $k_2 > \left(\frac{d}{4}\right)^4$, no three-bound signal can exist.

Theorem 4.4.5. *The minimum enclosing circle of a n-bound signal is contained within the minimum enclosing circle of a p-bound signal ($p > n$) if both the signals have same d and $k_n = k_p$ with $d > (p+1)\left(\frac{p}{n}\right)^{\frac{n}{p-n}}$.*

Proof. We can write $d_{min,p}\left(\frac{d-d_{min,p}}{p}\right)^p = k_p$ using Lemma 4.4.3. Let

$$\begin{aligned} H(n) &= d_{min,p}\left(\frac{d-d_{min,p}}{p}\right)^p - d_{min,p}\left(\frac{d-d_{min,p}}{n}\right)^n \\ &= d_{min,p}\left(d-d_{min,p}\right)^n\left(\frac{(d-d_{min,p})^{p-n}}{p^p} - \frac{1}{n^n}\right) \end{aligned}$$

If $d > d_{min,p} + p\left(\frac{p}{n}\right)^{\frac{n}{p-n}}$ then $H(n) > 0$.
Since $d_{min,p} \in \left(0, \frac{d}{p+1}\right]$

$$H(n) > 0 \text{ if } d > (p+1)\left(\frac{p}{n}\right)^{\frac{n}{p-n}} \tag{4.4.2}$$

Again $H(n) > 0$ implies $k = d_{min,p}\left(\frac{d-d_{min,p}}{p}\right)^p > d_{min,p}\left(\frac{d-d_{min,p}}{n}\right)^n$. Since $f(x) = x\left(\frac{d-x}{n}\right)^n$ is an increasing function for $x \in \left(0, \frac{d}{n+1}\right]$, there exists $\hat{x} > d_{min,p}$ such that $\hat{x}\left(\frac{d-\hat{x}}{n}\right)^n = k_n$. Using Lemma 4.4.3, $\hat{x} = d_{min,n}$. Finally,

$$H(n) > 0 \text{ implies } d_{min,n} > d_{min,p} \tag{4.4.3}$$

So, $d_{min,n} > d_{min,p}$ for all $d > (p+1)\left(\frac{p}{n}\right)^{\frac{n}{p-n}}$. Using Theorem 4.4.1, we can conclude that the minimum enclosing circle of a n-bound signal is contained within the minimum enclosing circle of a p-bound signal if both the signals have same d and $k_p = k_n$ with $d > (p+1)\left(\frac{p}{n}\right)^{\frac{n}{p-n}}$. □

4.5 Area of Presence for an Unknown-Bound Signal

Practically it is not possible to know the actual value of n of a received $n-bound$ signal. Hence we can not calculate k_n for unknown n (Ref. equation 4.4.1). In this section we analyze and find conditions on d such that localizing a sensor is possible after receiving any n-bound signal, where n is unknown, using received signal strength S_r. However, we assume that the value N, of maximum possible bound in the system is known.

Theorem 4.5.1. *For a n-bound signal ($n \leq N$), the sensor lies within a circle calculated assuming the signal is N-bound if $d \geq (N+1)\left(\frac{N+1}{N}\right)^N \sqrt{\frac{c(100-h)}{100}}$.*

Proof. Let a sensor receives a signal with signal strength S_r and let distance traveled by the signal be d, measured by TOA technique. The number of bounds for the signal is not known to the receiver. Let originally the received signal be a n-bound signal. We can establish the following relation using equation 4.4.1, assuming that it is a N-bound signal,

$$k_N = k_n\left(\frac{c(100-h)}{100}\right)^{\frac{N-n}{2}} \tag{4.5.1}$$

Using Lemma 4.4.2, if $k_N \leq \left(\frac{d}{N+1}\right)^{N+1}$, then for the signal, n may be equal to N. So, there exists $d_{min,N}$ such that $d_{min,N}\left(\frac{d-d_{min,N}}{N}\right)^N = k_N$. We find a range of d such that $k_N \leq$

$\left(\frac{d}{N+1}\right)^{N+1}$ always occurs. From the equation 4.5.1 and Lemma 4.4.2, we can rewrite this expression as $\left(\frac{d}{n+1}\right)^{n+1}\left(\frac{c(100-h)}{100}\right)^{\frac{N-n}{2}} \leq \left(\frac{d}{N+1}\right)^{N+1}$, i.e., $d \geq (N+1)\left(\frac{N+1}{n+1}\right)^{\left(\frac{n+1}{N-n}\right)}\sqrt{\frac{c(100-h)}{100}}$. Since $(N+1)\left(\frac{N+1}{n+1}\right)^{\left(\frac{n+1}{N-n}\right)}\sqrt{\frac{c(100-h)}{100}}$ is an increasing function for $n = 1$ to $N-1$, we can conclude if $d \geq (N+1)\left(\frac{N+1}{N}\right)^{N}\sqrt{\frac{c(100-h)}{100}}$, then $k_N \leq \left(\frac{d}{N+1}\right)^{N+1}$ always occurs.

For the n-bound signal, there exist $d_{min,n}$ such that $d_{min,n}\left(\frac{d-d_{min,n}}{n}\right)^{n} = k_n$. Let $W(n)$ be a function defined below:

$$\begin{aligned} W(n) &= d_{min,N}\left(\frac{d-d_{min,N}}{N}\right)^{N} - \left(\frac{c(100-h)}{100}\right)^{\frac{N-n}{2}} d_{min,N}\left(\frac{d-d_{min,N}}{n}\right)^{n} \\ &= d_{min,N}(d-d_{min,N})^{n}\left(\frac{(d-d_{min,N})^{N-n}}{N^{N}} - \frac{\left(\frac{c(100-h)}{100}\right)^{\frac{N-n}{2}}}{n^{n}}\right) \end{aligned}$$

If $d \geq d_{min,N} + N\left(\frac{N}{n}\right)^{\frac{n}{N-n}}\sqrt{\frac{c(100-h)}{100}}$ then $W(n) \geq 0$,
i.e., if $d \geq (N+1)\left(\frac{N}{n}\right)^{\frac{n}{N-n}}\sqrt{\frac{c(100-h)}{100}}$, then $W(n) \geq 0$ since $d_{min,N} \in (0, \frac{d}{N+1}]$.

As $(N+1)\left(\frac{N}{n}\right)^{\frac{n}{N-n}}\sqrt{\frac{c(100-h)}{100}}$ is an increasing function for $n = 1$ to $N-1$, we can conclude if $d \geq (N+1)\left(\frac{N}{N-1}\right)^{N-1}\sqrt{\frac{c(100-h)}{100}}$ then $W(n) \geq 0$.

Again, $W(n) \geq 0$ implies $d_{min,N}\left(\frac{(d-d_{min,N})}{N}\right)^{N} \geq \left(\frac{c(100-h)}{100}\right)^{\frac{N-n}{2}} d_{min,N}\left(\frac{(d-d_{min,N})}{n}\right)^{n}$ which implies $k_n \geq d_{min,N}\left(\frac{d-d_{min,N}}{n}\right)^{n}$, using equation 4.5.1.

Since $f(c) = c\left(\frac{d-c}{n}\right)^{n}$ is increasing in $\left(0, \frac{d}{n+1}\right]$, $k_n \geq d_{min,N}\left(\frac{d-d_{min,N}}{n}\right)^{n}$ implies $d_{min,n} \geq d_{min,N}$. So, $W(n) \geq 0$ implies that $d_{min,n} \geq d_{min,N}$.

Again, $(N+1)\left(\frac{N+1}{N}\right)^{N}\sqrt{\frac{c(100-h)}{100}} > (N+1)\left(\frac{N}{N-1}\right)^{N-1}\sqrt{\frac{c(100-h)}{100}}$. So, we can conclude if $d \geq (N+1)\left(\frac{N+1}{N}\right)^{N}\sqrt{\frac{c(100-h)}{100}}$ then minimum enclosing circle of any n-bound signal where $n \leq N$ is contained within the minimum enclosing circle of a N-bound signal with same received signal strength S_r. □

4.6 Proposed Localization Algorithm

4.6.1 System model

All anchors are equipped with an omnidirectional antenna for sending beacons and also a directional antenna for the measurement of AOA of a signal from other sensors. Other sensors are equipped with directional antennas to avoid collision when it receives more than one beacon from an anchor coming through different paths at different angles. An anchor is said to be a *neighbor* of another anchor if it is located within twice the transmission range of the second anchor. Anchors are synchronized with some global clock (possibly through GPS) such that at a time only one anchor sends a beacon to avoid collision with the beacons from the neighboring anchors. This ensures that a receiving sensor receives only one beacon at a time from a particular anchor.

4.6.2 The algorithm

Based on the above discussions, Algorithm 2 (LocalizeSensor) given below finds the position of a sensor Q using the beacon signals from an anchor S.

Algorithm 2 LocalizeSensor

1: Anchor S sends beacon by omnidirectional antenna with $< anchor\_id >$ first, using electromagnetic signal and second, using ultrasonic signal.
2: **for** each sensor Q who hears the beacons **do**
3: Receives electromagnetic signal and measures receiving signal strength S_r.
4: Measures the angles of arrival (θ) of the ultrasonic signal and transmits back $< sensor\_id, \theta, S_r, \phi >$ to S via the same path.
5: **end for**
6: S measures the angles of arrival (δ) while receiving the reply and computes the corresponding distances (d) traveled by the beacon by measuring the TOA.
7: Anchor computes the area of presence of the sensor according to section 4.5.
8: If Q receives different signals then intersection of all such areas (calculated in the preceding step) is the area of presence of Q.

4.7 Simulation Results

Simulation is done in Matlab platform. First, we present simulation for the case of two-bound signals by randomly deployed sensors and reflectors over a square area with sides 100 meter. The anchors are also deployed randomly over the square. The range of sensors and anchors are taken as 30 meter. If total distance traveled by a two-bound signal is d then possible position of the sensor is inside the circle of area πd^2, which is the red

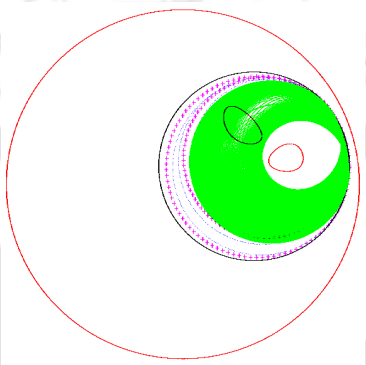

Figure 4.8: Sensor Q lie on any one of the infinitely many green circles when Q receives a two-bound signal

(largest) circle shown in Fig. 4.8. The union of infinitely many green circles in Fig. 4.8 is the exact area of presence of the sensor which is covered by finite circles. We compute the possible area as $\pi(d - x_m - y_m)^2$ for Q which is the black (second largest) circle. Fig. 4.8 shows that if we cover the area by two (pink-dotted) or three (blue-dotted) circles, then area of presence can be further reduced as discussed in the section 4.3.1. For each run of our simulation 100 two-bound signals are generated. The average reduced area is calculated for one circle. The Table 4.1 is showing the area reduced by our proposed algorithm with a two-bound signal. On an average 50% area of presence has been reduced when one two-bound signal is received by a sensor.

Table 4.1: Percentage of average area reduced using one two-bound signal

No of Runs →	1	2	3	4	5	6	7	8	9	10
Percentage of reduction	48.2	53.7	51.9	54.1	49.4	47.6	50.5	50.9	52.3	49.8

Table 4.2: Reduction in average area compared to trilateration when sensor receives three two-bound signals

No of Runs →	1	2	3	4	5	6	7	8	9	10
Percentage of reduction	34.2	37.7	32.1	41.3	33.2	39.8	42.2	37.2	30.4	30.9

Table 4.3: Error comparison when sensor receives three two-bound signals

No of Runs →	1	2	3	4	5	6	7	8	9	10
Error in our technique (in meter)	3.7	4.8	3.1	3.1	3.7	3.9	3.3	2.9	3.2	3.8
Error in trilateration (in meter)	5.3	6.9	6.2	5.2	8.0	6.2	6.4	4.6	6.5	6.4
Percentage of improvement	30.2	30.7	49.1	39.9	53.2	37.0	48.2	37.2	50.4	40.4

Table 4.4: Reduction in average area compared to trilateration when sensor receives three unknown-bound signals

Maximum number of bounds →	3	4	5	6	7	8
Percentage of reduction	24.54	14.7	8.6	6.1	4.5	4.1

Table 4.5: Error comparison when sensor receives three unknown-bound signals

Maximum number of bounds →	3	4	5	6	7	8
Error in our technique (in meter)	8.17	9.60	10.19	9.70	7.28	10.76
Error in trilateration (in meter)	9.45	10.16	10.46	9.80	7.33	10.78
Percentage of improvement	13.54	5.49	2.63	1.00	0.60	0.25

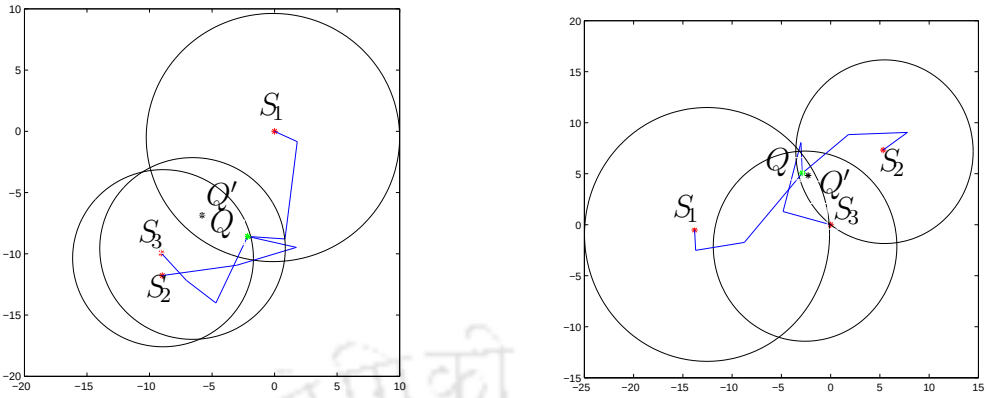

(a) (b)

Figure 4.9: Figures showing localization using three two-bound signals

We generate three two-bound signals, found corresponding circles, to compute the center of gravity of the intersection area of the three circles as the position of the sensor. Average area of presence as well as average error of our method are compared with trilateration method by applying trilateration over same set of data. The results in Table 4.2 and Table 4.3 show on an average 35% improvement in terms of area of presence and 40% improvement in terms of average error over trilateration. All the error values are in meter. Sample outputs of our simulation are shown in Fig. 4.9 where positioning are done using three received two-bound signals by the sensor. In this figure, S_1, S_2, S_3 are the anchors represented by red stars, Q is the actual position of the sensor represented by green star and Q' is the computed position of Q using our method.

Next, simulation are done for unknown-bound signal assuming the maximum possible bound of the environment is known. Sensor receives three unknown-bound signals and its position is computed using our method varying the number of maximum possible bound from three to eight. We compare average area of presence as well as average error of our method with trilateration and show percentage of improvement in Table 4.4 and Table 4.5. On an average, 10% improvement in terms of area of presence and 4% improvement in terms of average error over trilateration is achieved by our technique. Sample outputs of our simulation are shown in Fig. 4.10, where positioning is done using three received unknown-bound signals by the sensor. In this figure, S_1, S_2, S_3 are the

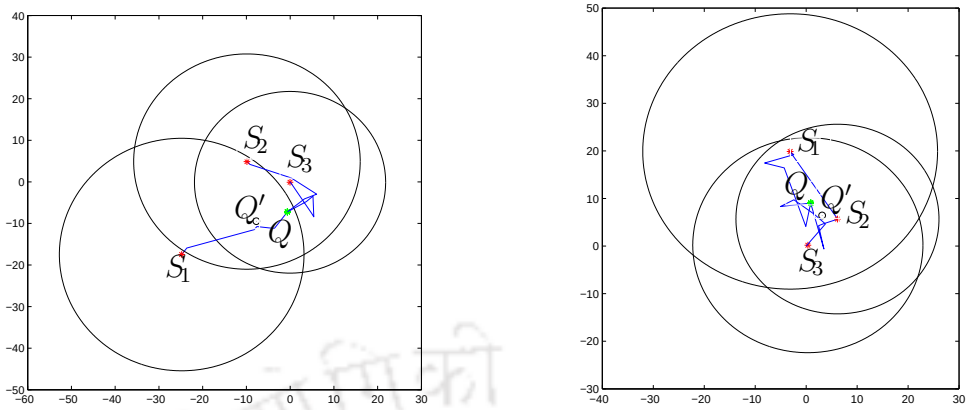

(a) (b)

Figure 4.10: Figures showing localization using three unknown-bound signals

Table 4.6: Reduction in average area assuming maximum number of bound is 7

Actual maximum number of bounds →	3	4	5	6	7
Percentage of reduction	2.2	3.6	4.7	3.8	4.9

anchors represented by red stars, Q is the actual position of the sensor represented by green star and Q' is the computed position of Q using our method. In Table 4.6 and

Table 4.7: Error comparison by assuming maximum number of bound is 7

Actual maximum number of bounds →	3	4	5	6	7
Error in our technique (in meter)	9.72	5.42	8.5	9.9	7.4
Error in trilateration (in meter)	9.73	5.47	8.6	10	7.5
Percentage of improvement	0.10	0.86	1.37	0.6	1.38

Table 4.7, we show improvement over trilateration in terms of both area of presence and average error assuming that the value of actual maximum bound signal in the environment is not known. The value of possible maximum bound is taken as 7 and computed average improvement varying actual maximum bound from 3 to 7.

4.8 Conclusions

In this work we have proposed a localization algorithm under a model where multiple-bound (up to N-bound, any known N) signals are allowed. To the best of our knowledge there is no deterministic algorithm for localization where the received multiple-bound (more than one-bound) signals are used in absent of LOS signals. Comparison with trilateration shows on an average 35% improvement when sensor receives three two-bound signals from different anchors and on an average 10% improvement when sensor receives three unknown-bound signals from different anchors in terms of area of presence. In future we will try to solve the localization problem under a more practical model relaxing the condition of known N and introducing measurement errors.

Chapter 5

Mobile Sensor Localization using Static Anchor under Constrained Motion

5.1 Introduction

Mobile wireless sensor networks (MWSNs) is a recent development of WSNs. In MWSN mobile sensors are needed to be localized in such a way that their position can be known at any time instant. This work is motivated by the beacon point selection strategy used in [46, 75, 84] for static sensor localization using mobile anchors. In all these three schemes since static sensors receive beacons from mobile anchors, sensors know the co-ordinates of the beacon points. Hence chord formed by two beacon points is unique in [75]. Similarly unique circular lamina with known equations of the circles can be formed using a beacon point in [46]. Contrary to that in our proposed algorithm, as anchors are static and mobile sensors are receiving beacons at different positions, so co-ordinate of beacon points are not known and a unique chord can not be formed using two beacon points. Hence we use communication circles of two different anchors to identify the chord and localize the mobile sensor in proposed Algorithm 3. We modify the definition of beacon point accordingly and propose range-free deterministic localization algorithms under different circumstances.

5.1.1 Our contribution

According to our proposed algorithm LWCD, a mobile sensor can localize itself within any predefined error bound when it passes through communication circles of two different anchors. As it passes through more communication circles, positioning error can be further reduced. Simulation results of LWCD show around 75% improvement of the positioning error over the existing algorithm [90]. When mobile sensor passes through three and five more communication circles, 40% and 55% further reduction in error are shown respectively. In presence of obstacles, our proposed algorithm LWCDPO can localize mobile sensors within same error bound as LWCD.

The rest of the chapter is organized as follows. We propose a localization algorithm LWCD assuming mobile sensor does not change its direction during movement in section 5.2. With the same assumption, we propose another algorithm LWCDPO to localize mobile sensors in presence of obstacles in section 5.3. The simulation results of our algorithms are presented in section 5.4, along with performance comparison with relevant algorithms. Finally we conclude in section 5.5.

5.2 Localization without Change of Direction

In this section we propose a mobile sensor localization algorithm assuming sensors do not change their direction during localization. System model for the algorithm is given below.

5.2.1 System model

Static anchors with equal communication range are deployed sparsely in a two dimensional plane. All mobile sensors have the information about the communication range of the anchors. Also mobile sensors and anchors have equal communication range r. Anchors are identified by their locations. The anchors periodically broadcast beacons with their locations. The time interval between two consecutive broadcasts of beacons is t, which is fixed and same for all anchors. The mobile sensors move according to the requirement of underlying application. During localization phase, mobile sensors move with a uniform velocity until localization.

When a mobile sensor receives first beacon from an anchor, it recognizes that it is in the communication range of that anchor. The position of receiving first beacon is an approximate end point of the chord of the communication circle of that anchor, along which it is moving. Similarly, the position of receiving the last beacon from that anchor denotes the approximate position of the other end point of that chord. As mobile sensor does not know the positions of receiving beacons, it records the time of receiving the first and last beacon according to it's own clock to calculate the approximate chord length. We denote the time of receiving any beacon according to the sensor's clock as the time stamp of the beacon. Definition of the key terms used in this paper are given below.

Definition 5.2.1. (Beacon distance) Distance traveled by the mobile sensor between receiving two consecutive beacons from an anchor is called *beacon distance*.

The beacon distance is denoted by u and is equal to vt, where v is uniform velocity of the mobile sensor during localization and t is time interval of periodical broadcasts of beacon by the anchor.

Definition 5.2.2. (Beacon point) Beacon received by a mobile sensor from an anchor at time x is marked as a beacon point by the sensor if and only if the sensor does not receive any beacon either in time interval $[x - t_0, x)$ or in time interval $(x, x + t_0]$ from the same anchor, where $t < t_0 < 2t$ and t is time interval of periodical broadcasts of beacon by the anchor.

Definition 5.2.3. (Communication circle) The circle with radius r centering at an anchor, where r is the communication range of the anchor.

Beacon distance should be much lesser than communication range in order to receive a good number of beacons. When a mobile sensor moves into the transmission area of an anchor and receives a beacon, it knows the equation of the communication circle in which it is moving since the communication range and position of the anchor is known. We call the line along which a mobile sensor is moving within a communication circle as it's *actual line of movement*. The mobile sensors are equipped with a electronic compass [65] for knowing the direction of movement and a timer to record the time stamps of the received beacons. Electronic compass yields an in-plane heading accuracy of ± 1 degree [65].

5.2.2 Beacon list

Each mobile sensor maintains a *beacon list* with two columns. Each entry of the list contains time stamp ($time\_stamp$) of the received beacon and corresponding anchor id ($anchor\_id$) according to it's own clock. When a mobile sensor receives a beacon from an anchor, it records $< time\_stamp, anchor\_id >$ in the beacon list. Here a beacon is represented as $< time\_stamp, anchor\_id >$. At the beginning, list is empty. Let a sensor receives a beacon from an anchor with $anchor\_id = i$. It records $< time\_stamp, i >$ in the first column and marks it as a beacon point. If another beacon is received from the same anchor by time t_0 then sensor replaces the last beacon with latest one provided the last beacon is not marked as beacon point. If last beacon is marked as beacon point then it adds this beacon in the same column. If no beacon is received by the time t_0 then the last beacon is marked as beacon point. A sensor may receive many beacons but the beacons marked by above rule, are the beacon points. In between whenever any beacon comes from a different anchor with $anchor\_id = j$, say, $(j \neq i)$, it records $< time\_stamp, j >$ in the second column and marks it as a beacon point. If both the columns are non-empty and a beacon is received from an anchor with $anchor\_id = s$ $(s \neq i, j)$, then that beacon is ignored. Following the procedure discussed above, sensor records at most two beacon points for each anchor. There is possibility of receiving only one beacon from an anchor, in that case only one beacon point appears in a column of the list. So, there can be maximum of four entries in the list. After localizing itself, the sensor deletes those marked beacon points to make the list empty, as explained in section 5.2.6.

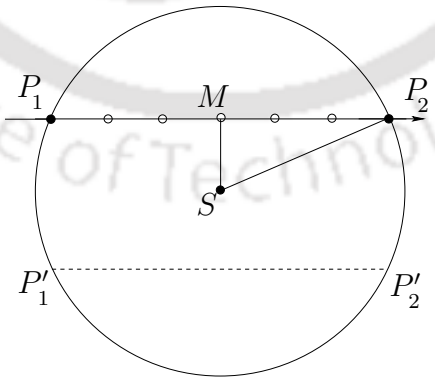

Figure 5.1: Showing two possible lines of movement including the actual one (P_1P_2)

5.2.3 Finding line of movement

We explain how a mobile sensor can identify its actual line of movement based on beacon points corresponding to two anchors. A mobile sensor calculates the time difference between receiving two beacon points from an anchor, to calculate the chord length $2l$. Using the electronic compass, the sensor also knows the gradient of the line along which it moves. As there exist only two possible chords of same length and gradient in a circle, the sensor is moving along any one of those two lines (Ref. Fig. 5.1). For simplicity, let the sensor moves along a line parallel to X-axis. Throughout the chapter, in the figures, filled circles denote beacon points and unfilled circles denote received beacons except beacon points, on the line of movement of a mobile sensor.

Let one anchor be placed at $S = (0, 0)$ and P_1P_2 is the actual line of movement of the mobile sensor, where filled circles labeled as P_1 and P_2 are the beacon points as shown in Fig. 5.1. The equation of the communication circle is $x^2 + y^2 = r^2$ and $SM = \sqrt{r^2 - l^2}$, where $P_1P_2 = 2l$. Hence, the possible line of movement of the mobile sensor is either P_1P_2 or $P_1'P_2'$, whose equations are $y = \pm\sqrt{r^2 - l^2}$. More information is needed to identify the actual line. For which the sensor continues its movement along the same line until it crosses the communication circle of another anchor. Let $S' = (a, b)$, $b \neq 0$ be a different anchor as shown in Fig. 5.2. Let P_3, P_4 be the beacon points corresponding to S' and $S'M' = \sqrt{r^2 - l'^2}$, where $P_3P_4 = 2l'$. Similarly, the possible line of movement of the mobile sensor is either P_3P_4 or $P_3'P_4'$, whose equations are $y = b \pm \sqrt{r^2 - l'^2}$. Now, among these four lines, equations of two lines should be same with the actual line of movement, since there is exactly one line along which the sensor is moving. According to Fig. 5.2, the equation of the actual line is $y = \sqrt{r^2 - l^2}$ i.e., $y = b + \sqrt{r^2 - l'^2}$.

Using the selected equation of the line of movement, the sensor can calculate the coordinates of the points P_1, P_2, P_3, P_4. Current position of the mobile sensor can be calculated based on any P_i for $i = 1$ to 4, and elapsed time from timer. To localize itself, a sensor has to pass through communication circles of two different anchors where the line joining those two anchors should not be parallel with the line of the sensor, i.e., $SS' \nparallel P_1P_4$.

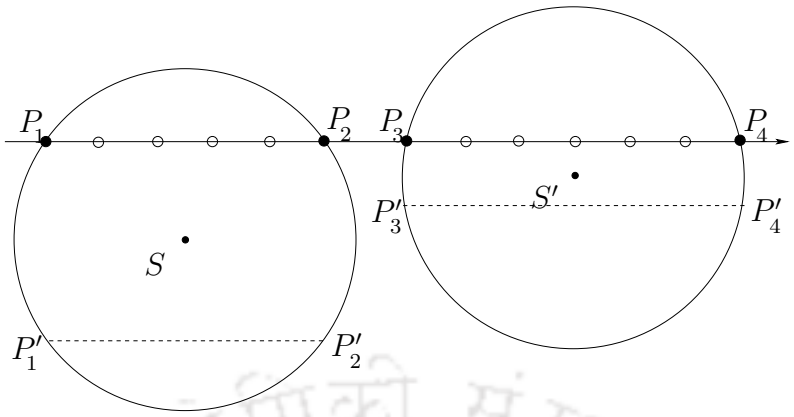

Figure 5.2: Two communication circles are required to find the correct line of movement

5.2.4 Error analysis

The above technique of choosing the line of movement among four calculated chords is not applicable for finding actual line of movement unless beacon points are located on the perimeter of the communication circles of the respective anchors. In practice beacon points, C, C' marked with filled circles (Ref. Fig. 5.3) may lie inside the communication circles due to periodic broadcast of anchors. This may lead to a situation where equation of no two chords are common. In that case mobile sensor finds *approximate line of movement* instead of actual one. Hence localization error occurs.

Again, $P_1C \leq u$ and $P_2C' \leq u$, where P_1 and P_2 are the points of intersection of the actual line of movement of the mobile sensor with communication circle of the anchor S. For some $h_1, h_2 \in [0, 1]$, we can write

$$\begin{aligned} P_1C &= h_1u \\ P_2C' &= h_2u \end{aligned} \tag{5.2.1}$$

According to Fig. 5.3, possible approximate lines of movement are $P'_1P'_2$ and $P''_1P''_2$. Mobile sensor can measure the length CC' from its velocity and time stamps of the beacon points. The sensor misinterprets the length CC' as the length of the chords P_1P_2 along which it is moving. So, the actual line of movement P_1P_2 is projected to the approximate line of movement $P'_1P'_2$ such that $CC' = P'_1P'_2$. Due to the symmetric nature of circle, we

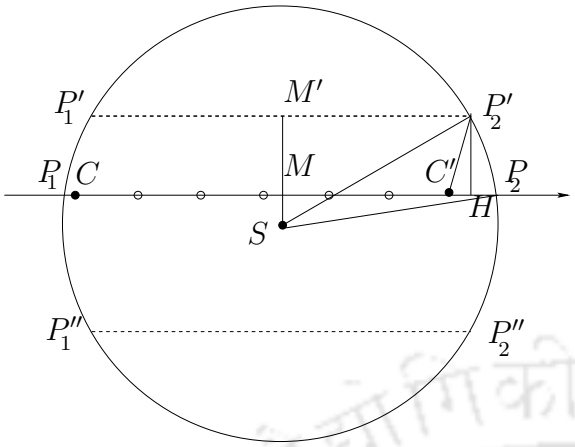

Figure 5.3: Showing error $C'P_2'$ for the line of movement P_1P_2, where P_2' is the calculated position with respect to the actual position C'

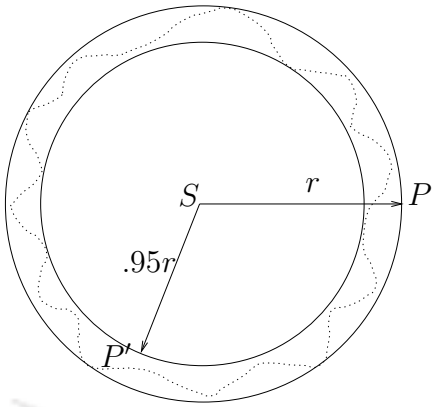

Figure 5.4: SP and SP' are radii of the maximum and minimum possible communication range of S due to effect of irregular radio propagation where $SP - SP' = .05r$.

get another possible line of movement $P_1''P_2''$. It is possible to discard $P_1''P_2''$ as a line of movement using one more communication circle of another anchor as discussed later. The error in calculating line of movement is $C'P_2'$ as shown in Fig. 5.3. According to Fig. 5.3 the actual line of movement is P_1P_2 and the selected approximate line of movement is $P_1'P_2'$. Let T be the time stamp of receiving beacon at C'. The mobile sensor calculates position of the beacon point as P_2' instead of C' with the knowledge of $P_1'P_2'$. So, error in positioning is equal to $C'P_2'$. $P_1'P_2' = 2l$, say. $C'P_2' = \sqrt{(P_2'H)^2 + (C'H)^2}$. Again $P_1'P_2' = CC'' = P_1P_2 - (h_1u + h_2u)$.

Hence, $C'H = C'P_2 - HP_2 = (h_2 - h_1)\frac{u}{2}$.

Also, $P_2'H = MM' = SM' - SM = \sqrt{r^2 - l^2} - \sqrt{r^2 - \left(l + \frac{h_1u + h_2u}{2}\right)^2}$.

Here, $P_2'H$ and $C'H$ are the perpendicular and horizontal components of the error $C'P_2'$. We denote perpendicular component of error as *perpendicular error* E_P and horizontal component of error as *horizontal error* E_H. The error in positioning, $C'P_2'$ is denoted as

ζ which is equal to $\sqrt{E_P^2 + E_H^2}$.

$$\begin{aligned} E_H &= (h_2 - h_1)\frac{u}{2} \\ E_P &= \sqrt{r^2 - l^2} - \sqrt{r^2 - \left(l + \frac{h_1 u + h_2 u}{2}\right)^2} \\ \zeta &= \sqrt{E_P^2 + E_H^2} \end{aligned} \tag{5.2.2}$$

For any chord length $2l$, maximum E_P is denoted by $MaxE_P(2l)$. We find maximum possible value of perpendicular component of error considering all possible chord lengths.

Lemma 5.2.4. *The value of the possible perpendicular component of the error is maximum when mobile sensor passes along the diameter of the communication circle of any anchor.*

Proof. Perpendicular component of positioning error is equal to MM' as shown in Fig. 5.3. Hence, maximum possible value of MM' for all possible chords is the maximum possible perpendicular component of error in localization. As the values of P_1C and P_2C' increases, MM' also increases. Without considering the irregularity in signal propagation, $[0, u]$ is the range of possible values of P_1C and $C'P_2$, where u is the beacon distance. When $P_1C = u = C'P_2$, then the length of the actual chord along which the sensor is moving becomes $2l + 2u$, where $2l$ is the calculated chord length.
So, length of $MM' = MaxE_P(2l) = \sqrt{r^2 - l^2} - \sqrt{r^2 - (l + u)^2}$.
This expression gives maximum value when $u + l = r$. That is, if the sensor moves along diameter and calculates chord length as $2(r - u)$ instead of $2r$, then error becomes maximum and hence the maximum possible perpendicular error is $\sqrt{r^2 - (r - u)^2}$. □

We denote ϵ as the maximum possible perpendicular error and $\epsilon = \sqrt{r^2 - (r - u)^2}$.

In case of irregular radio propagation (Ref. Fig. 5.4) if radius of larger circle is the communication range, due to irregular radio propagation, sometimes signal reaches only up to the boundary of the smaller circle in some direction. Now, according to Fig. 5.3, the range of possible values of P_1C and $C'P_2$ is $[0, u + 0.01\rho r)$, where ρ is the percentage of maximum possible reduction of the communication range due to radio propagation irregularity. Expression of the maximum possible error becomes $\epsilon = \sqrt{r^2 - (r - u - .01\rho r)^2}$.

We can keep ϵ under control by choosing appropriate values of u and r. For our simulation study we consider $\rho = 5$ in section 5.4. Simulation results are also shown varying ρ from 0 to 20. However, if ρ is not known, it can be estimated by sending radio signals and measuring the maximum and minimum communication ranges of environments. In a dynamic environment when the radio irregularity changes frequently and sensor node also moves out quickly from the communication range of the anchor, it is not easy to estimate ρ perfectly because of low number of sampling. But in such a dynamic environment, instead of online estimation of ρ, we can use minimum communication range for maximum value of ρ i.e., the maximum possible radio irregularity of the environment. The upper bound of ρ could be estimated off line with large sample for such a dynamic environment.

Now error in localization is less than the maximum of $\sqrt{\epsilon^2 + \left(\frac{(h_2-h_1)u}{2}\right)^2}$, for all $h_1, h_2 \in [0, 1]$ (according to equation 5.2.2). Error ζ, is less than $\sqrt{\epsilon^2 + \left(\frac{u}{2}\right)^2}$. But this is an upper bound of ζ. We now find the least upper bound of ζ in the following lemma.

Lemma 5.2.5. *Least upper bound of ζ is ϵ.*

Proof. For any calculated chord length $2l$, the horizontal component of error is $E_H = |h_2 - h_1|\frac{u}{2}$ (Ref. equation 5.2.2). Let $|h_2 - h_1| = f$. So $f \in [0, 1]$. If horizontal error is nonzero then $f > 0$. Then value of horizontal error is $\frac{fu}{2}$. Without loss of generality, let $h_2 = h_1 + f$. Perpendicular error increases as $h_1 + h_2$ increases, i.e., calculated chord length decreases. So, maximum possible value of $h_1 = 1 - f$ and $h_2 = 1$. Hence using equation 5.2.2, for any l, perpendicular error becomes $E_P = \sqrt{r^2 - l^2} - \sqrt{r^2 - \left(l + \frac{(2-f)u}{2}\right)^2}$.
From Lemma 5.2.4, for any f, E_P is maximum when the original line passes along the diameter, i.e., $l + \frac{(2-f)u}{2} = r$. So, for any f, ζ also attains maximum if $l + \frac{(2-f)u}{2} = r$ and the expression of maximum value of ζ becomes $\sqrt{r^2 - \left(r - \frac{(2-f)u}{2}\right)^2 + (\frac{uf}{2})^2}$, which is a decreasing function of $f \in (0, 1]$.
Using limit of function and existence of $\sqrt{r^2 - \left(r - \frac{(2-f)u}{2}\right)^2 + (\frac{uf}{2})^2}$ at $f = 0$, we can say, it attains maximum at $f = 0$ i.e., least upper bound of error ζ is $\sqrt{r^2 - (r-u)^2} = \epsilon$. □

The value of maximum possible error is ϵ if we can select the line of movement which is closer to the original line of movement among two calculated lines of movement. An interesting observation is that if there is any error while selecting the line of movement,

the erroneous line is always far from the anchor than the actual line of movement. It happens because the length of the chord always decreases in case of wrong chord length estimation. As discussed in section 5.2.3, a sensor chooses the actual line of movement among four lines calculated by passing through two communication circle of different anchors in ideal situation, when beacon points are on the perimeter of the communication circles. But the following result ensures that the sensor chooses the approximate line of movement with error bound ϵ in practical situation, when beacon points may lie inside the communication circles.

Theorem 5.2.6. *Among four equations of possible lines of movements, a mobile sensor finds the pair of line such that perpendicular distance between them is the least. If the sensor chooses a line from that pair then error would always be at most ϵ, where perpendicular distance between the lines passing through the anchors with same gradient with the actual line of movement is at least ϵ.*

Proof. For simplicity, we prove the theorem assuming that the mobile sensor is moving along a line parallel to X-axis. Let coordinates of two anchors, S and S', be (a, b) and (c, d) respectively where $a \geq 0$, $b \geq 0$, $c \geq 0$, $d > 0$ and $(d - b) \geq \epsilon$. There are two possible cases:

Case 1: If actual line of movement passes through same side of two anchors. According

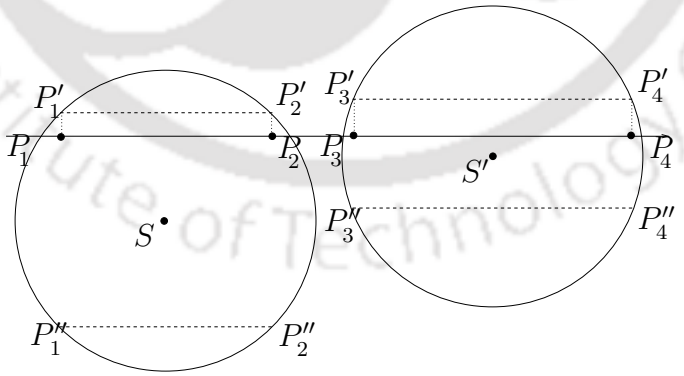

Figure 5.5: Anchors are at same side of the line of movement

to Fig. 5.5 the actual line of movement is P_1P_4, passes through upper side of the anchors

S and S'. Let equation of the actual line of movement which passes through both the circles be

$$y = dk \text{ where } k \geq 1 \tag{5.2.3}$$

Let the chord length corresponding to the communication circles of the anchors S and S' be $2l$ and $2l'$ respectively. Sensor calculates equation of the line $P_1'P_2'$ and $P_1''P_2''$ as,

$$y = dk + \frac{MaxE_P(2l)}{q_1} \text{ where } q_1 \geq 1 \text{ and} \tag{5.2.4}$$

$$y = 2b - dk - \frac{MaxE_P(2l)}{q_1} \text{ where } q_1 \geq 1 \tag{5.2.5}$$

respectively. Similarly, sensor calculates equation of the line $P_3'P_4'$ and $P_3''P_4''$ as

$$y = dk + \frac{MaxE_P(2l')}{q_2} \text{ where } q_2 \geq 1 \text{ and} \tag{5.2.6}$$

$$y = 2d - dk - \frac{MaxE_P(2l')}{q_2} \text{ where } q_2 \geq 1 \tag{5.2.7}$$

respectively. Distance between the lines (equation 5.2.4 and equation 5.2.6) is equal to $\left|\frac{MaxE_P(2l')}{q_2} - \frac{MaxE_P(2l)}{q_1}\right| \leq \max\left(\frac{MaxE_P(2l)}{q_1}, \frac{MaxE_P(2l')}{q_2}\right)$.
We denote distance between lines (equation 5.2.i) and (equation 5.2.j) by $D(i,j)$ hereafter. So, $D(4,6) \leq \max\left(\frac{MaxE_P(2l)}{q_1}, \frac{MaxE_P(2l')}{q_2}\right)$.
Let it be the smallest distance among those six possible distances $D(i,j)$. If we choose equation 5.2.4 or equation 5.2.6, we are choosing lines within $\max\left(\frac{MaxE_P(2l)}{q_1}, \frac{MaxE_P(2l')}{q_2}\right)$ error, since $D(3,4) = \frac{MaxE_P(2l)}{q_1}$ as well as $D(3,6) = \frac{MaxE_P(2l')}{q_2}$. Actually we are finding distances between correct line (equation 5.2.3) and the line we are choosing according to our technique and checking it is less or equal to ϵ or not. Equation 5.2.4 and equation 5.2.6 make sure that there is at least one pair of lines whose perpendicular distance is less than or equal to $\max\left(\frac{MaxE_P(2l)}{q_1}, \frac{MaxE_P(2l')}{q_2}\right)$.

Let $D(4,5)$ be the least. We have to check $D(3,5)$ only.

$D(3,5) = 2dk - 2b + \frac{MaxE_P(2l)}{q_1} \leq 2dk - 2b + 2\frac{MaxE_P(2l)}{q_1} = D(4,5) < D(4,6)$
$= \left|\frac{MaxE_P(2l')}{q_2} - \frac{MaxE_P(2l)}{q_1}\right| \leq \max\left(\frac{MaxE_P(2l)}{q_1}, \frac{MaxE_P(2l')}{q_2}\right)$.

Let $D(4,7)$ be the least. We have to check $D(3,7)$ only.

$D(3,7) = 2dk - 2d + \frac{MaxE_P(2l')}{q_2} \leq 2dk - 2d + \frac{MaxE_P(2l)}{q_1} + \frac{MaxE_P(2l')}{q_2} = D(4,7) < D(4,6) =$
$\left|\frac{MaxE_P(2l')}{q_2} - \frac{MaxE_P(2l)}{q_1}\right| \leq \max\left(\frac{MaxE_P(2l)}{q_1}, \frac{MaxE_P(2l')}{q_2}\right)$.

$D(5,6) = 2dk - 2b + \frac{MaxE_P(2l)}{q_1} + \frac{MaxE_P(2l')}{q_2} > 2dk - 2d + \frac{MaxE_P(2l)}{q_1} + \frac{MaxE_P(2l')}{q_2} = D(4,7)$, since $d > b$. So, it cannot be the least.

$D(5,7) = 2d - 2b + \frac{MaxE_P(2l)}{q_1} - \frac{MaxE_P(2l')}{q_2} \geq \epsilon$, since $d \geq b + \epsilon$. So it cannot be the least.

Let $D(6,7)$ be least. We have to check $D(3,7)$ only.

$D(3,7) = 2dk - 2d + \frac{MaxE_P(2l')}{q_2} \leq 2dk - 2d + 2\frac{MaxE_P(2l')}{q_2} = D(6,7) \leq \left|\frac{MaxE_P(2l')}{q_2} - \frac{MaxE_P(2l)}{q_1}\right| \leq$
$\max\left(\frac{MaxE_P(2l)}{q_1}, \frac{MaxE_P(2l')}{q_2}\right)$.

Hence we show that if $D(i,j)$ is the least and we choose any one of the 5.2.i-th and 5.2.j-th equation, then we are choosing a line of movement which is within
$\max\left(\frac{MaxE_P(2l)}{q_1}, \frac{MaxE_P(2l')}{q_2}\right)$ perpendicular error with the actual line of movement.

Case 2: If actual line of movement passes through different sides of two anchors. According to Fig. 5.6, the actual line of movement is P_1P_4 passes through the different

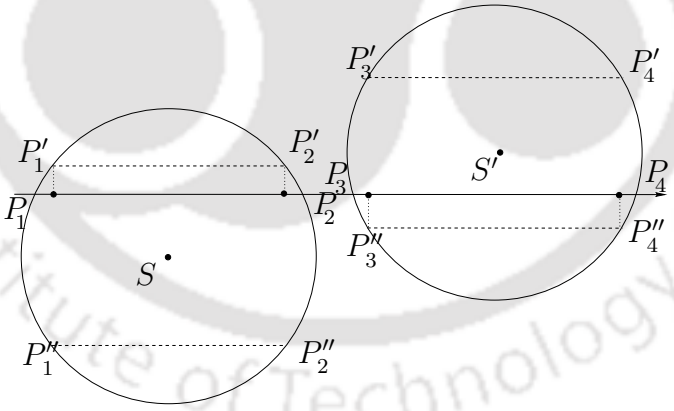

Figure 5.6: Anchors are at different sides of the line of movement

sides of S and S'. Let the equation of the actual line of movement which passes through both the circles be

$$y = \frac{d}{k} \text{ where } k \geq 1 \tag{5.2.8}$$

Let the chord length corresponding to the communication circles of the anchors S and S' be $2l$ and $2l'$ respectively. Sensor calculates equation of the line $P_1'P_2'$ and $P_1''P_2''$ as,

$$y = \frac{d}{k} + \frac{MaxE_P(2l)}{q_1} \text{ where } q_1 \geq 1 \text{ and} \tag{5.2.9}$$

$$y = 2b - \frac{d}{k} - \frac{MaxE_P(2l)}{q_1} \text{ where } q_1 \geq 1 \tag{5.2.10}$$

respectively. Similarly, sensor calculates equation of the line $P_3'P_4'$ and $P_3''P_4''$ as,

$$y = \frac{d}{k} - \frac{MaxE_P(2l')}{q_2} \text{ where } q_2 \geq 1 \text{ and} \tag{5.2.11}$$

$$y = 2d - \frac{d}{k} + \frac{MaxE_P(2l')}{q_2} \text{ where } q_2 \geq 1 \tag{5.2.12}$$

respectively. Now perpendicular distance between equation 5.2.9 and equation 5.2.11 is equal to $\left|\frac{MaxE_P(2l')}{q_2} + \frac{MaxE_P(2l)}{q_1}\right| \leq 2\max\left(\frac{MaxE_P(2l)}{q_1}, \frac{MaxE_P(2l')}{q_2}\right)$.
So, $D(9,11) = \frac{MaxE_P(2l)}{q_1} + \frac{MaxE_P(2l')}{q_2} \leq 2\max\left(\frac{MaxE_P(2l)}{q_1}, \frac{MaxE_P(2l')}{q_2}\right)$.
Let it be the smallest distance among those six possible distances. If we choose equation 5.2.9 or equation 5.2.11, we are choosing lines within $\max\left(\frac{MaxE_P(2l)}{q_1}, \frac{MaxE_P(2l')}{q_2}\right)$ error, since $D(8,9) = \frac{MaxE_P(2l)}{q_1}$ as well as $D(8,11) = \frac{MaxE_P(2l')}{q_2}$. Equation 5.2.9 and equation 5.2.11 make sure that there is at least one pair of lines whose perpendicular distance is less than or equal to $2\max\left(\frac{MaxE_P(2l)}{q_1}, \frac{MaxE_P(2l')}{q_2}\right)$.

Let $D(9,10)$ be least. We have to check $D(8,10)$ only.
$D(8,10) = 2\frac{d}{k} - 2b + \frac{MaxE_P(2l)}{q_1} \leq 2\frac{d}{k} - 2b + 2\frac{MaxE_P(2l)}{q_1} = D(9,10) < \frac{MaxE_P(2l)}{q_1} + \frac{MaxE_P(2l')}{q_2} = D(8,11)$, implies, $D(8,10) = 2\frac{d}{k} - 2b + \frac{MaxE_P(2l)}{q_1} \leq \frac{MaxE_P(2l')}{q_2}$.

Let $D(9,12)$ be least. We have to check $D(8,12)$ only.
$D(8,12) = 2\frac{d}{k} - 2d - \frac{MaxE_P(2l')}{q_2} \leq 2\frac{d}{k} - 2d + \frac{MaxE_P(2l)}{q_1} - \frac{MaxE_P(2l')}{q_2} = D(9,12) < \frac{MaxE_P(2l)}{q_1} + \frac{MaxE_P(2l')}{q_2} = D(9,11)$, implies, $D(8,12) = 2\frac{d}{k} - 2d - \frac{MaxE_P(2l')}{q_2} \leq \frac{MaxE_P(2l')}{q_2}$.

$D(10,11) = 2\frac{d}{k} - 2b + \frac{MaxE_P(2l)}{q_1} + \frac{MaxE_P(2l')}{q_2} > 2\frac{d}{k} - 2d + \frac{MaxE_P(2l)}{q_1} + \frac{MaxE_P(2l')}{q_2} = D(9,12)$, since $d > b$. So, it cannot be the least.

$D(10,12) = 2d - 2b + \frac{MaxE_P(2l)}{q_1} - \frac{MaxE_P(2l')}{q_2} \geq 2\epsilon$, since $d \geq (b+\epsilon)$. So it cannot be the least.

Let $D(11,12)$ be least. We have to check $D(9,12)$ only.
$D(9,12) = 2\frac{d}{k} - 2d + \frac{MaxE_P(2l')}{q_2} \leq 2\frac{d}{k} - 2d + 2\frac{MaxE_P(2l')}{q_2} = D(11,12) < D(9,11) = \frac{MaxE_P(2l)}{q_1} + \frac{MaxE_P(2l')}{q_2}$, implies, $D(8,12) = 2\frac{d}{k} - 2d + \frac{MaxE_P(2l')}{q_2} \leq \frac{MaxE_P(2l)}{q_1}$.

Hence in this case also, if $D(i,j)$ is the least and we choose any one of the 5.2.i-th or 5.2.j-th equation, that means we select a line of movement which is within
$\max\left(\frac{MaxE_P(2l)}{q_1}, \frac{MaxE_P(2l')}{q_2}\right)$ perpendicular error with the actual line of movement.

Without loss of generality, let 5.2.i-th equation is chosen. Now 5.2.i-th equation is generated from first(second) communication circle. Then according to Lemma 5.2.5, if sensor localizes itself corresponding to the last beacon received from the first(second) communication circle, then the error remains less than equal to ϵ. □

5.2.5 Error minimization

Sensor localizes itself using the above theorem within error bound ϵ. There is a possibility of reducing error by updating the line of movement whenever it passes through communication circle of some anchor as explained below. Suppose a sensor computed its approximate line of movement $y = mx + c$. Currently the sensor is passing through the communication circle of an anchor S'', where the actual line of movement is P_1P_2 and the approximate line of movement is $P_1'P_2'$ as shown in Fig. 5.7. Error can be reduced

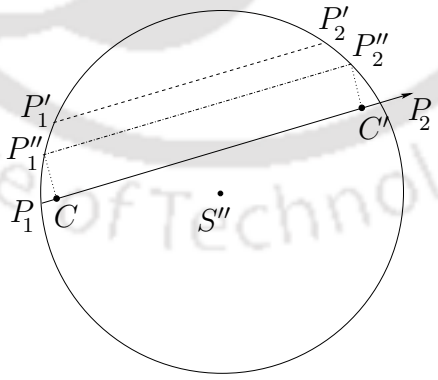

Figure 5.7: Sensor minimizes error by updating line of movement from $P_1'P_2'$ to $P_1''P_2''$

by finding a suitable approximate line of movement between $P_1'P_2'$ and P_1P_2. To do this,

the sensor approaches as follows: The sensor calculates length l (say) of $P_1'P_2'$ from the equations of the communication circle and the line $y = mx + c$. The sensor also calculates length L (say) of the chord along which it is moving using two beacon points C, C' corresponding to the anchor S''. If it finds $L > l$, error usually reduces by updating the approximate line of movement $P_1'P_2'$ to $y = mx + c'$, which is equation of the chord of length L, where $c' = \left[ma - b \pm \frac{\sqrt{(4r^2-l^2)(m^2+1)}}{2}\right]$ and (a, b) is the position of S''. Among these two lines $y = mx + c'$ (for different values of c'), which is closer to $P_1'P_2'$ is chosen as the new approximate line of movement. According to Fig. 5.7, $P_1''P_2''$ is the updated line. If the sensor finds $L \leq l$, no improvement in error is possible, hence it does not change the approximate line of movement.

5.2.6 Position calculation

When a mobile sensor finds four marked beacon points in its beacon list, it calculates the time difference in the time stamps of two beacon points corresponding to an anchor for calculating approximate chord length of the communication circle of the same anchor. It calculates two equations of possible lines according to the chord length. Similarly, it calculates two equations of possible lines for the second anchor. According to Theorem 5.2.6, finds the pair of lines with minimum distance between them. Our technique selects any one of those lines. Let the equation is generated from first(second) communication circle. Find the time stamp of the last beacon received by the sensor from first(second) anchor. Find the coordinate of the intersection point of the communication circle of the same anchor with the selected equation of line. Since it is moving along the same line until localization, using the current time in its clock find its current position. The sensor removes used beacon point entries from the beacon list. Once a sensor localizes itself, if it keeps track of its direction changes and corresponding time using the directional antenna, then it can calculate its position at any time instance.

5.2.7 Algorithm for localization without change of direction

The algorithm for localization without change of direction (LWCD) is presented below. Each mobile sensor localizes itself using the Algorithm 3 (LWCD). The expression of ϵ is

chosen for the algorithm depending on the presence of radio propagation irregularity as described in section 5.2.4.

Algorithm 3 LWCD

1: Mobile sensor begins localization process by moving with a uniform velocity until localization.
2: Maintains beacon list as described in section 5.2.2.
3: **if** there are four marked beacon points in beacon list such that the distance between the lines, which are passing through the anchors parallel to the direction of the sensor's movement is at least ϵ **then**
4: The sensor calculates the current position according to section 5.2.6.
5: **end if**

5.3 Localization without Change of Direction in Presence of Obstacles

In this section we localize mobile sensors in presence of obstacles. By obstacles, we mean anything which are blocking the beacons from reaching to the sensor. In this method, the perpendicular error remains same with LWCD, i.e., maximum perpendicular error on any calculated chord length $2l$ is $MaxE_P(2l)$. Beacons are obstructed by the obstacles as shown in Fig. 5.8. Here, the actual line of movement is P_1P_2, whereas $P_1'P_2'$ is the calculated chord length corresponding to the beacon points. In presence of obstacles, there are two possible cases which effect localization as mentioned below. In case 1, the sensor receives at least two beacons including the first and last beacons but the remaining beacons are blocked by the obstacles. Here the problem is, whenever beacons are blocked after receiving at least the first beacon c_1, sensor marks the beacon c_2 as the last beacon point for the communication circle as the waiting time t_0 (Ref. section 5.2.2) exceeds before receiving next beacon c_3. So last beacon point is selected wrongly. Hence the actual last beacon c_4 is received but is not marked as beacon point as shown in Fig. 5.8a. We can avoid this problem by increasing the waiting time t_0 of the sensor to t_{2r}, where t_{2r} is defined as the time required for a sensor to travel $2r$ distance. Since $2r$ is the length of the diameter of the communication circle, by setting the waiting time equal to t_{2r}, a sensor always detects the actual last beacon in case 1. So, according to Fig. 5.8a, now

sensor marks c_4 as the last beacon point instead of c_2. In case 2, either first or last or both beacons are blocked. Here sensor marks two beacons as the first and last beacons wrongly since it does not receive the actual first or(and) last beacon(s). It calculates wrong chord length accordingly. Case 2 is illustrated in Fig. 5.8b-5.8d.

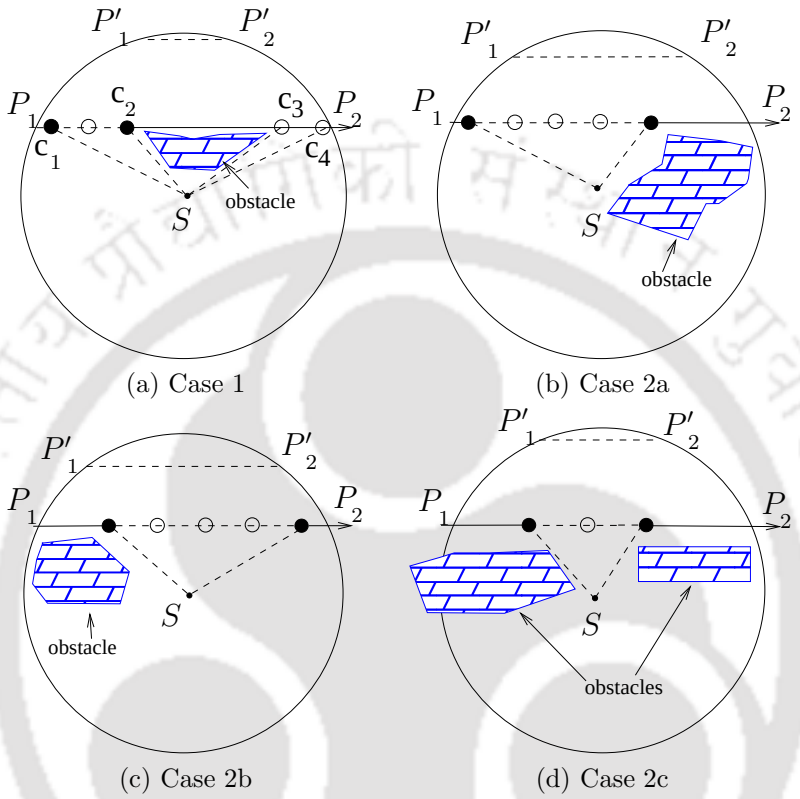

Figure 5.8: Wrong chord length ($P'_1P'_2$) estimation due to obstacles located at different positions

Our aim is to detect obstacles where it may cause larger localization errors. We localize sensors when we are sure that the perpendicular error lies within $MaxE_P(2l)$ for any calculated chord of length $2l$. We prove that for any calculated chord of length $2l$, sensor localizes itself within perpendicular error $MaxE_P(2l)$ on the same communication circle and detects obstacles in those cases where perpendicular error may become greater than $MaxE_P(2l)$. Fig. 5.8 shows the mobile sensor moves along the line P_1P_2 and enters in the communication circle of anchor S. Due to the obstacles in the figure, the sensor receives the first beacon or the last beacon or both, well inside the communication circle. The calculated chord length may be less than $2l - 2u$, where $2l$ is the length of the chord

P_1P_2, which creates an error greater than $MaxE_P(2l)$ according to the section 5.2.4. We prevent this by detecting obstacles by the following theorem.

Theorem 5.3.1. *A sensor either localizes itself within $MaxE_P(2l)$ perpendicular error on the communication circle where it calculates a chord of length $2l$ or detects presence of obstacles, if distance between lines which are passing through the anchors parallel to the actual line of movement is at least r.*

Proof. For simplicity, we prove it considering the line of movement is parallel to X-axis. Only two equations of lines among four calculated lines pass through both the communication circles. It is because sensor localizes itself only when it finds that the difference between the Y-coordinates of the anchors are at least equal to their radius.

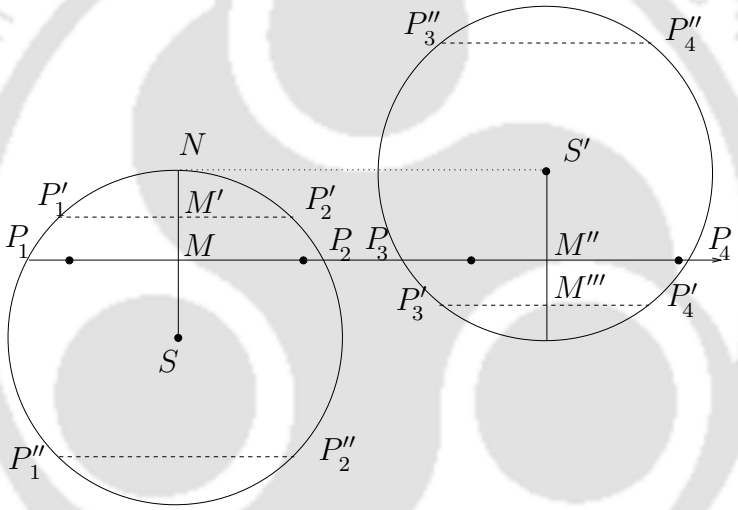

Figure 5.9: Showing communication circles for localization in presence of obstacles such that only two chords ($P'_1P'_2$ and $P'_3P'_4$) out of four calculated chords pass through both the circles

According to Fig. 5.9, let coordinates of two anchors, S and S', be (a, b) and (c, d) respectively where $a \geq 0$, $b \geq 0$, $c \geq 0$, $d > 0$ and $(d - b) \geq r$. Let P_1P_4 be the actual line of movement which passes through both the circles and equation of the line of movement be $y = \frac{d}{k}$, for some $k > 1$. Let $2l$ $(= P'_1P'_2)$ and $2l'$ $(= P'_3P'_4)$ be the calculated lengths of the chords P_1P_2 and P_3P_4 respectively. Without loss of generality, let $2l \geq 2l'$.

If there are no obstacles, then the equations of the calculated chords $P'_1P'_2$ and $P'_3P'_4$ which pass through both the communication circles are $y = \frac{d}{k} + \frac{MaxE_P(2l)}{q_1}, q_1 \geq 1$ and

$y = \frac{d}{k} - \frac{MaxE_P(2l')}{q_2}, q_2 \geq 1$ respectively. MM' and $M''M'''$ are the perpendicular errors corresponding to the chords of length $2l$ and $2l'$ respectively. Then the distance between those two calculated chords $MM' + M''M'''$ should be less or equal to $MaxE_P(2l) + MaxE_P(2l')$ when $q_1 = 1 = q_2$.

If $MM' + M''M''' > MaxE_P(2l) + MaxE_P(2l')$ then either $MM' > MaxE_P(2l)$ or $M''M''' > MaxE_P(2l')$. Without loss of generality let $MM' > MaxE_P(2l)$, which implies sensor failed to receive first and/or last beacon corresponding to the anchor S due to presence of obstacles. So it is possible to conclude presence of obstacles if $MM'+M''M''' > MaxE_P(2l) + MaxE_P(2l')$.

Otherwise, if $MM' + M''M''' \leq MaxE_P(2l) + MaxE_P(2l')$, sensor is not sure about presence of obstacles and localizes itself. Sensor chooses the line which lies exactly in between two calculated lines $P_1'P_2'$ and $P_3'P_4'$ on the circle where it calculated the chord of larger length $2l$. Now we show that the perpendicular error bound is $MaxE_P(2l)$ in this case.

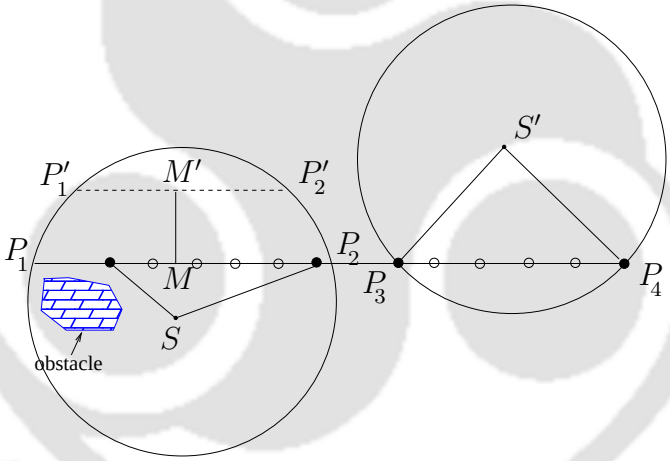

Figure 5.10: In presence of obstacle, error in the first communication circle may greater than $MaxE_P(2l)$ but using second communication circle, the resultant error becomes less than $MaxE_P(2l)$

Since $2l \geq 2l'$, so $MaxE_P(2l) \geq MaxE_P(2l')$. The worst case occurs when either $P_1'P_2'$ or $P_3'P_4'$ coincides with the original line of movement and distance $MM' = MaxE_P(2l) + MaxE_P(2l')$ due to presence of obstacles as shown in Fig. 5.10. Then perpendicular error becomes $\frac{MaxE_P(2l)+MaxE_P(2l')}{2}$. The maximum perpendicular error is $MaxE_P(2l)$ as $MaxE_P(2l) \geq MaxE_P(2l')$. So sensor localizes in such cases where obstacle affects

localization but the perpendicular error remains within its bound. □

In presence of obstacles, percentage of localization is an important factor along with localization error. For better localization percentage, we can relax the condition from $MM' + M''M''' \leq MaxE_P(2l) + MaxE_P(2l')$ to $MM' + M''M''' \leq 2(MaxE_P(2l) + MaxE_P(2l'))$ for doing localization. Then perpendicular error increases accordingly and perpendicular error bound becomes $2MaxE_P(2l)$. Section 5.4 shows average errors for both these cases.

5.3.1 Position calculation in presence of obstacles

Sensor calculates two lines which pass through both the communication circles using the calculated chord lengths $2l$, $2l'$, say, from the communication circles of the anchors as explained above. If distance between these two lines is less than equal to $MaxE_P(2l) + MaxE_P(2l')$, it chooses the line lies exactly in between of those two lines and on the communication circle on which it calculated the chord with greater length. Then it localizes itself using the elapsed time between the current time and time stamp of the last beacon received from that anchor. Otherwise sensor avoids localization detecting obstacles and looks for beacons from other anchors for localization.

5.3.2 Algorithm in presence of obstacles

The algorithm for localization without change of direction in presence of obstacles (LWCDPO) is given below. Each sensor localizes itself using the proposed Algorithm 4 (LWCDPO) in presence of obstacles.

Algorithm 4 LWCDPO

1: Mobile sensor does not change its direction of movement during localization.
2: Maintains beacon list as described in section 5.2.2 with waiting time t_{2r}.
3: **if** there are at least four marked beacon points in beacon list such that the distance between the lines, which are passing through the anchors parallel to the actual line of movement is at least r **then**
4: Sensor either detects obstacles or calculates the current position according to Theorem 5.3.1.
5: **end if**

5.4 Simulation Results

We use MATLAB platform to study the performances of our proposed schemes. Simulation is done under different communication range r varying from 10 to 50 meter and beacon distance varying from 1 to 5 meter. To be more practical, we consider irregular radio model for the simulation study. Through out the simulation, we take $\rho = 5$ for radio irregularity as discussed in section 5.2.4 if not otherwise mentioned.

5.4.1 Simulation for LWCD

Random straight lines are generated as the equation of actual lines of movement corresponding to two communication circles of distinct anchors, such that the distance between the lines passing through those two anchors with same direction as of the sensor is at least ϵ. Table 5.1 shows the average error with and without considering irregular radio model

Table 5.1: Showing values (in meter) of average error (AE), average error under radio irregularity (AERI) and maximum possible error under radio irregularity (MERI) for different communication range (CR) and beacon distance (BD)

BD→	**1**			**3**			**5**		
CR↓	AE	AERI	MERI	AE	AERI	MERI	AE	AERI	MERI
10	0.87	1.18	5.26	1.82	2.21	7.59	2.47	2.86	8.93
20	1.02	1.79	8.71	2.36	2.91	12.00	3.29	3.89	14.28
30	1.15	2.36	11.98	2.61	3.60	15.80	3.70	4.58	18.64
40	1.22	2.80	15.19	2.87	4.14	19.36	4.16	5.35	22.60
50	1.28	3.36	18.37	3.02	4.77	22.79	4.39	6.06	26.33

with respect to different communication ranges as well as beacon distances. The average error is very much less than the maximum possible error, which makes the algorithm very effective. It also shows that the average error under irregular radio model increases compared to the average error without radio irregularity. For each beacon distance (BD), there are three columns in Table 5.1 showing the values of average error (AE), average error under radio irregularity (AERI) and maximum possible error under radio irregularity (MERI) for different communication ranges (CR). All data are in meter. This table is also represented in Fig. 5.11. We show errors along Z-axis. For each communication range (along Y-axis) and beacon distance (along X-axis), AERI is greater than AE, whereas

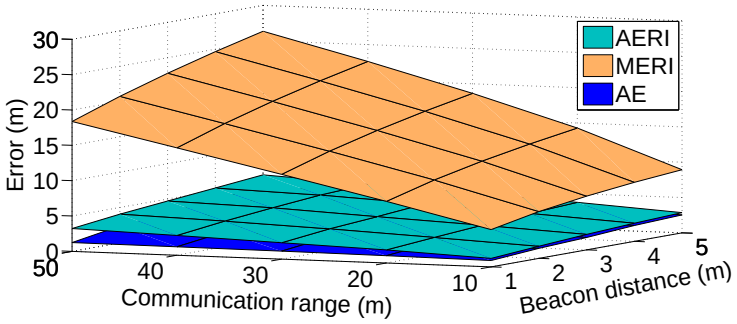

Figure 5.11: Errors varying communication range and beacon distance

Table 5.2: Showing values (in meter) of average error after passing through three more communication circles (AE3) and five more communication circles(AE5) under radio irregularity for different communication range (CR) and beacon distance (BD)

BD →	**1**		**2**		**3**		**4**		**5**	
CR↓	AE3	AE5	AE3	AE5	AE3	AE5	AE3	AE5	AE3	AE5
10	0.71	0.57	1.09	0.89	1.44	1.21	1.82	1.54	2.16	1.85
20	0.99	0.78	1.41	1.15	1.82	1.48	2.17	1.82	2.56	2.14
30	1.26	1.01	1.73	1.38	2.12	1.74	2.53	2.07	2.85	2.39
40	1.54	1.20	2.01	1.63	2.41	1.91	2.87	2.30	3.28	2.65
50	1.80	1.43	2.28	1.80	2.65	2.13	3.17	2.52	3.54	2.85

MERI is greater than AERI.

As discussed in the section 5.2.5, that sensor can minimize the localization error as it passes through the communication circles of other anchors. Following Table 5.2 shows the average error (AE3) as the mobile sensor passes through three more communication circles and the average error (AE5) as the mobile sensor passes through five more communication circles after localization. For each beacon distance, AE3 and AE5 are shown in two columns. Average error reduces to $0.07r$ and $0.057r$ respectively from $0.12r$ after sensor passes through three and five more communication circles. So error reduces around 40% and 55% after passing through three and five more communication circles respectively. In Fig. 5.12, surface plot of Table 5.2 shows that the average error (AE5) along Z-axis as the mobile sensor passes through five more communication circles is lesser than the average error (AE3) as the mobile sensor passes through three more communication circles for any communication range and beacon distance.

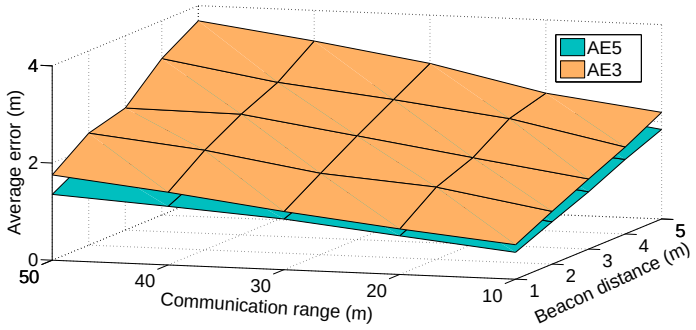

Figure 5.12: Average errors AE3 and AE5 after passing through three and five communication circles respectively

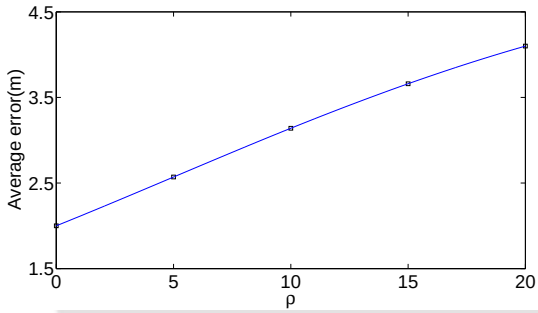

Figure 5.13: Average errors versus radio irregularity ρ

In Table 5.3, we compare our result with some of the existing mobile sensor localization algorithms WMCL-A [90], WMCL-B [90], MCL [33] and MCB [7]. Communication range is taken as 20 meter, beacon distance 2 meter and radio irregularity as discussed before. Among those, WMCL-A and WMCL-B give best results. These two are sequential monte carlo analysis based algorithms. Simulation results show around 75% improvement over WMCL-A of the positioning error as shown in Table 5.3.

Table 5.3: Average error (r) of our proposed algorithm compared with some existing algorithms, where r is the communication range of anchor

Algorithm	Proposed algorithm	WMCL-A	WMCL-B	MCB	MCL
Error(r)	0.1205	0.5034	0.5683	0.6628	0.7669

In Fig. 5.13, we show a two dimensional plot of average error versus ρ, where ρ is varying from 0 to 20. Here communication range and beacon distance are 20 meter and 2 meter respectively. Average error is varying from 2 meter to 4.1 meter according to the figure.

5.4.2 Simulation for LWCDPO

Simulation of LWCDPO are performed under different communication ranges and beacon distances with different level of obstacles varying from 20% to 50% considering irregular radio model. Here by 20% obstacle level, we mean, blockage of up to 20% beacons by the obstacles within a communication circle of an anchor. We generate random straight lines as the equation of actual line of movement corresponding to communication circles of two distinct anchors, such that the distance between the lines passing through those two anchors in the same direction of the actual line is at least equal to the communication range r. In Table 5.4 and Table 5.5, we show average localization error in presence of radio irregularity (AERI) and percentage of localization (%) for different communication ranges and beacon distances keeping the obstacle level at 0% (no obstacles) and 30% respectively. It shows that under this model we get better positioning accuracy and 100% localization if there are no obstacles. If percentage of localization is ℓ, that indicates $(100 - \ell)$ percent of cases sensor detects obstacles. Results of Table 5.4 and Table 5.5 reflect the cases where sensor localizes if distance between the calculated lines passing through both the circles are less than or equal to $MaxE_P(2l) + MaxE_P(2l')$ according to section 5.3. In Table 5.5, for fixed communication range r, localization percentage increases with increasing beacon distance since $MaxE_P(2l) + MaxE_P(2l')$ also increases at the same time. In Fig. 5.15 we show that percentage of obstacle detection increases as obstacle level increases for different obstacle levels varying from 20% to 50%. For the same, the localization percentage is shown in Fig. 5.14. In this figure percentage of

Table 5.4: Showing values (in meter) of average error in presence of radio irregularity (AERI) and localization percentage (%) under irregular radio range for different communication range (CR) and beacon distance (BD) in absence of obstacle

BD →	**1**		**2**		**3**		**4**		**5**	
CR↓	AERI	%	AERI	%	AERI	%	AERI	%	AERI	%
10	0.74	100	1.05	100	1.37	100	1.60	100	1.83	100
20	1.10	100	1.49	100	1.86	100	2.10	100	2.42	100
30	1.43	100	1.83	100	2.20	100	2.52	100	2.89	100
40	1.73	100	2.18	100	2.61	100	2.97	100	3.27	100
50	2.04	100	2.55	100	2.95	100	3.32	100	3.73	100

Table 5.5: Showing values (in meter) of average error in presence of radio irregularity (AERI) and localization percentage (%) under irregular radio range for different communication range (CR) and beacon distance (BD) with 30% obstacle level when perpendicular error bound is $MaxE_P(2l)$ for calculated chord of length $2l$

BD →	**1**		**2**		**3**		**4**		**5**	
CR↓	AERI	%	AERI	%	AERI	%	AERI	%	AERI	%
10	0.87	34.43	1.24	53.48	1.60	64.25	1.86	72.60	2.18	79.49
20	1.26	23.83	1.72	35.25	2.13	45.73	2.49	51.75	2.84	59.88
30	1.68	19.59	2.15	27.57	2.56	34.94	3.03	41.85	3.38	47.85
40	2.00	17.40	2.49	23.16	3.01	29.57	3.45	35.67	3.83	39.38
50	2.42	15.88	2.88	21.79	3.39	26.68	3.81	30.50	4.35	34.93

Table 5.6: Showing values (in meter) of average error in presence of radio irregularity (AERI) and localization percentage (%) under irregular radio range for different communication range (CR) and beacon distance (BD) with 30% obstacle level perpendicular error bound is $2MaxE_P(2l)$ for calculated chord of length $2l$

BD →	**1**		**2**		**3**		**4**		**5**	
CR↓	AERI	%	AERI	%	AERI	%	AERI	%	AERI	%
10	1.23	65.25	1.70	84.85	2.04	91.93	2.30	95.68	2.53	97.34
20	1.84	47.83	2.46	64.99	2.96	76.31	3.40	84.74	3.75	89.23
30	2.42	42.44	3.12	55.23	3.67	64.87	4.22	73.65	4.66	79.82
40	3.06	37.24	3.68	48.49	4.31	58.04	4.91	65.57	5.45	72.74
50	3.61	34.66	4.33	43.55	4.97	51.70	5.54	60.09	6.17	65.25

localization decreases as obstacle level increases.

In Fig. 5.16, we show a graph of average error versus beacon distance and communication range for 30% obstacle level. In all these three figures, beacon distance and communication range is along X-axis and Y-axis respectively. Table 5.6 shows better localization percentage but larger average error where sensor localizes itself if distance between the calculated lines passing through both the circles are less than or equal to $2(MaxE_P(2l) + MaxE_P(2l'))$ according to section 5.3.

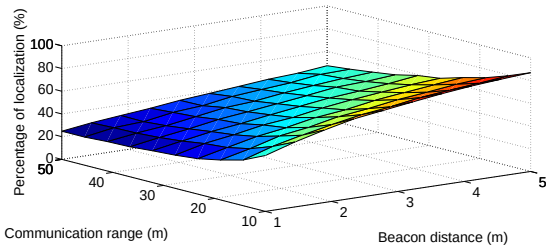

(a) 20% obstacle level

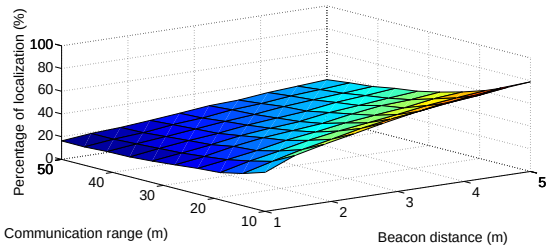

(b) 30% obstacle level

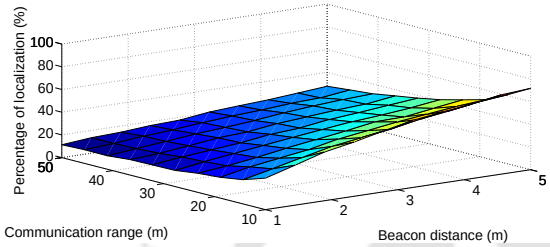

(c) 40% obstacle level

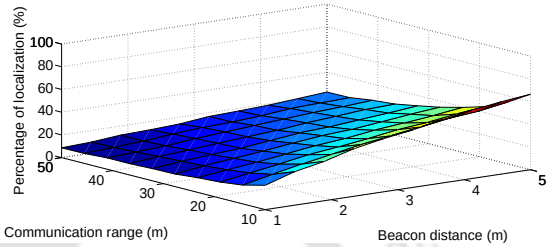

(d) 50% obstacle level

Figure 5.14: Percentage of localization decreases as obstacle level increases

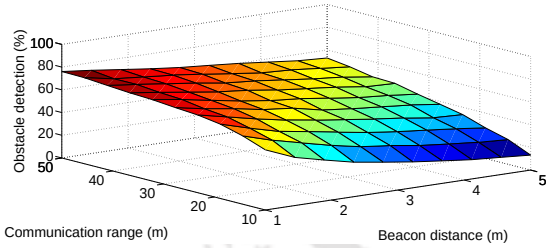

(a) 20% obstacle level

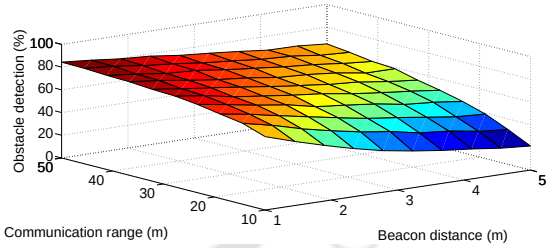

(b) 30% obstacle level

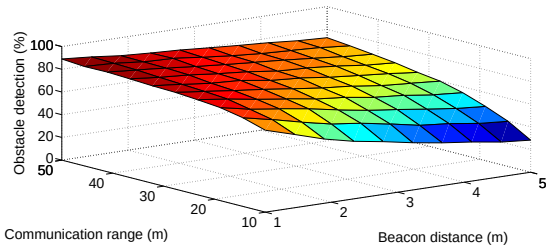

(c) 40% obstacle level

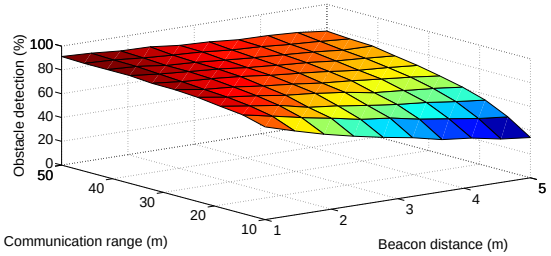

(d) 50% obstacle level

Figure 5.15: Obstacle detection increases as obstacle level increases

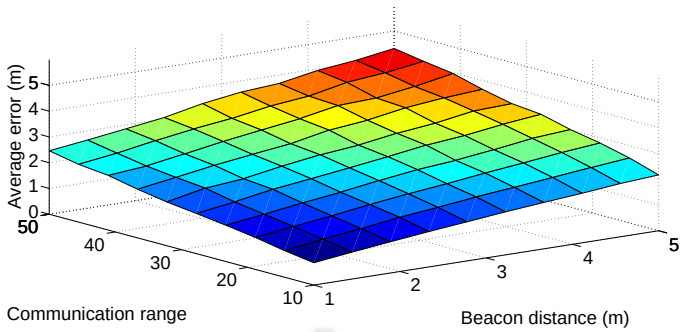

Figure 5.16: Average error increases with communication range and beacon distance

5.5 Conclusion

In this work we have proposed three deterministic range-free localization algorithms for mobile sensors with static anchors. We have given a bound on error for localization. Our algorithm LWCD is able to localize mobile sensor within any predetermined error bound by fixing appropriate beacon distance. To use LWCD, sensor needs to move in a straight line during localization. Simulation results show improvement over the existing approaches in terms of positional accuracy. Using our technique, a mobile sensor can further reduces localization error whenever it passes through the communication circle of different anchors by repeated calculations of the approximate line of movement. Sensor localizes itself using LWCDPO in presence of obstacles. Simulation results show good positioning accuracy for different levels of obstacle.

Chapter 6

Mobile Sensor Localization in Presence of Obstacles

6.1 Introduction

In the previous chapter, localization of mobile sensors is done assuming sensors do not change direction during localization. Practically, sensors may need to change direction within a communication circle depending on the requirements of the underlying applications. In this chapter we allow change of direction of mobile sensors during localization and propose the algorithm LCD. LCD localizes a sensor within the communication circle of one static anchor based on polygonal structures generated by direction changes of mobile sensor. Then we consider the problem where obstacles may present anywhere in the network and propose another algorithm LPO to localize sensors.

6.1.1 Our contribution

The algorithm LCD localizes mobile sensors which change direction during localization. Simulation results show 67% and 63% improvement of the positioning error over the existing algorithm [90] corresponding to two different selection criteria. We propose another algorithm LPO which localizes sensors in presence of obstacles with change of direction. It achieves 52% and 49% improvements corresponding to two different selection criteria in terms of localization accuracy compared to existing works.

In section 6.2, the localization algorithm LCD is proposed. We propose LPO in section 6.3. Simulation results of our algorithms are presented in section 6.4 along with performance comparison. Finally we conclude in section 6.5.

6.2 Localization with Change of Direction

Mobile sensors may change direction during localization. We start with one direction change of a mobile sensor within a communication circle. It enters the communication circle of anchor S along the line P_1P_2 as shown in Fig. 6.1. Mobile sensor marks the first and last received beacon as beacon points within the communication circle. It marks C as the first beacon point. The sensor changes it direction at P_2 and exits from the communication circle along the line P_2P_3. It records the time of changing direction at P_2 according to it's own clock. We denote the time of changing direction at some point according to sensor's clock as the time stamp of direction change at that point. Then it marks C' as the last beacon point. Beacon points are marked according to the definition given in chapter 5. Using compass, sensor knows the gradients of CP_2, P_2C' and hence

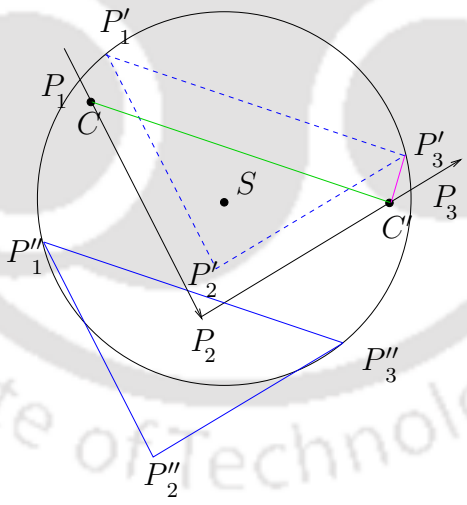

Figure 6.1: Sensor changes direction of movement once at P_2 within the communication circle of anchor S

can calculate the $\angle P_1P_2P_3$. It computes the length $\mathcal{L}$ of CC', which is the third side of

the $\triangle CP_2C'$ using the following formula.

$$(CC')^2 = (CP_2)^2 + (P_2C')^2 - 2(CP_2)(P_2C')\cos\angle CP_2C' \tag{6.2.1}$$

Now the sensor knows all three sides of the triangle and hence finds the $\angle P_2CC'$ and gradient $\mathcal{M}$ of CC'. It finds two possible chords $P_1'P_3'$ and $P_1''P_3''$ of the communication circle of S with length $\mathcal{L}$ and gradient $\mathcal{M}$ as shown in Fig. 6.1. Both P_1', P_1'' are the possible positions of C. Sensor draws line segments $P_1'P_2'$, $P_1''P_2''$ from P_1', P_1'' respectively with length and gradient equal to the length and gradient of CP_2. The points P_2' and P_2'' are the possible positions of P_2. It accepts $P_1'P_3'$ or $P_1''P_3''$ depending on whether P_2' or P_2'' lies within the communication circle respectively. The sensor accepts $P_1'P_3'$ as the correct chord as P_2' is inside the communication circle as shown in Fig. 6.1. Here P_3' is considered as the position of the sensor at that time when it marked C' as a beacon point. So error in positioning is equal to the Euclidian distance $C'P_3'$ between C' and P_3'. So for localization, three recorded time stamps are needed including two beacon points. If both P_2' and P_2'' lies inside or outside the communication circle, then this technique is unable to localize the sensor with those information.

We generalize this technique when the sensor changes it's direction several times within a communication circle of an anchor. As shown in Fig. 6.2, sensor changes it's direction thrice at P_2, P_3, P_4 while moving within the communication circle of S. Sensor records time stamps at P_2, P_3 and P_4 to calculate the lengths CP_2, P_2P_3, P_3P_4 and P_4C'. The sensor finds length and gradient of CP_3 from $\triangle CP_2P_3$. Similarly, from $\triangle CP_3P_4$, sensor finds length and gradient of CP_4. Finally, from $\triangle CP_4C'$, sensor finds length $\mathcal{L}$ and gradient $\mathcal{M}$ of CC'. Sensor computes chords $P_1'P_5'$ and $P_1''P_5''$ with length $\mathcal{L}$ and gradient $\mathcal{M}$. Sensor computes P_2', P_3', P_4' and P_2'', P_3'', P_4'' starting from both P_1' and P_1'' as possible positions of P_2, P_3, P_4.

Based on the possible positions P_i' or P_i'' of P_i for $i = 2, 3, 4$, we propose following two selection criteria to find approximate location of the mobile sensor.

Selection criterion 1: Sensor selects the chord corresponding to which all the points P_i' or P_i'', $i = 2, 3, 4$, but not both, lie within the communication circle.

Selection criterion 2: Sensor selects the chord corresponding to which more of the

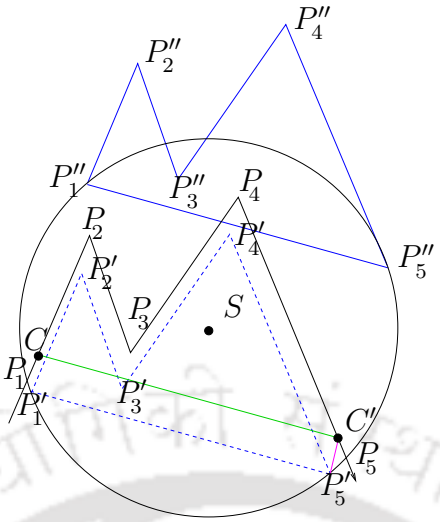

Figure 6.2: Sensor changes direction of movement thrice at P_2, P_3 and P_4 within the communication circle of anchor S

points among P'_i and P''_i, $i = 2, 3, 4$, lie within the communication circle.

Sensor uses either *selection criterion 1* or *selection criterion 2* for localization. If number of points lying inside the communication circle become equal for both the chords, then localization is not possible using any of the given criteria. In this circumstances, sensor avoids localization with the anchor S and looks for beacons from another anchor. According to Fig. 6.2, $P'_1P'_5$ is the chord selected using *selection criterion 1*. Hence it calculates P'_5 as it was the approximate location when it received the last beacon C' and P'_5C' is the localization error.

If sensor moves in curved shaped trajectories instead of straight lines, then also LCD can localize the sensor if it is possible to compute the trajectories based on the two possible approximate chords. *Selection criterion 1* is applicable if all points of exactly one of the two approximate trajectories lies within the communication circle. As vertex is not defined over curves, *selection criterion 2* can be modified such that it selects the trajectory, larger portion of which lies within the communication circle.

6.2.1 Algorithm for localization with change of direction

We propose a technique to localize mobile sensor when it changes it's direction randomly while moving. To do so, mobile sensor needs to enter and exit communication circle of

an anchor. Hence it marks two beacon points. But in addition to those two beacon points, sensor also records time stamps whenever it changes direction of movement within the communication circle. Like LWCD, sensor uses elapsed time and known direction of movement of itself from the last marked beacon point and localizes itself starting from the calculated position. We proposed the Algorithm 5 for localization with change of direction (LCD).

Algorithm 5 LCD

Mobile sensor records time stamp whenever it changes direction, say, N-times.
Maintains beacon list as described in section 5.2.2 and starts localization whenever two beacon points appears in the list from a particular anchor.
Computes approximate chord length and two possible chords as described in section 6.2.
Computes two possible sets of N points where the sensor changed directions with respect to those two chords as described in section 6.2.
Computes number of points, say n_1 and n_2, which lie within the communication circle from both sets.
if $n_1 \neq n_2$ **then**
  if sensor uses *selection criterion 1* **then**
    if $n_1 = N$ or $n_2 = N$ **then**
      Selects corresponding chord and computes the current position.
    end if
    if $n_1 \neq N$ and $n_2 \neq N$ **then**
      Sensor can not localize and looks for beacons from different anchors.
    end if
  end if
  if sensor uses *selection criterion 2* **then**
    Selects corresponding chord with more number of points inside the communication circle and computes the current position.
  end if
end if
if $n_1 = n_2$ **then**
  Sensor avoids localization with this anchor and looks for beacons from different anchor.
end if

LCD works in absence of obstacles. In the following section we propose an algorithm LPO which localizes sensors in presence of obstacles.

6.3 Localization in Presence of Obstacles

Obstacles may present anywhere in the network, which may block movement of mobile sensor as well as beacons from reaching to the sensor. If movement of the mobile sensor is obstructed by some obstacles, then sensor has to change its direction to continue movement. Here LWCD is not applicable but we can apply LCD unless beacons are blocked by the obstacles. The explanation is given in the following section.

6.3.1 Problems due to Obstacles

Problems due to obstacles are explained with examples shown in Fig. 6.3 and Fig. 6.4. According to Fig. 6.3, sensor enters in the communication circle of the anchor S along the line P_1P_2. Then it changes its direction at P_2 and moves along P_2P_3. As its path is obstructed by some obstacle (obs 1), it changes direction at P_3 and then again at P_4 (due to obstacle obs 2). After that the sensor leaves the communication circle of the anchor S along P_4P_5. Sensor marks C, C' as beacon points according to the definition given in chapter 5. Hence it is possible to localize the sensor using LCD since path

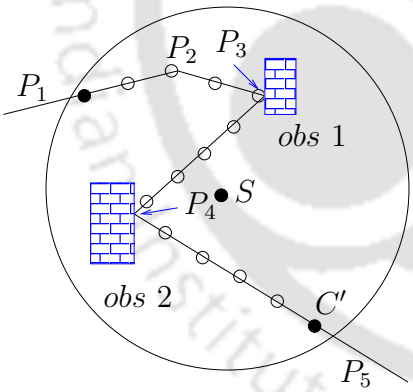

Figure 6.3: Direction changes due to obstruction

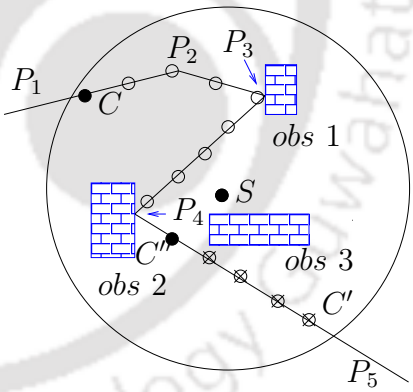

Figure 6.4: Wrong beacon point marking due to obstacle

of the mobile sensor is obstructed but no beacons are blocked by the obstacles. Now consider another obstacle (obs 3) as shown in Fig. 6.4. Due to this obstacle, sensor does not receive any beacon from S after receiving the beacon at C''. Those positions are indicated by circle with a cross in it as shown in Fig. 6.4. For the remaining part of this chapter, crossed circles are used in this purpose. Hence sensor marks the beacon received

at C'' as a beacon point instead of C'. Consequently sensor computes inappropriate chord length, which incurs larger localization error. So, in presence of obstacles, beacon points are marked using the definition given in chapter 5 may not be appropriate. Thus we introduce below a new system model for localization in presence of obstacle and propose a technique to select appropriate beacon points for reducing localization error.

6.3.2 System model in presence of obstacle

Static anchors are deployed sparsely in a two dimensional plane. Mobile sensors have equal communication range r. Anchors are identified by their locations and periodically broadcast beacons with their locations. The time interval between two consecutive broadcasts of beacons is t, which is fixed and same for all anchors. The beacon distance is denoted by u and is equal to the distance which a sensor can travel in time t during its movement. In this model activities of the static anchors and mobile sensors are as follows.

Anchor: Broadcasts beacons with two different signal strengths alternatively, such that one beacon reaches up to r distance (denoted by (r)) and other beacon reaches up to $r + u$ distance (denoted by $(r + u)$). That is, if anchor broadcasts first beacon which reaches up to r distance, then second beacon reaches up to $r + u$ distance, again third beacon reaches up to r distance and so on.

Mobile sensor: Performs *move-wait-move* movement during localization, i.e., sensor moves u distance with fixed velocity v, waits there for a time t, then moves another u distance, again waits for a time t, then moves u distance and so on.

Sensor detects obstacles as well as appropriate beacon points with the *move-wait-move* movement based on received beacons from the anchor. The logic behind introducing two different signal strengths is, if a sensor receives beacons $(r + u)$ and (r) at some position while waiting, then it must receive at least $(r + u)$ at the next position if there is no obstacle, since the next position is at a distance u from the previous one. How sensor marks beacon points are discussed below.

6.3.3 Beacon point selection in presence of obstacles

There are three possible states of a sensor based on receiving beacons by the sensor at any point. We define those states as $< 2, S >$, $< 1, S >$ and $< 0 >$, where receiving both beacons $(r + u)$ and (r) at a point from anchor S is denoted by $< 2, S >$, receiving only $(r + u)$ at a point is denoted by $< 1, S >$ and not receiving any beacon at a point is denoted by $< 0 >$. From now onwards, we write $< 2 >$, $< 1 >$ instead of $< 2, S >$, $< 1, S >$ respectively assuming beacons are received from same anchor. By $< 2 >$, $< 1 >$ and $< 0 >$, we also denote the corresponding points of receiving the beacons and achieving corresponding states. A sensor executes *move-wait-move* movement during localization and may need to change its state. It is possible to make some decisions whenever sensor achieves different states at two consecutive positions. Different decisions are explained below.

- If a sensor achieves state $< 2 >$ after achieving state $< 1 >$ at the previous point, then $< 2 >$ is marked as beacon point. Following example clarify this. A sensor is moving along P_1P_4 as shown in Fig. 6.5, where S is the anchor, radius of larger dotted circle is $r + u$ and radius of smaller solid circle is r with respect to two different signal strengths of S. At P_1, sensor updates its state $< 1 >$ after waiting t time. It is possible only when the sensor lies within the circular lamina formed by two circles. At the next point C, it updates its state $< 2 >$ after waiting t time, which implies it is within the circle of radius r now. Hence the beacon received at C is marked as a *beacon point*.

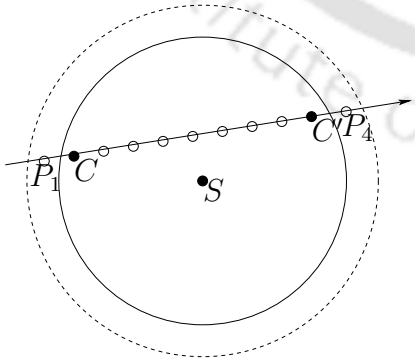

Figure 6.5: Beacon point marking

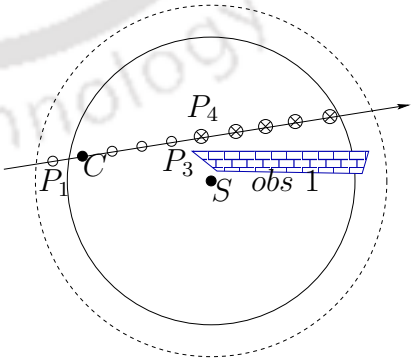

Figure 6.6: Obstacle detection

- If a sensor achieves state $< 1 >$ after achieving state $< 2 >$ at the previous point, then $< 2 >$ is marked as *beacon point*. According to Fig. 6.5, at C', sensor receives $< 2 >$, but it receives $< 1 >$ at P_4. P_4 must be in the circular lamina otherwise sensor should have received $< 2 >$ also at P_4, since presence of obstacle between S and P_4 is ruled out as sensor receives $< 1 >$. Hence sensor marks the beacon received at C' as a *beacon point*.

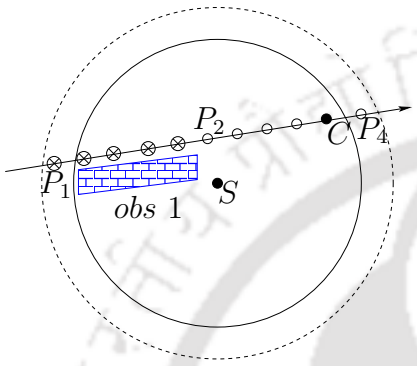

Figure 6.7: Obstacle detection

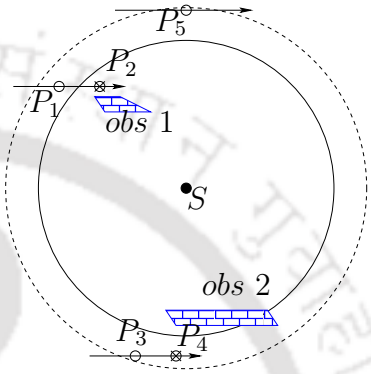

Figure 6.8: Obstacle detection

- If a sensor achieves state $< 0 >$ after achieving state $< 2 >$ at the previous point, obstacles are detected. As shown in Fig. 6.6, there is an obstacle within the communication circle, which obstructs receiving beacon at P_4. The sensor moving along P_1P_3 achieves state $< 2 >$ by receiving beacons $(r+u)$ and (r) at P_3 but it does not receive any beacon at the next point P_4 of its movement. Hence the sensor detects presence of an obstacle in between the sensor and the anchor along that path.

- If a sensor achieves $< 2 >$ after receiving $< 0 >$ at the previous point, obstacles are detected. According to Fig. 6.7, the sensor moving along P_1P_2 updates its state $< 2 >$ by receiving beacons $(r+u)$ and (r) at P_2 and it did not receive any beacon before P_2. The sensor realizes presence of obstacles since otherwise at least it should have achieved state $< 1 >$ when it passed through the circular lamina at some point P_1.

- If a sensor achieves $< 0 >$ after achieving $< 1 >$ at the previous point, obstacles are detected. According to Fig. 6.8 the sensor moving along P_1P_2 and receives $(r+u)$ at P_1 and it does not receive any beacon at the next point P_2. The sensor detects

presence of obstacle. Similar observation is also occur when a sensor moves along P_3P_4 in the same figure. It may also be the case that the sensor is going out of the larger circle after receiving beacon only at P_5 as shown in Fig. 6.8.

- Sensor achieves $< 1 >$ after achieving $< 0 >$ implies sensor is in the circular lamina. This happens at P_1 in Fig. 6.5.

From above discussion we can say, sensor makes some decisions if it achieves different states at two consecutive points. According to those decisions, sensor takes some actions such that it can mark correct beacon points in presence of obstacles. Those decisions and actions are shown in Table 6.1 where $< a > \rightarrow < b >$ implies a sensor changes state to $< b >$ from $< a >$ at two consecutive positions. However, a sensor can change its direction of movement if it achieves same state in two consecutive points. But like LCD, it has to record time stamp whenever it changes direction.

Table 6.1: Decisions and actions taken by sensor after receiving two consecutive beacons with different states to select correct beacon points in presence of obstacles

Case	Decision	Action
$< 2 > \rightarrow < 1 >$	$< 2 >$ is a beacon point	Sensor returns to previous position, marks $< 2 >$ as a beacon point and changes direction if needed
$< 2 > \rightarrow < 0 >$	Obstacle is detected	Sensor returns to previous position then changes direction and records time stamp simultaneously
$< 1 > \rightarrow < 2 >$	$< 2 >$ is a beacon point	Sensor marks $< 2 >$ as a beacon point and continues movement along same direction
$< 1 > \rightarrow < 0 >$	Obstacle is detected or sensor is passing through the larger circle only	Sensor returns to previous position then changes direction and records time stamp simultaneously
$< 0 > \rightarrow < 1 >$	Sensor is in the circular lamina	Sensor continues movement along same direction
$< 0 > \rightarrow < 2 >$	Obstacle is detected	Sensor continues movement along same direction

To localize a sensor, when it changes direction during the process, according to section 6.2, at least formation of a triangular structure is needed whose one side is a possible chord of the communication circle. So it needs two beacon points with at least one direction change. That is, time stamps of at least three events are needed including two beacon points. Now, if sensor receives two consecutive beacon points without any direction change in between, it needs another point within the circle to formulate a triangle. So it changes direction from the last beacon point in search of another time stamp of either a direction change or of a beacon point, whichever comes earlier. From Table 6.1, one can see, when a sensor achieves $< 0 >$ at some point, it always returns to previous point and change it's direction. Also when it achieves $< 1 >$ at some point P_1 after achieving $< 2 >$ at the previous point P_2, it marks the beacon atP_2 as a beacon point and if it requires time stamps of more events, it returns back to P_2 and changes direction to stay within the communication circle. This confirms that a sensor always marks time stamps of at least three events including two beacon points.

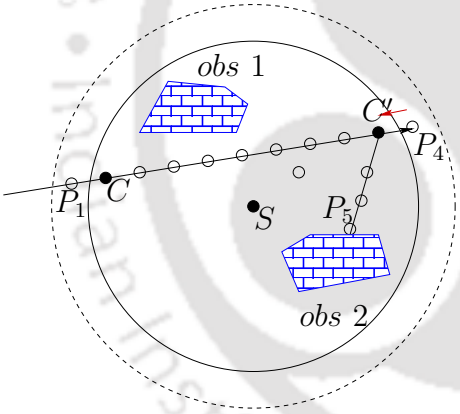

Figure 6.9: Sensor marks consecutive beacon points

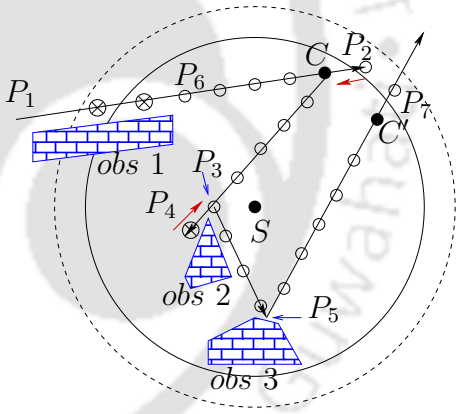

Figure 6.10: Direction changes in between beacon points

Now we show by example how this beacon point selection method works in presence of obstacle. Let sensor achieves $< 1 >$, $< 2 >$ at P_1, C respectively as shown in Fig. 6.9. Sensor marks the beacon received at C as a beacon point and continue it's movement. Then it achieves $< 2 >$, $< 1 >$ at C', P_4 respectively, returns to C', marks the beacon received at C' as a beacon point and changes it's direction in the search of time stamp of another event. As it already has two beacon points, localization can be done if it changes

direction or receives another beacon point, whichever is earlier. According to Fig. 6.9, sensor changes direction at P_5 due to obstacle (obs 2). It records the time stamp at P_5. Now sensor can compute length CC', $C'P_5$ and $\angle CC'P_5$. So it can form a triangle by finding CP_5 to localize itself as explained in section 6.2.

Consider another case where sensor does not receive two beacon points without any direction change in between. Sensor received $< 2 >$ first at P_6 as shown in Fig. 6.10. Then it achieves $< 2 >$, $< 1 >$ at C, P_2 respectively, returns to C, marks the beacon received at C as a beacon point and changes it's direction. Then sensor achieves $< 2 >$, $< 0 >$ at P_3, P_4 respectively. So it detects obstacle (obs 2), returns back to P_3, records the time stamp and changes it's direction. Then sensor changes direction at P_5 after obstructed by obstacle (obs 3). It records the time stamp at P_5. Then it achieves $< 2 >$, $< 1 >$ at C', P_7 respectively. It marks the beacon received C' as another beacon point and finds four time stamps along with two beacon points. Sensor has to calculate lengths of the line segments for localization. In this model, while calculating distance from those recorded time stamps of beacon points and points of direction changes, sensor has to take care of *move-wait-move* movement as well as the event of returning back from some point to the previous position. Let sensor wants to compute distances between two points P_1, P_2 with recorded time stamps t_1, t_2 respectively. Let v be the velocity of the mobile sensor. The distance calculation is as follows. If movement path was obstructed at P_2, then length of P_1P_2 is equal to $\frac{(t_2-t_1)v}{2}$. If sensor returns to P_2, then length of P_1P_2 is equal to $\frac{(t_2-t_1-3)v}{2}$.

6.3.4 Algorithm for localization with change of direction in presence of obstacle

Here we adopt the Algorithm 5 along with beacon point selection technique from section 6.3.3 to localize sensors in presence of obstacles. Like earlier algorithms LWCD and LCD, sensor uses elapsed time and known direction of movement from the last marked beacon point and localizes itself starting from the calculated position. We present the Algorithm 6 for localization with change of direction in presence of obstacle (LPO).

Algorithm 6 LPO

1: Sensor marks beacon points, records time stamps of direction changes and computes lengths of line segments according to section 6.3.3.
2: Computes two possible chords as described in section 6.2.
3: Computes two possible sets of N (say), points where the sensor changed directions excluding two beacon points with respect to those two chords as described in section 6.2.
4: Use *selection criterion 1* or *selection criterion 2* according to the Algorithm 5 for localization.

6.4 Simulation Results

We use MATLAB platform to study the performances of our proposed schemes. We simulate it under different communication range r varying from 10 to 50 meter and beacon distance varying from 1 to 5 meter. To be more practical, we use irregular radio model for the simulation study. Through out the simulation, we consider $\rho = 5$ for radio irregularity as discussed in section 5.2.4, if not mentioned otherwise. Values of average errors are given in meters.

6.4.1 Simulation for LCD

We place an anchor at the origin $(0, 0)$ on a two dimensional plane and simulate random movements of a sensor within the communication circle of the anchor. Mobile sensor changes its direction randomly up to 5 times. We calculate localization error for each random movement of a sensor considering radio irregularity. Then average localization error for 10000 such random movements of the sensor are calculated for each communication range and beacon distance as shown in Table 6.2 and Table 6.3 according to Algorithm 5.

For *selection criterion 1*, Table 6.2 shows average error (AE_{sc1}) in presence of radio irregularity and percentage of localization (LP_{sc1}) of Algorithm 5. The percentage of localization decreases and average error increases with respect to increasing beacon distance for fixed communication range. These happens because of greater beacon distances, usually sensor calculates lesser chord length than the actual chord length. As a result approximate chord moves further from the actual chord and consequently few points of both the calculated trajectories, where sensor changed direction, go out of the communication circle. Hence 100% localization is not possible. Table 6.3 shows a much better percentage of localization (LP_{sc2}) for *selection criterion 2*, since it does not require

Table 6.2: Average error in presence of radio irregularity and percentage of localization using *selection criterion 1* of LCD

BD →	**1**		**2**		**3**		**4**		**5**	
CR↓	LP_{sc1}	AE_{sc1}	LP_{sc1}	AE_{sc1}	LP_{sc1}	AE_{sc1}	LP_{sc1}	AE_{sc1}	LP_{sc1}	AE_{sc1}
10	72.66	1.60	65.32	2.37	60.04	3.15	54.10	3.76	48.83	4.45
20	75.42	2.32	72.16	3.23	67.77	4.04	62.70	4.91	59.86	5.60
30	76.43	3.04	73.21	3.95	69.86	4.79	67.50	5.70	64.55	6.56
40	76.63	3.67	74.09	4.71	71.98	5.59	69.32	6.46	67.60	7.39
50	76.57	4.52	74.49	5.48	71.86	6.50	70.57	7.42	70.27	8.21

Table 6.3: Average error in presence of radio irregularity and percentage of localization using *selection criterion 2* of LCD

BD →	**1**		**2**		**3**		**4**		**5**	
CR↓	LP_{sc2}	AE_{sc2}	LP_{sc2}	AE_{sc2}	LP_{sc2}	AE_{sc2}	LP_{sc2}	AE_{sc2}	LP_{sc2}	AE_{sc2}
10	86.59	1.81	86.23	2.71	85.63	3.49	84.67	4.23	84.12	4.80
20	86.95	2.63	86.89	3.69	86.42	4.61	85.97	5.62	85.15	6.33
30	86.31	3.41	86.09	4.49	85.65	5.51	86.18	6.44	86.11	7.46
40	86.60	4.21	86.75	5.40	86.76	6.44	86.44	7.44	85.68	8.35
50	85.66	4.99	86.17	6.10	86.58	7.21	86.00	8.39	86.33	9.23

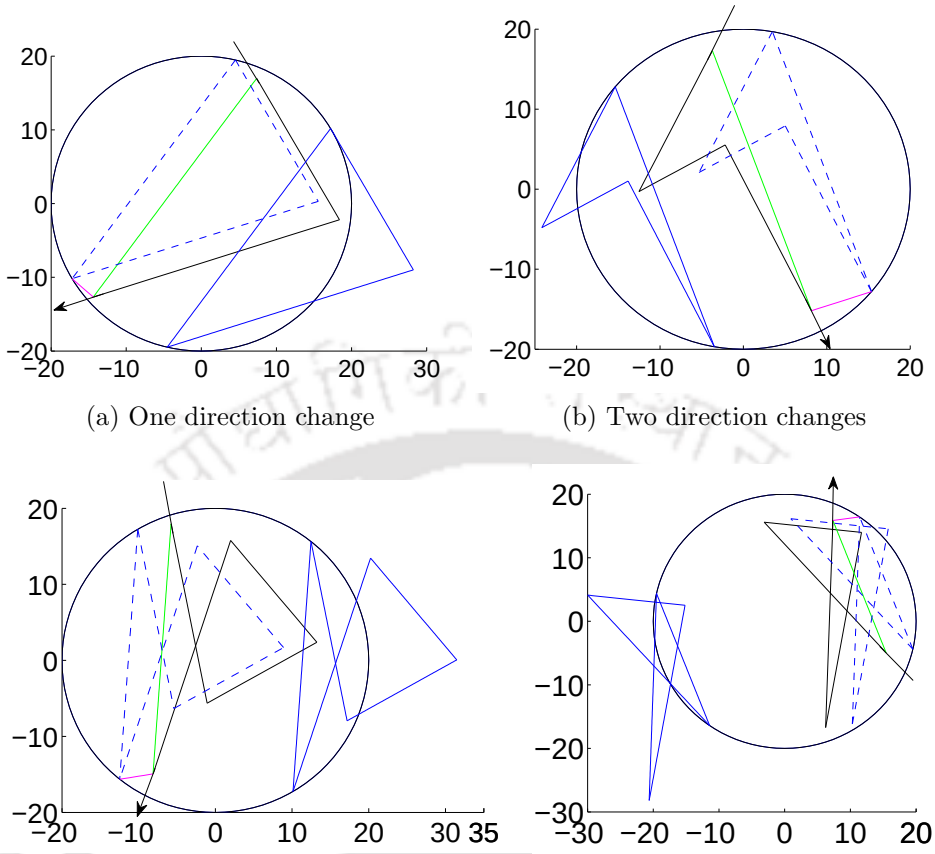

(a) One direction change (b) Two direction changes

(c) Three direction changes (d) Three direction changes

Figure 6.11: Simulation outputs as sensor changes direction during localization

all points of a trajectory to be inside the communication circle to localize the sensor. Percentage of localization decreases and average error (AE_{sc2}) increases with respect to increasing beacon distance according to Table 6.3 for *selection criterion 2*.

Four simulation outputs are shown in Fig. 6.11 with the actual trajectory and two calculated trajectories of a mobile sensor in each of the figures. The dashed trajectory is selected to localize the sensor in each of Fig. 6.11. *Selection criterion 1* is used in Fig. 6.11a - 6.11c and *selection criterion 2* is used in Fig. 6.11d. Fig. 6.12 shows graphical representations of the tables. In Fig. 6.12a, it can be observed that localization percentage in *selection criterion 2* is higher than localization percentage in *selection criterion 1* for any communication range and beacon distance. Also average error in *selection criterion 2* is higher than average error in *selection criterion 1* as shown in Fig. 6.12b. In Table 6.4,

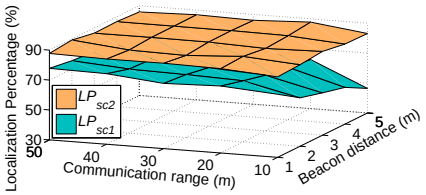

(a) Localization percentage with respect to *selection criterion 1 & 2*

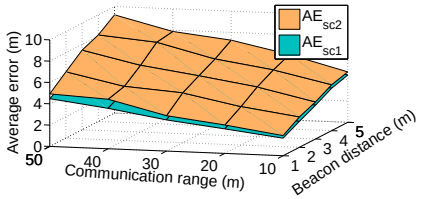

(b) Average error with respect to *selection criterion 1 & 2*

Figure 6.12: Performance of *selection criterion 1* and *selection criterion 2*

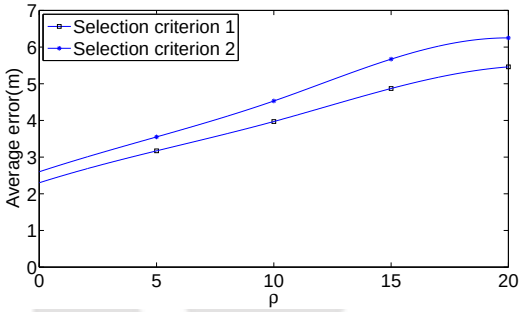

Figure 6.13: Average errors of LCD versus radio irregularity ρ

we compare our proposed algorithm with existing algorithms. Simulation results show around 67% and 63% improvement over WMCL-A for *selection criterion 1* and *selection criterion 2* of LCD respectively in terms of average localization error.

Table 6.4: Average error (r) of our proposed algorithm compared LCD with some existing algorithms, where r is the communication range of anchor

Algorithm	LCD		WMCL-A	WMCL-B	MCB	MCL
	selection criterion 1	*selection criterion 2*				
Error(r)	0.165	0.185	0.503	0.568	0.662	0.766

In Fig. 6.13, we show a two dimensional plot of AE_{sc1} and AE_{sc2} versus ρ, where ρ is varying from 0 to 20. Here communication range and beacon distance are 20 meter and 2 meter respectively. AE_{sc1} is varying from 2.3 meter to 5.6 meter whereas AE_{sc2} is varying from 2.7 meter to 6.3 meter according to the figure.

6.4.2 Simulation for LPO

We place an anchor at the origin $(0, 0)$ on a two dimensional plane. We considere different level of obstacles within the communication circle. According to our simulation, 20% obstacle level implies, at each position where sensor waits, there is 20% possibility that obstacles either obstruct path of the sensor or block beacons. Mobile sensor enters in the communication circle randomly, find beacon points in spite of obstacles and localizes itself. Few simulation outputs are shown in Fig. 6.14 and Fig. 6.15. Sensor receives $< 1 >$ first at the point which is marked using blue star. Direction of movement is shown using black arrows. Green solid lines are the lines joining beacon points. Fig. 6.14a shows that

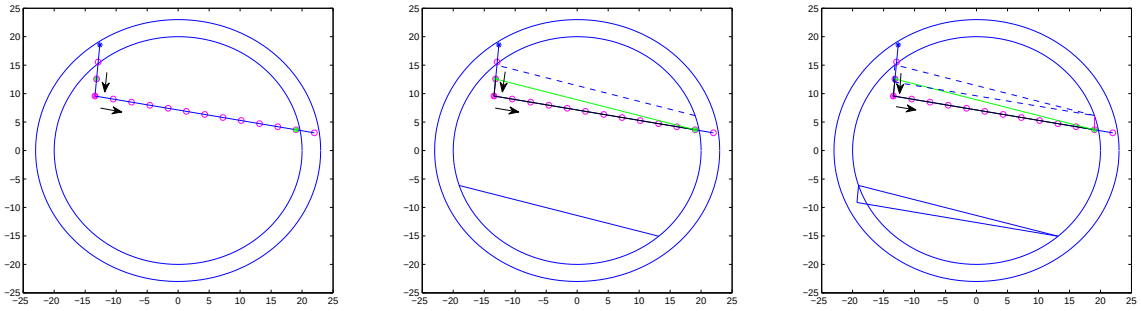

(a) Marking beacon points (b) Computing chords (c) Localization

Figure 6.14: Simulation output of localization using LPO

a sensor changes it's direction once before finding two beacon points. Fig. 6.14b shows sensor computes approximate chord length and find two possible chords. Blue solid and

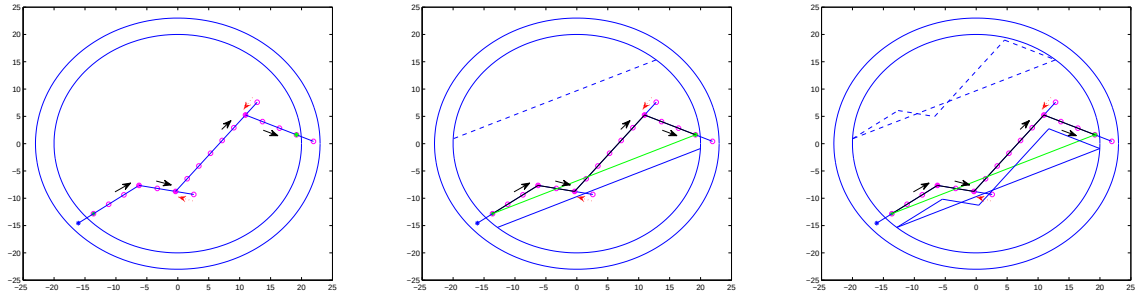

(a) Marking beacon points (b) Computing chords (c) Localization failure

Figure 6.15: Simulation output of a failure of localization using LPO

Table 6.5: Average error in presence of radio irregularity and percentage of localization using *selection criterion 1* of LPO for 20% obstacle level

BD →	**1**		**2**		**3**		**4**		**5**	
CR↓	LP_{sc1}	AE_{sc1}	LP_{sc1}	AE_{sc1}	LP_{sc1}	AE_{sc1}	LP_{sc1}	AE_{sc1}	LP_{sc1}	AE_{sc1}
10	75.70	2.72	68.30	3.26	63.20	4.46	53.50	5.24	44.00	6.27
20	69.30	3.74	65.0	4.80	62.70	5.81	65.70	7.04	63.50	7.79
30	61.30	5.92	63.20	6.58	61.60	7.83	63.40	7.97	62.60	9.81
40	54.20	11.14	58.60	8.40	61.50	9.15	57.70	9.43	59.30	11.32
50	45.50	13.50	54.80	9.49	59.90	11.16	53.10	11.72	57.10	11.29

blue dotted lines show two approximate chords with same length and gradient. Finally in Fig. 6.14c, sensor finds that the blue dotted trajectory is within the circle of radius r centering at the anchor and localizes accordingly. Fig. 6.15 shows failure of localization. Sensor changes direction thrice before finding two beacon points in Fig. 6.15a. For the last two direction changes, sensor returns back to previous positions and then changes direction which happened due to receiving no beacon at those points. Returning back to previous positions are shown using red dotted arrows. Fig. 6.15b shows sensor computes approximate chord length and find two possible chords. Blue solid and blue dotted lines show two approximate chords with same length and gradient. In Fig. 6.15c, sensor finds both the trajectories are entirely within the circle with radius r centering at the anchor, hence localization can not be done.

We calculate localization error for each run of LPO by a sensor considering radio irregularity. Average localization error for 10000 such runs for each communication range and beacon distance are calculated as shown in Table 6.5 and Table 6.6 according to Algorithm 6. For *selection criterion 1*, Table 6.5 shows average error (AE_{sc1}) in presence of radio irregularity and percentage of localization (LP_{sc1}) of Algorithm 6 considering 20% obstacle level. For *selection criterion 2*, Table 6.6 shows average error (AE_{sc2}) in presence of radio irregularity and percentage of localization (LP_{sc2}) of Algorithm 6 considering 20% obstacle level. In most of the cases, average localization errors increase as communication range increases for any fixed beacon distance in both Tables 6.5 and 6.6. In most of the cases, percentage of localization (LP_{sc1}) for *selection criterion 1* in Table 6.5 decreases as communication range increases for any fixed beacon distance. On the other hand, percentage

Table 6.6: Average error in presence of radio irregularity and percentage of localization using *selection criterion 2* of LPO for 20% obstacle level

BD →	**1**		**2**		**3**		**4**		**5**	
CR↓	LP_{sc2}	AE_{sc2}	LP_{sc2}	AE_{sc2}	LP_{sc2}	AE_{sc2}	LP_{sc2}	AE_{sc2}	LP_{sc2}	AE_{sc2}
10	85.30	2.79	84.40	3.33	81.60	4.62	80.50	5.41	79.00	6.29
20	89.90	4.02	87.30	5.07	85.60	6.14	83.30	7.10	84.20	7.94
30	91.30	6.53	90.60	6.49	87.40	8.01	86.10	8.23	85.10	10.44
40	92.50	11.31	91.00	8.56	88.30	9.41	87.30	9.73	86.80	11.11
50	93.40	13.33	93.20	10.50	91.30	11.23	89.80	11.69	88.50	12.11

Table 6.7: Average number of direction changes in LPO for 20% obstacle level

BD → CR↓	1	2	3	4	5
10	7.8700	5.7700	5.4650	5.3320	4.7440
20	12.1140	7.6360	6.6060	5.9580	5.4510
30	17.0100	10.2160	7.6990	6.7500	6.1300
40	22.4360	12.7290	9.2670	7.9420	7.0700
50	30.9790	13.9330	10.9960	9.1810	7.9480

of localization (LP_{sc2}) for *selection criterion 2* in Table 6.6 increases as communication range increases for any fixed beacon distance. Values of (LP_{sc2}) in Table 6.6 are larger than (LP_{sc1}) in Table 6.5 for LPO, since *selection criterion 2* does not require all points of a trajectory to be inside the communication circle to localize the sensor. Average number of direction changes required to localize a sensor is shown in Table 6.7 for 20% obstacle level. Number of direction changes increases for fix beacon distance as communication range increases. It happens since sensor needs to travel more distance within larger circle. For a fixed communication range, number of direction changes decrease with increasing beacon distance since number of beacon decreases with larger beacon distance.

In Fig. 6.16, three dimensional plots of average error of LPO *selection criterion 1* are shown for different communication range and beacon distances keeping obstacle level 20% and 30%. Similarly in Fig. 6.17, three dimensional plots of average error of LPO *selection criterion 2* has been shown for different communication range and beacon distances keeping obstacle level 20% and 30%. In both the figures, average errors are along Z-axis. Figures suggest that average errors increase with obstacle degree. In Fig. 6.18, we show

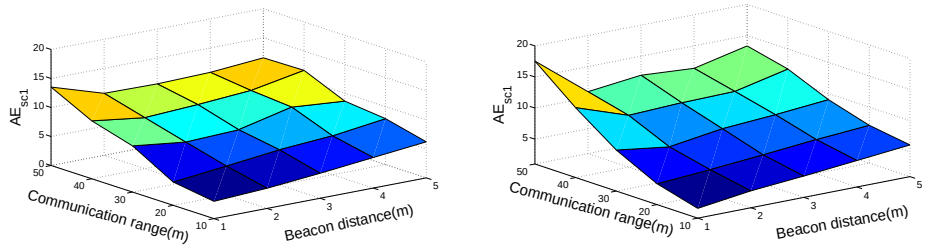

(a) 20% obstacle level (b) 30% obstacle level

Figure 6.16: Average error for *selection criterion 1* of LPO for different obstacle levels

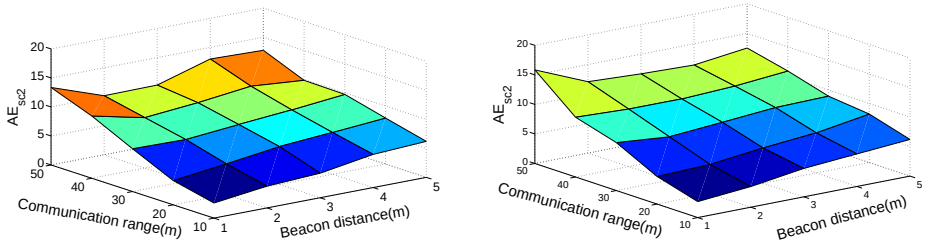

(a) 20% obstacle level (b) 30% obstacle level

Figure 6.17: Average error for *selection criterion 2* of LPO for different obstacle levels

a two dimensional plot of AE_{sc1} and AE_{sc2} versus ρ, where ρ is varying from 0 to 20. Here communication range and beacon distance are 20 meter and 2 meter respectively. AE_{sc1} is varying from 3.5 meter to 8.1 meter whereas AE_{sc2} is varying from 4.2 meter to 8.3 meter according to the figure. Fig. 6.19 shows graphical representations of the localization percentages for both selection criteria of LPO in presence of 20% obstacle level. Localization percentages are along Z-axis. From Fig. 6.19, it can be observed that localization percentage in *selection criterion 2* is higher than localization percentage in *selection criterion 1*.

Average time (in second) needed to localize a sensor using proposed schemes LWCD (in chapter 5), LCD and LPO are shown in Table 6.8, when the speed of mobile sensor is 2 meter/second, r=20 meter and u=2 meter. We find the averages of minimum distances which a sensor needs to travel for localization and divide it by speed of the sensor to find the average localization time. Distance values are in meters. Sensor takes double time in LPO to move same distance due to *move-wait-move* movement compared to LWCD and LCD. That is why localization time is largest for LPO.

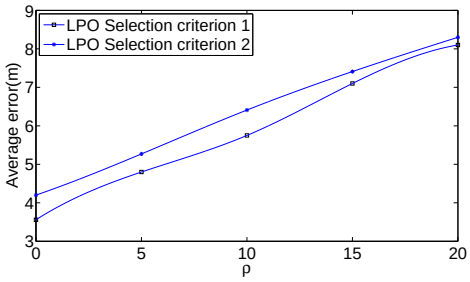

Figure 6.18: Average errors of LPO versus radio irregularity ρ

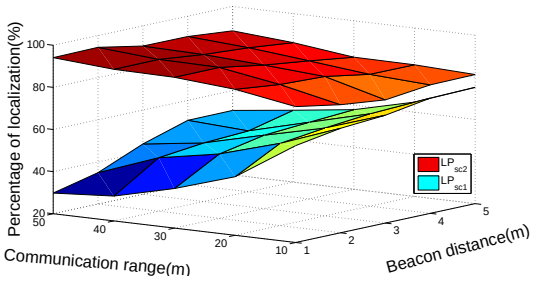

Figure 6.19: Localization percentages LP_{sc1} and LP_{sc2} for the *selection criterion 1* and *2* respectively

Table 6.8: Average time taken by our proposed schemes

Algorithm $\rightarrow$	LWCD	LCD	LPO
Average distance (in meters)	78.4	39.7	52.2
Average time (in seconds)	39.2	19.85	52.2

In Table 6.9, we compare our results with some of the existing mobile sensor localization algorithms WMCL-A [90], WMCL-B [90], MCL [33] and MCB [7]. In this table, average errors are given in terms of communication range r. Communication range is taken as 20 meter, beacon distance 2 meter and radio irregularity as discussed before. Among those, WMCL-A gives best results. Results show 67% and 63% improvement over WMCL-A for *selection criterion 1* and *selection criterion 2* of LCD respectively in terms of average localization error. Table 6.9 shows 52% and 49% improvement over WMCL-A for *selection criterion 1 (SC 1)* and *selection criterion 2 (SC 2)* of LPO respectively in terms of average localization error.

Table 6.9: Average error (r) of our proposed algorithms LCD and LPO compared to some existing algorithms, where r is the communication range of the anchor

Algorithm	LCD		LPO		WMCL-A	WMCL-B	MCB	MCL
	SC 1	*SC 2*	*SC 1*	*SC 2*				
Error(r)	0.165	0.185	0.24	0.253	0.503	0.568	0.662	0.766

6.5 Conclusion

In this chapter we have proposed LCD for localization considering sensors change direction while localization. Another algorithm LPO is proposed which localizes sensors in presence of obstacles. LPO selects appropriate beacon points in presence of obstacles using a different system model. Simulation results of LPO show good positioning accuracy for different levels of obstacles. Better positioning accuracy is observed in simulation for LCD and LPO compared to existing works.

Chapter 7

Path Planning for Mobile Anchor in Connected Networks

7.1 Introduction

A number of static anchors are used to localize static senors in the localization schemes [14, 20, 68, 92]. To minimize the number of static anchors and to avoid range measurements, range-free localization schemes [46, 75, 84] using mobile anchor are proposed. One mobile anchor with a suitable path planning is equivalent to many static anchors, which localizes whole network. By a single mobile anchor we can save large number of static anchors with deployment cost in the expense of the mobility of the mobile anchor. Therefore, reducing path length of the mobile anchor becomes an important issue in the area of localization. Range measurements are done in most of the existing works [47, 48, 36], where path planning are proposed for connected network. Our aim is to propose a path planning using only connectivity information which can adapt an existing range-free localization scheme for better accuracy. In this chapter we propose a movement strategy for a mobile anchor to localize sensors of a connected network with connectivity guided movement. We use range-free localization scheme proposed by Lee et al. [46] which yields better positioning accuracy.

7.1.1 Our contribution

We introduce a hexagonal movement strategy for mobile anchors. Our proposed distributed range-free movement strategy localizes all sensors within $r/2$ error-bound in a connected network, where r is the transmission range of the sensors and the mobile anchor. To the best of our knowledge, this is the first work where localization and path planning both are done using connectivity of the network without range estimation. Simulation results show improvement over existing work [48] in terms of both path length and localization accuracy. Full localization is guaranteed in absence of irregular radio propagation. Simulation results show, also in presence of radio irregularity, all the sensors are being localized using proposed movement strategy.

The organization of the remaining part of this work is as follows. The theoretical results of our proposed path planning on a connected network are explained in section 7.2. The algorithm along with system model and correctness proof, complexity analysis are given in section 7.3. Effect of irregular radio propagation is discussed in section 7.4. The simulation results are presented in section 7.5. Finally we conclude in section 7.6.

7.2 Path Planning

In this section we discuss path planning to localize an arbitrary connected network of any number of sensors. The mobile anchor broadcasts beacon with its position information after every t time interval. We may use the term 'anchor' instead of 'mobile anchor' in the rest part of this paper.

Definition 7.2.1. (Beacon distance) Distance traveled by the mobile anchor between two consecutive broadcasts of beacon is called *beacon distance* and is denoted by u.

Definition 7.2.2. (Communication circle) The circle with radius r centering at the sensor, where r is the communication range of the sensor.

Definition 7.2.3. (LRH) Largest regular hexagon inscribed within the communication circle of any sensor.

Definition 7.2.4. (Beacon point) The position of the anchor that is extracted from the beacon received by a sensor at time x is denoted as a beacon point for the sensor if and

only if the sensor does not receive any other beacon either in time interval $[x - t_0, x)$ or in time interval $(x, x + t_0]$, where t_0 is the waiting time such that $t < t_0 < 2t$ and t is time interval of periodical broadcasts of beacon by the anchor.

The algorithm begins with localizing a sensor by random movement of the anchor. The localized sensor broadcasts its position which is received by the anchor. After a finite amount of movement, the anchor reaches at any point on the communication circle of the localized sensor. The anchor computes vertices of the LRH inscribed within the communication circle with that point as a vertex. Then the anchor starts moving along the LRH broadcasting beacons with its current position along with all vertices of the LRH at regular interval so that any sensor which receives a beacon knows the LRH. At the same time all the neighbors of the localized sensor marks at least two beacon points according to our scheme. Those beacon points help the neighbors to compute two probable positions of themselves according to the scheme [46]. We briefly discuss below how the localization scheme [46] works.

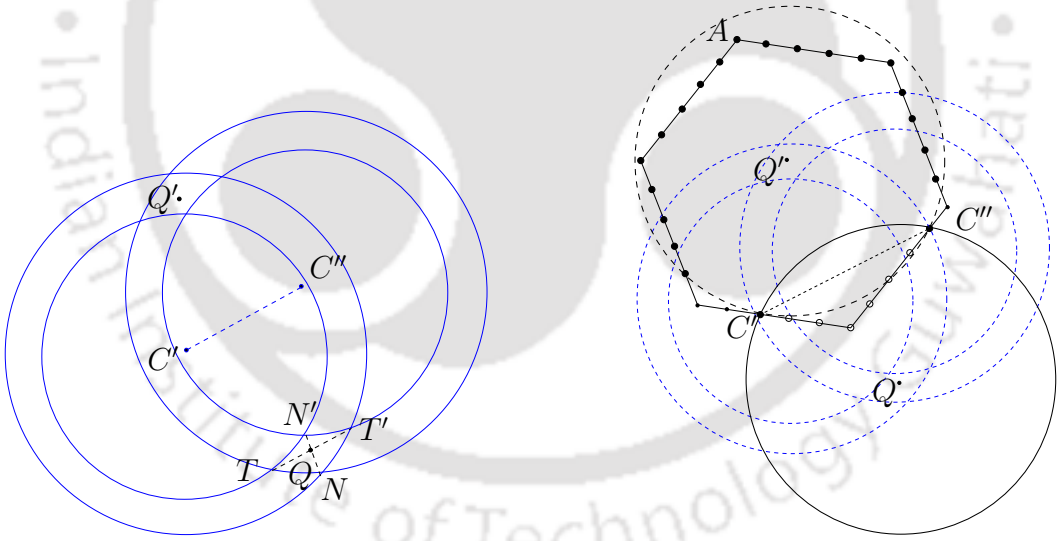

(a) Q and Q' are the two possible positions (b) Sensor chooses its position at Q

Figure 7.1: Detection of correct position using hexagonal movement pattern of mobile anchor

Let C' and C'' be two beacon points marked by a sensor as shown in Fig. 7.1a. Sensor lies on one of the two regions of intersection of the circular laminae with radius $(r - u)$ and r centering at the beacon points C' and C'', where u is the beacon distance.

The position of the sensor is approximated as the intersection point Q of NN' and TT'. So maximum localization error is equal to $\max(NN'/2, TT'/2)$. Similarly, Q' is another possible position. A third beacon point helps the sensor to choose the correct one among Q and Q'.

In our work we do not need the third beacon point to localize the sensor. Hexagonal movement strategy helps to choose the correct one among those two. With the knowledge of the LRH, the sensor can compute the set of beacons it supposed to receive for different possible positions Q and Q'. The sensor chooses Q as its position since it received beacons marked with unfilled circles on the LRH as shown in Fig. 7.1b. Similarly, the sensor would choose Q' as its position if it received beacons marked with filled circles on the LRH. This selection method will fail only if there exist a common set of beacons for two different sensor positions, which is not possible.

We impose a condition on the distance between two beacon points for which the error bound of the scheme [46] remains less than $r/2$. This error bound ensures localization of all sensors within $r/2$ error according to our proposed path planning.

Theorem 7.2.5. *Using the localization scheme [46], if $l \geq (r - u)$ then the localization error remains less than $r/2$ for beacon distance $u < r/7.5$, where l is the distance between two beacon points and r is the communication range.*

Proof. There are two cases depending on the length of l.

Case 1 ($r - u \leq l \leq 2r - 2u$): Fig. 7.2 illustrates the case. According to Fig. 7.2a, C' and C'' be the beacon points received by a sensor such that $r - u \leq l \leq 2r - 2u$, where $C'C'' = l$.

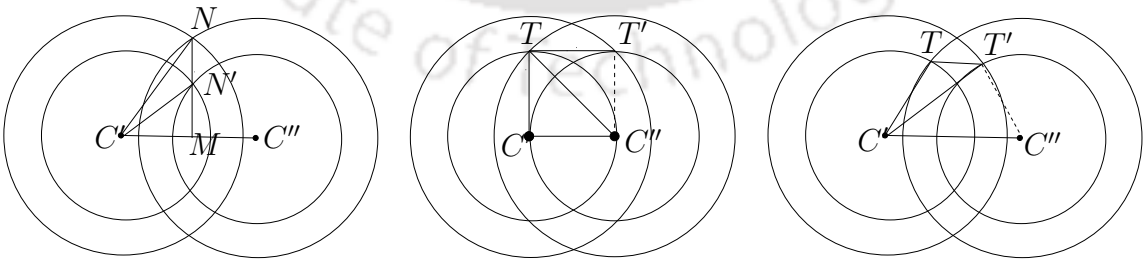

(a) Showing the line segment NN'

(b) $\angle C'TT' = \pi/2$

(c) $TT' < r$ when $\angle C'TT' > \pi/2$

Figure 7.2: Illustration of case 1

From the figure, $NN' = \sqrt{r^2 - (l/2)^2} - \sqrt{(r-u)^2 - (l/2)^2} < r$.

Now consider the $\angle C'TT'$ in Fig. 7.2b. Since TT' is parallel with $C'C''$, so $\angle C'TT' = \pi/2$ implies $\angle TC'C'' = \pi/2$. Then from $\triangle C'C''T$, $(C'T)^2 + (C'C'')^2 = (C''T)^2$. Since the minimum value of $C'C''$ is $(r-u)$, so, $(C'T)^2 + (C'C'')^2 = (C''T)^2$ implies $\sqrt{2}(r-u) = r$, which is same as $u = (\sqrt{2}-1)r/\sqrt{2}$. Therefore, $\angle C'TT' = \pi/2$ implies $u = (\sqrt{2}-1)r/\sqrt{2}$. Hence, $u < (\sqrt{2}-1)r/\sqrt{2} = r/3.5$ implies $\angle C'TT' > \pi/2$.

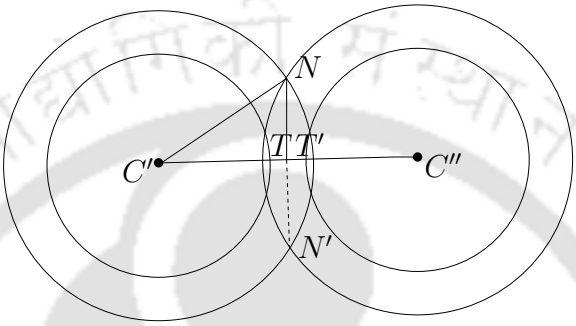

Figure 7.3: Illustration of case 2

From $\triangle C'TT'$ in Fig. 7.2c, we can say, $TT' < r$ when $\angle C'TT' > \pi/2$, i.e., $TT' < r$ when $u < r/3.5$. Hence,

$$\max(TT'/2, NN'/2) \quad < \quad r/2 \text{ when } u < r/3.5 \tag{7.2.1}$$

Case 2 ($l > 2r - 2u$): From Fig. 7.3, $NN' = 2\sqrt{r^2 - (l/2)^2}$. This is maximum when l is minimum, i.e., $l = 2r - 2u$. Now, $NN' < r$ if $2\sqrt{r^2 - (r-u)^2} < r$, i.e., $NN' < r$ if $u < (2-\sqrt{3})r/2 = r/7.5$. Again from Fig. 7.3, $TT' < 2u$. So, $TT' < r$ if $u < r/2$. Hence,

$$\max(TT'/2, NN'/2) \quad < \quad r/2 \text{ when } u < r/7.5 \tag{7.2.2}$$

From the above two inequalities 7.2.1 and 7.2.2, for $l \geq (r-u)$, the error bound of the scheme [46] is $r/2$ if $u < \min(r/3.5, r/7.5)$, i.e., error is less than $r/2$ if $u < r/7.5$. □

Following theorems guarantee that all neighbors of any sensor can localize by one complete movement of the mobile anchor along the LRH around the sensor.

Theorem 7.2.6. *If an anchor completes its movement along the LRH around a sensor Q, then all other sensors lying inside the circle of radius $3r/2$ centering at Q can be localized with error less than $r/2$ for suitable beacon distance u, if Q has been localized within $r/2$ error.*

Proof. In Fig. 7.4, Q is the calculated position of a sensor and the anchor moves along LRH around Q. Here the LRH is $ABCDEF$. Due to localization error, Q may lie

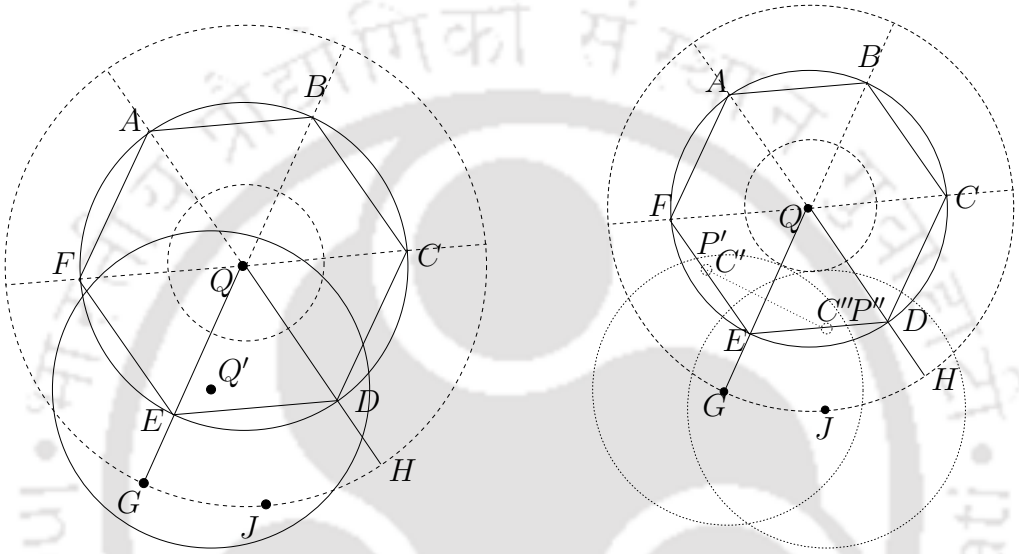

(a) Position of the sensor is within the $\triangle QDE$

(b) Position of the sensor is within the region bounded by GE, ED, DH and the arc HJG

Figure 7.4: Position of a sensor within the sector QGH

anywhere within the smallest dotted circle in Fig. 7.4 with radius $r/2$ centering at Q. We prove that if a sensor lies anywhere within the largest dotted circle with radius $3r/2$ centering at Q then it marks at least two beacon points such that distance between them is at least $(r - u)$, where u is the beacon distance. Length of each side of the regular hexagon $ABCDEF$ is r and $QA = QB = QC = QD = QE = QF = r$. The anchor starts its movement from a vertex of the hexagon and broadcasts beacon maintaining beacon distance $u = r/k$ for some integer k, which ensures that the anchor broadcasts beacon at every vertex of the LRH along with some other points on the LRH.

We divide the largest dotted circle shown in Fig. 7.4 in six symmetric sectors by joining each vertex of the hexagon with Q and then extending the line up to the boundary of the

largest circle. Therefore any sensor lying within the largest circle must lie in any one of the six symmetric sectors. If a sensor lies on the common boundary of any two sectors then it can be considered within any of the sector. Without loss of generality, let a sensor lie in the sector bounded by the line segments GQ, QH and by the arc HJG, where J is the mid-point of GH on the arc. We further divide the sector in two parts i.e., $\triangle QED$ and the region $GEDHJG$ bounded by GE, ED, DH and the arc HJG, where $\triangle QED$ defines the triangle with vertices Q, E and D. There are two cases based on the position of a sensor belonging to $\triangle QED$ or region $GEDHJG$.

Case 1. Q' is the location of sensor inside $\triangle QED$ as shown in Fig. 7.4a, where $\triangle QED$ is an equilateral triangle with side length r. Then irrespective of the position of Q', $Q'E < r$, $Q'D < r$. Hence if the communication circle of Q' intersects CD then it intersects EF or FA. Similarly, if the communication circle of Q' intersects EF then it intersects CD or CB. So distance l between two beacon points is at least r i.e., $l > (r - u)$. Therefore, Q' can be localized within $r/2$ error using Theorem 7.2.5.

Case 2. The location of sensor is inside the region $GEDHJG$ as shown in Fig. 7.4b. The distance l between the beacon points decreases, if distance between the sensor and the center Q of the LRH decreases. As any point on the arc GJH is furthest from Q, it is sufficient to prove that $l > (r - u)$ when Q' lies on the arc GJH. Due to the symmetric nature of the arcs JG and JH, we show the proof for sensor positions on arc JG. Let J be the position of the sensor. Since $JE = JD < r$, circle with radius r centering at J intersects CD and EF as shown in Fig. 7.4b. Hence sensor marks two beacon points such that $l \geq r > (r - u)$. One can easily verify that as the position of the sensor changes along the arc JG towards G, distance l between two beacon points decreases and l is least when the sensor is at G. So, it is sufficient to show that $l > (r - u)$ when the sensor is at G. Communication circle centering at G, intersects DE and EF at P' and P'' respectively i.e., $GP' = GP'' = r$. Beacon points are located anywhere within the line segments $P'C'$ and $P''C''$ such that $P''C'' = P'C' = u$. Distance between the beacon points decreases as position of beacon points move towards C', C''. Let C', C'' be the position

of the beacon points considering the worst case. Therefore, $EC' = EP' - u$ and $EC'' = EP'' - u$. Let $EP' = EP'' = L$. Then from $\triangle GEP''$ of Fig. 7.4b, $L^2 + (r/2)^2 - 2L(r/2)\cos(2\pi/3) = r^2$. Solving this equation, we get $L = (\sqrt{13} - 1)r/4$. Now from $\triangle EC'C''$, $C'C'' = \sqrt{(L-u)^2 + (L-u)^2 - 2(L-u)^2\cos(2\pi/3)}$, i.e., $C'C'' = \sqrt{3}\left((\sqrt{13}-1)(r/4) - u\right)$. So, $C'C'' \geq (r-u)$ if $\sqrt{3}((\sqrt{13}-1)r/4 - u) \geq (r-u)$, i.e., $u \leq (\sqrt{3}(\sqrt{13}-1) - 4)r/(4(\sqrt{3}-1))$, i.e., $u \leq r/5$.

Using Theorem 7.2.5, as $r/7.5 < r/5$, we can conclude that for $u < r/7.5$, all the sensors which lie within the circle of radius $3r/2$ and centering at Q, can be localized with error less than $r/2$. □

Theorem 7.2.7. *If a mobile anchor completes its movement along the LRH around a sensor which is localized within $r/2$ error, then all its neighbors are localized within $r/2$ error.*

Proof. If a sensor is localized within $r/2$ error, its neighbors lie within the circle of radius $3r/2$ centering the sensor. Hence the statement follows by Theorem 7.2.6. □

7.3 Distributed Algorithm for Path Planning

We assume sensors form a connected network. The number of sensors in the network is not an input of our algorithm. Each sensor has unique id and knows the id of its one hop neighbors. The set of one hop neighbors of a sensor i is denoted by $nbd(i)$. We define NLN-degree(i) as the number of non-localized neighbors of a sensor i. Initially NLN-degree(i) = $|nbd(i)|$, where $|nbd(i)|$ is the cardinality of the set $nbd(i)$. At the beginning of localization, a sensor i localizes itself by random movement of the mobile anchor such that the localization error is within $r/2$, where r is the communication range. This can be done by choosing beacon points such that they are at least $(r-u)$ distance apart (Ref. Theorem 7.2.5), where u is the beacon distance. After localization, i broadcasts its id and position. Whenever the mobile anchor hears the position of i, it starts moving along the sides of the LRH of i and broadcasts beacon. Each beacon has the information about sensor id i and the LRH around i, along which the anchor is moving. Computation of LRH is explained in section 7.2. Hence each $j \in nbd(i)$ localizes itself within the error bound

$r/2$ by Theorem 7.2.7 and broadcasts the position to $nbd(j)$. A sensor localizes itself only

Algorithm 7 HexagonalLocalization

1: Mobile anchor localizes a sensor by its random movement then PUSH id of the sensor into the STACK.
2: Computes LRH centering at the sensor whose id i is at the TOP of the STACK and broadcasts beacons periodically with period t until the LRH movement completes.
3: The anchor moves $r/2$ distance towards i and sends a message to i for next destination of its movement.
4: Sensor i sends a message to all $j \in nbd(i)$ for NLN-degree(j) along with their positions.
5: On receiving the replies, sensor i selects a neighbor sensor j' that achieves the value $\max\{\text{NLN-degree}(j)|j \in nbd(i)\}$ and sends position of j' with NLN-degree(j') to the anchor for next destination of movement.
6: If NLN-degree(j') > 0 then the anchor PUSH j' into the STACK and moves to the closest point of the communication circle of j' and executes step 2, otherwise POP from the STACK.
7: The algorithm terminates if STACK is empty, otherwise the anchor revisits the sensor whose id is at the TOP of the STACK and executes step 3.

if it is a neighbor of sensor i. After receiving position of a neighbor $j \in nbd(k)$, sensor k updates NLN-degree(k) by NLN-degree(k) -1. During the process of completion of LRH, each sensor which receives a neighbor's position, keeps updating its NLN-degree. So, when all neighbors of sensor i are localized at the end of a LRH movement, each $j \in nbd(i)$ has computed their NLN-degree(j). After completing LRH, the anchor moves $r/2$ distance towards i. Moving $r/2$ distance towards i is required to ensure communication between the anchor and i because the positional error is bounded by $r/2$ according to Theorem 7.2.6. Then anchor sends a message to i for its next destination of movement. To do so, i sends a request to all $j \in nbd(i)$ for NLN-degree(j) along with their positions. Then i selects a neighbor sensor j' that achieves the value $\max\{\text{NLN-degree}(j)|j \in nbd(i)\}$ and sends position of j' with NLN-degree(j') to the anchor for next destination of movement. The anchor moves to the closest point of the communication circle of j' and starts the LRH movement around j' to continue localization process. The mobile anchor maintains a STACK along with its operations PUSH, POP and variable TOP with usual dynamic stack data structure during its travel through the connected network. Initially the STACK is empty. Before making LRH movement around a sensor i, the anchor PUSH id i on the STACK. If $\max\{\text{NLN-degree}(j)|j \in nbd(i)\} = 0$ then anchor POP i from the STACK.

When the STACK becomes empty, the algorithm terminates, otherwise anchor revisits the communication circle of the sensor i' (say), which is at the TOP of the STACK and then sends a message to i' for its next destination of movement. Mobile anchor decides its path according to the Algorithm 7 (HexagonalLocalization).

7.3.1 Correctness and complexity analysis

Theorem 7.3.1. *Algorithm 7 ensures localization of all sensors in a connected network.*

Proof. We prove correctness of the algorithm by method of contradiction. Let us assume that one sensor i is not localized but the algorithm terminates, i.e., the STACK becomes empty. Since all sensors are in a connected network, then there exist at least one sensor j, which is a neighbor of i and is localized. According to the algorithm, j localizes itself by marking beacon points on a LRH movement of the anchor around one of its neighbors k. At this moment k is at the TOP of the STACK. As i is not localized, j would send non zero NLN-degree(j) and its position to k. Since other sensors are localized, NLN-degree(j) is the maximum among those received by k. Hence k should send the position of j to the anchor for the next destination of movement according to Algorithm 7. Whenever anchor visits j and makes LRH movements, i becomes localized. So k cannot be popped without pushing j which implies localization of i. Hence k is in the STACK until i is localized. It contradicts our assumption that the STACK is empty but i is not localized. Hence proved. □

Theorem 7.3.2. *The time complexity of Algorithm 7 is* $O(|V| + |E|)$.

Proof. To analyze complexity of Algorithm 7, we calculate maximum travel distance of the mobile anchor to localize all sensors in any connected graph $G = (V, E)$ topology in absence of radio irregularity. Here V and E are the set of vertices corresponding to the sensors and the set of edges of G respectively. If degree of the graph decreases then the anchor needs to make more LRH movements. The line graph achieves lowest degree among connected graphs and hence the anchor attends maximum LRH movements to localize all sensors. In the worst case, for a line graph our algorithm matches with DFS visit of G. In this case anchor has to make LRH movement around $|V| - 1$ sensors if it

initiates its movement from one end of the graph. Total LRH movement is $6r(|V|-1)$ since each LRH movement equals to perimeter $6r$ of LRH, where r is the communication range of the sensors. In addition to this, anchor has to move maximum $2r(|E|-1)$ distance to reach other sensors and then to return to the initiator. Hence both time complexity and complexity in terms of distance traveled by the anchor are same and equal to $O(|V|+|E|)$. □

Communication Cost: We find communication cost in terms of number of messages being broadcasted during the path planning scheme. This depends on communication range r, beacon distance u, average degree z of the connected network and number of LRH movements H the anchor completes. By average degree, we mean average number of one hop neighbors each node have. During one LRH movement, anchor broadcasts $\frac{6r}{u}$ beacons and then one message to the sensor around which the LRH movement is done. That sensor broadcasts one message to its neighbors and receives the replies. So, for one LRH movement, $(\frac{6r}{u}+1+1+z)$ messages are needed on an average. Hence a total of $H \times (\frac{6r}{u}+z+2)$ number of messages being broadcasted during the algorithm.

7.4 Effect of Irregular Radio Propagation

Due to irregular radio propagation, sometimes signals broadcasted by the anchor may not reach up to r distance at every direction. Consequently, few neighbors of a sensor may not be localized even after a complete LRH movement around that sensor by the anchor. Fig. 7.5 illustrates one such case where i is the actual position and i' is the computed position of a sensor with id i. The distance between i and i' is less or equal to $r/2$. j is a neighbor of i and located within r distance from i. Anchor moves along the LRH computed within the circle of radius r centering at i'. C', C'' are the beacon points as shown in the figure. Due to radio irregularity, j may not receive beacons broadcasted by the anchor from C' and C'' but receives from P', P'' as first and last beacons, since distances from j to P', P'' are lesser compared to C', C''. Hence j marks P', P'' as beacon points. If distance between P' and P'' is less than $(r-u)$ then localization of j is not possible during this LRH movement, as $r/2$ error bound is not guaranteed which is necessary in our algorithm to localize all the sensors.

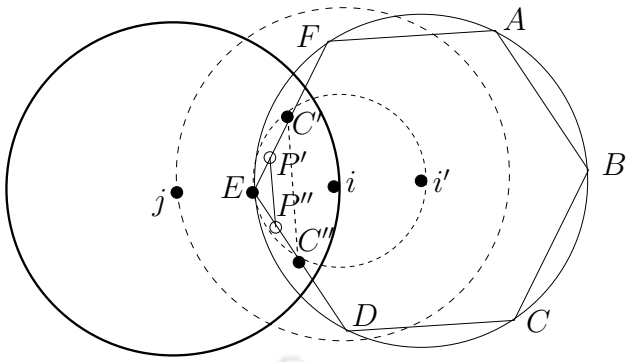

Figure 7.5: Sensor j is not localized after one LRH movement around computed position of neighbor i

If j is not localized after anchor completed LRH movement around i' then NLN-degree(i) remains nonzero. Here we have to add one more condition in step 6 of the Algorithm 7 to ensure localization of j. If $\max\{NLN - degree(k)|k \in nbd(i)\} = 0$, then POP is executed only if NLN-degree $(i) = 0$, otherwise anchor executes step 2. With this modification, i cannot be popped from the stack until NLN-degree(i) $= 0$. So, eventually j becomes localized during repeated LRH movement. Simulation results show that in presence of different degree of radio irregularity, path length increases due to repetitions of LRH movement around few sensors. Average error also increases as average distance between two beacon points may decrease due to radio irregularity.

7.5 Simulation Results

MATLAB platform is used to study the performances of our proposed schemes. We randomly generate connected graphs of sensors in a 50 meter $\times$ 50 meter square region. According to the section 7.2, we take values of beacon distance $u < r/7.5$. Following Fig. 7.6 and Fig. 7.7 show the hexagonal movement path (red solid lines) of a mobile anchor through the network during localization, where black bold lines are transition path between LRHs. The blue crosses and red circles are the actual and calculated positions of the sensors respectively and pairs are joined by dotted lines. The number of sensors n, communication range r, path length D and average positioning error are given in the caption of each figure. All the values showing in the tables and figures are in meters. As

the area remains fixed and connectivity is maintained by increasing number of sensors along with decreasing communication range of sensors and the anchor, path length does not increase much with the number of sensors. Considering irregular radio model,

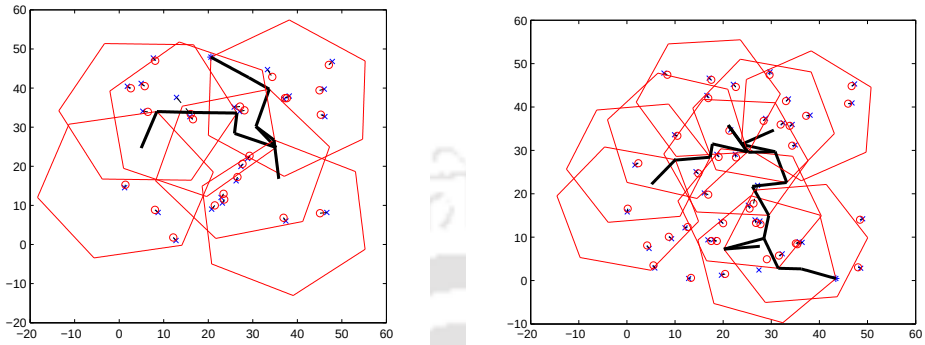

(a) $n = 25$, $r = 20$, $D = 966$, Average error=1.42 (b) $n = 50$, $r = 15$, $D = 1097$, Average error=1.09

Figure 7.6: Hexagonal movement pattern in a connected network

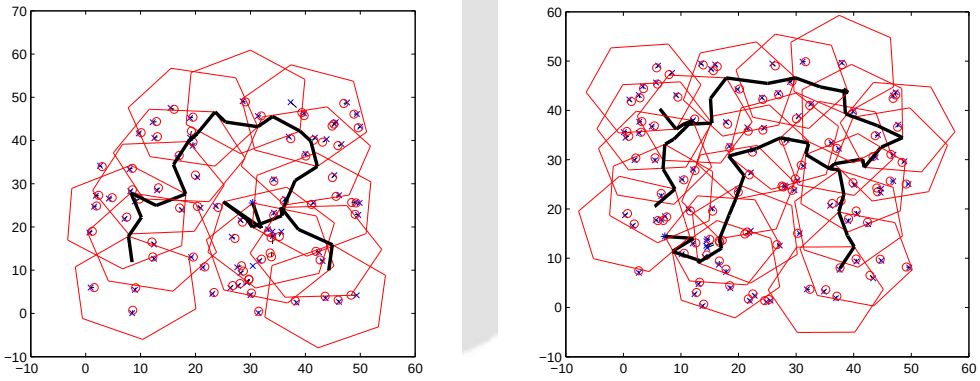

(a) $n = 75$, $r = 12$, $D = 1158$, Average error=0.92 (b) $n = 100$, $r = 10$, $D = 1481$, Average error=0.76

Figure 7.7: Hexagonal movement pattern in a connected network

path length and localization error are simulated. In Table 7.1, we show localization error for different communication range r and beacon distance u considering 0.1 degree of radio irregularity. According to Table 7.1, localization error decreases as beacon distance decreases for any fixed communication range. Here, $u = r/k$, where $k > 7.5$ according to Theorem 7.2.5 and Theorem 7.2.6. We also show path length of the mobile anchor

Table 7.1: Showing average error (in meters) for different communication range and beacon distance

Beacon distance → Communication range(↓)	$r/10$	$r/15$	$r/20$	$r/25$	$r/30$
10	1.52	1.13	0.63	0.42	0.33
15	2.39	1.42	1.07	0.75	0.54
20	2.84	1.97	1.33	0.96	0.67
25	4.45	2.48	1.59	1.28	0.98
30	5.98	3.22	2.20	1.71	1.21

Table 7.2: Average path length (in meters) and number of messages of our scheme varying number of sensors

No. of sensors	100	150	200	250	300
Average path length (meter)	1490	1550	1640	1675	1754
Average no. of messages	1620	1818	2017	2096	2277

for different number of sensors forming a connected network in a square region of fixed side length 50 meter in Table 7.2. Here we keep the communication range fixed at 10 meter with 0.1 degree radio irregularity. Results show that path length does not increase much with number of sensors. It happens since average degree increases with the number of sensors in a fixed region and one LRH movement localizes more number of sensors (approximately equal to the average degree). Table 7.2 also shows average number of messages being broadcasted by anchor and sensors to localize all sensors of the network.

Fig. 7.8a shows path length for mobile anchor increases as degree of radio irregularity increases from 0 to 0.2 to localize 100 sensors, where r=10 meter and u=1 meter. As we discussed in section 7.4, path length increases with radio irregularity because more than one LRHs are required to localize all the neighbors of some sensors as shown in Fig. 7.8b. Communication circle of such sensors are marked by blue dashed line in the figure.

We compare path length and average error of our algorithm with [48]. For comparison, we consider same parameters as in [48]. Sensors are randomly deployed over a square region of side length 1000 meter forming a connected graph. Average degree of vertices in the connected graph is varied from 7 to 35 by increasing number of sensors, where a sensor represents a vertex. We consider 0.1 degree of radio irregularity. Li et al. simulated four variants of *DREAMS* strategy in [48]. Among them *DREAMS-Random*

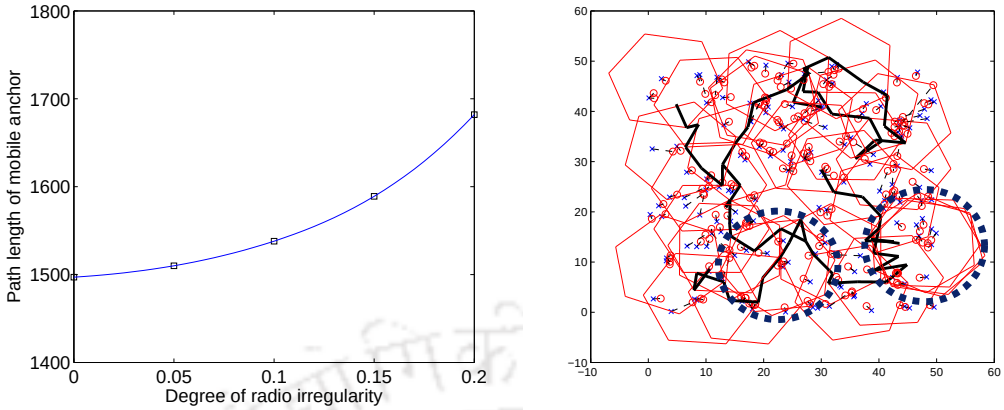

(a) Path length increases with degree of redio irregularity

(b) Multiple LRHs arond a sensor

Figure 7.8: Effect of radio irregularity

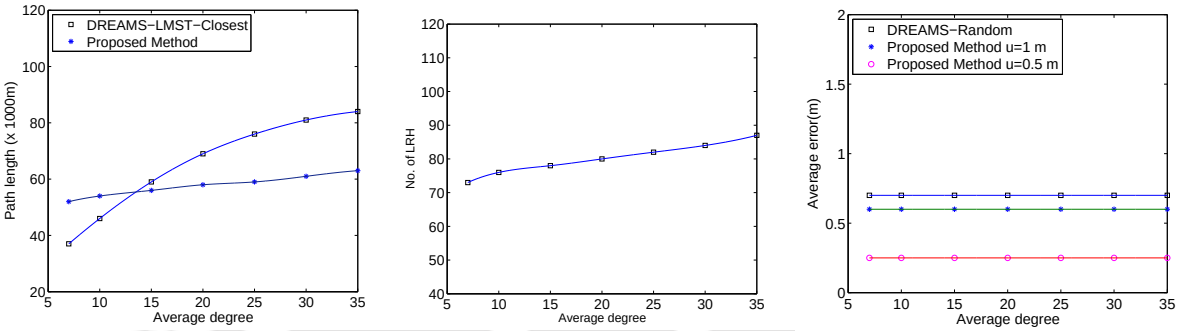

(a) Path length comparison

(b) No of hexagon vs average degree of a vertex

(c) Average error comparison

Figure 7.9: Performance evaluation of the proposed algorithm

yields minimum average error and *DREAMS-LMST-Closest* yields minimum path length. However, *DREAMS-Random* provides largest path length and *DREAMS-LMST-Closest* provides larger average error. We compare path length of our proposed algorithm with *DREAMS-LMST-Closest* as it provides minimum path length among the methods proposed in [48]. Simulation results show that path length of our technique is higher than *DREAMS-LMST-Closest* for average degree 7 and 10. But as average degree increases, our method outperforms [48] in terms of path length as shown in Fig. 7.9a. The reason behind this is that as average degree increases, one LRH movement localizes more number of sensors because all the neighbors (approximately equal to average degree of the

network) are being localized by one such movement. So path length does not increase much with increasing average degree according to our algorithm. Fig. 7.9b shows very small increment of average number of LRHs (73 to 87) with respect to increasing average degree. We compare average error with *DREAMS-Random* [48] and lesser localization errors are shown in Fig. 7.9c for different beacon distances 1 meter and 0.5 meter where $r = 100$ meter in presence of 0.1 degree radio irregularity. According to [48], localization error of *DREAMS-Random* is independent of average degree. The average error of our algorithm is independent of the average degree because we are using Lee's scheme [46] for localization, which does not depend on degree. Table 7.1 shows that average error decreases along the main diagonal of the table, i.e., average error decreases when beacon distance is 1 meter and communication range increases from 10 to 30. Following that trend, our error becomes 0.6 meter when beacon distance is 1 meter and communication range is 100 meter as shown in Fig. 7.9c.

7.6 Conclusion

In this paper we have proposed path planning algorithms for a mobile anchor using hexagonal movement. Our movement strategy reduces the requirement of three beacon points for localization to two beacon points. In a connected network, once a sensor is localized, proposed path planning is able to localize all its neighbors with one hexagonal movement around the sensor. The novelty is that without knowing the boundary of the network, our distributed algorithm localizes all sensors using connectivity without any range estimation. We have also computed the length of the path traversed by the anchor for different number of sensors with good localization accuracy based on simulation. Simulation results show improvement over [48] in terms of both path length and localization accuracy. In future we will try to investigate path planning in presence of obstacles.

Chapter 8

Path Planning for Mobile Anchor in Rectangular Regions

8.1 Introduction

In this chapter we consider the path planning problem for a mobile anchor where the region of interest is known beforehand like indoor networks. Our aim is to propose a movement strategy in a bounded region for a mobile anchor such that it can use existing range-free localization schemes which yields better accuracy while reducing the path length. In our strategy, only boundary information is used to localize all the sensors irrespective of deployment and underlying network topology. Comparison with existing literature shows reduction in path length along with good positioning accuracy.

8.1.1 Our contribution

We propose a movement strategy for mobile anchor which localizes all the sensors lying within the region using hexagonal tiling to cover a rectangular region with known boundary information. Theoretically we show that the length of the path traversed by the anchor is lesser in the proposed strategy compared to other existing path planning methods [25, 34, 37, 59] for covering a rectangular region. Results show 7.35% to 27.74% improvement of our scheme over different schemes in terms of path length. Good localization accuracy is also observed in simulation.

The organization of the remaining part of the work is as follows. The theoretical results of our proposed path planning in a rectangular region are explained in section 8.2. The simulation results are presented in section 8.3, along with performance comparison with existing approaches. Finally we conclude in section 8.4.

8.2 Path Planning for Rectangular Region

The mobile anchor broadcasts beacon with its position information after every t time interval. We may use the term 'anchor' instead 'mobile anchor' in the rest of this chapter. Definitions of beacon distance and beacon points are same as given in chapter 7. Here also we use localization scheme [46]. How this scheme works and our hexagonal movement strategy reduces the requirement of three beacon points to two beacon points are already discussed in section 7.2 of chapter 7.

In this section we discuss path planning for a mobile anchor which covers a given rectangular region to ensure localization of all sensors deployed in that region. Let $ABCDEF$ be a regular hexagon with side length r and center O as shown in Fig. 8.1a. If communication circle of a sensor touches the hexagon then we say that the sensor is within the coverage area of the hexagon. Obviously the area inside the hexagon is a part of the coverage area. As shown in Fig. 8.1a, $A'B'C'D'E'F'$ is a regular hexagon with side $2r$ and center O. The communication circles of the sensors located at the vertices of the larger hexagon touch the smaller hexagon at one vertex. Communication circle of any sensor which lies within or on the larger hexagon except at the vertices, intersects the smaller hexagon at at least two points. So $A'B'C'D'E'F'$ forms a coverage area of $ABCDEF$.

Let the anchor moves along $ABCDEF$ broadcasting beacons periodically with time period t. To localize itself following the scheme [46], each sensor should mark at least two beacon points on $ABCDEF$. To ensure marking of two beacon points, we reduce the coverage area by reducing the hexagon $A'B'C'D'E'F'$ to $A''B''C''D''E''F''$ with side $2r-X$ as shown in Fig. 8.1b. Now, we have to find a suitable value of X such that all sensors located inside $A''B''C''D''E''F''$ can be localized. As the vertices of $A''B''C''D''E''F''$ are the furthest points from $ABCDEF$, so if we find X in such a way that a sensor which lies at any vertex of $A''B''C''D''E''F''$, marks at least two beacon points, then so does

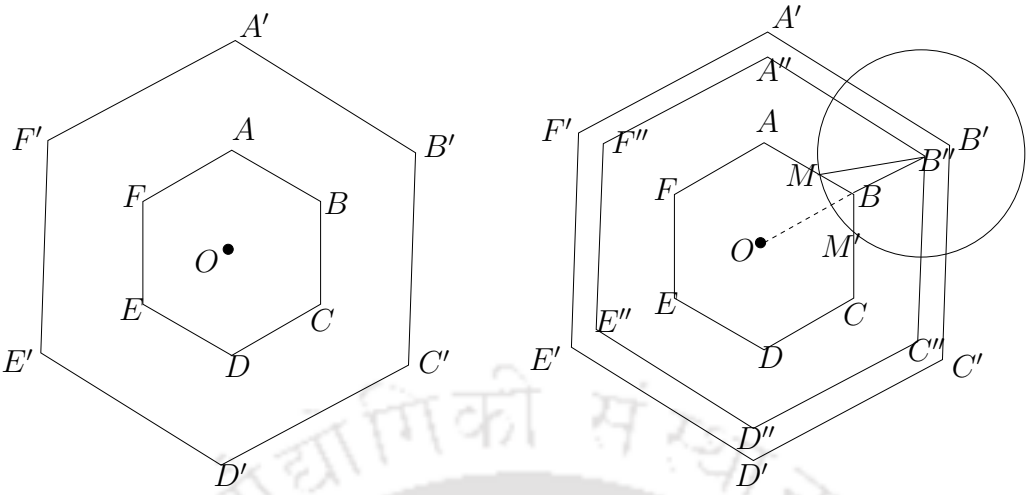

(a) The hexagon $A'B'C'D'E'F'$ is the coverage area when mobile anchor moves along the hexagon $ABCDEF$

(b) The coverage area $A''B''C''D''E''F''$ ensures two beacon points on $ABCDEF$

Figure 8.1: Showing coverage area when a mobile anchor moves along the regular hexagon $ABCDEF$

all other sensors which lies on or inside $A''B''C''D''E''F''$ for that same X. According to our strategy, anchor starts broadcasting beacon from some vertex of each hexagon with beacon distance $u = r/n$ for some integer n. This ensures that anchor broadcasts beacon at every vertex of any hexagon.

As shown in Fig. 8.1b, let $BM' = u$. Then the sensor at B'' marks two beacon points at B, M', if $B''M' = r$. Let $BB'' = r - X$. From $\triangle BMB''$, $(r - X)^2 + u^2 - 2(r - X)u\cos(2\pi/3) = r^2$, which implies $X = r + \frac{u}{2} - \frac{\sqrt{4r^2-3u^2}}{2}$. Approximately $X = \frac{u}{2}$ as $u << r$. Hence, if mobile anchor moves along a regular hexagon of side r, then all the sensors which lie within a regular hexagon with side $2r - X$, mark at least two beacon points, where $X \geq r + \frac{u}{2} - \frac{\sqrt{4r^2-3u^2}}{2}$.

As shown in Fig. 8.2, the mobile anchor moves along the blue solid lines starting from A to cover the rectangle $R_1R_2R_3R_4$. Anchor broadcasts beacons with $u = r/n$ for some integer n, so that beacon is broadcasted from each vertex along with other positions. Each beacon contains the information about the hexagon along which the anchor is moving. The movement terminates at Z. The directions of movement are shown by red dashed arrows. We now compute the path length of the movement. According to Fig. 8.2, each hexagon with blue solid lines and side r covers one larger hexagon with black dotted

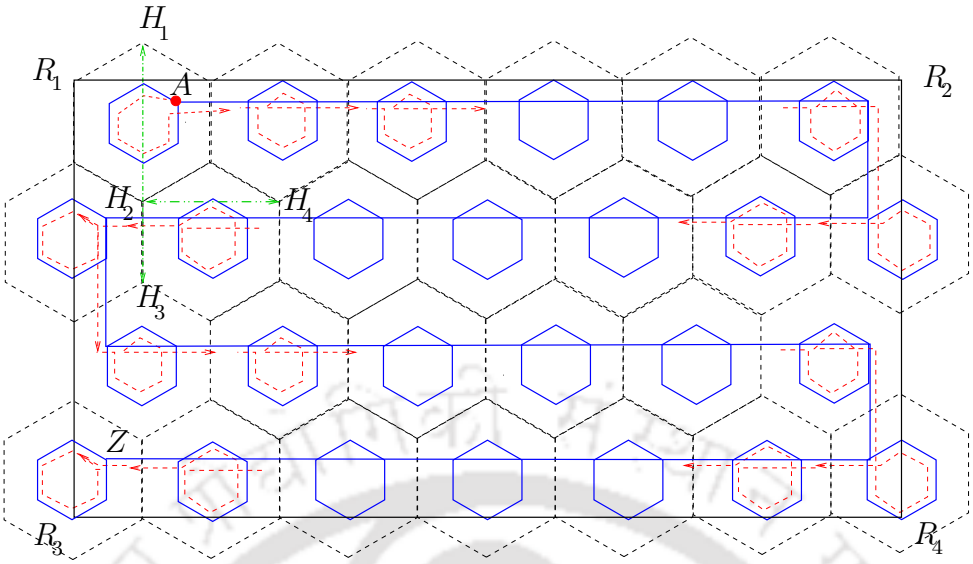

Figure 8.2: Showing path planning to cover a rectangular region $R_1R_2R_3R_4$

lines whose width is equal to $H_2H_4 = \sqrt{(2r-X)^2 + (2r-X)^2 - 2(2r-X)^2\cos(2\pi/3)} = \sqrt{3}(2r-X)$. If L is the width of the rectangle, then the number of hexagon in a row would be $\left\lceil \frac{L}{\sqrt{3}(2r-X)} \right\rceil$. Two rows of hexagon cover an area with height equal to $H_1H_3 = H_1H_2 + H_2H_3 = 3(2r-X)$. If L is the height of the rectangle, then the number of rows of hexagon would be $\left\lceil \frac{L}{3(2r-X)/2} \right\rceil$. Then total number of hexagon with side r required to cover a $L \times L$ rectangle is $\left\lceil \frac{L}{\sqrt{3}(2r-X)} \right\rceil \left\lceil \frac{2L}{3(2r-X)} \right\rceil$. Total path length required to reach all the hexagons in a row by moving from one hexagon to another hexagon is at most L. So, total distance traversed to connect the hexagons for all rows is equal to $L \left\lceil \frac{2L}{3(2r-X)} \right\rceil$. Total path length required to reach all the rows by moving from one row to another row is at most L again. In each pair of consecutive rows, an extra hexagon is needed i.e., an extra $3r$ movement is required in each row on an average. So, total path traversed to cover $L \times L$ rectangle is equal to

$$D_{Hexagon} = \left\lceil \frac{L}{\sqrt{3}(2r-X)} \right\rceil \left\lceil \frac{2L}{3(2r-X)} \right\rceil 6r + L \left\lceil \frac{2L}{3(2r-X)} \right\rceil + 3r \left\lceil \frac{2L}{3(2r-X)} \right\rceil + L.$$

Number of beacons transmitted by the mobile anchor throughout the traversal is equal to number of hexagons multiplied by $6r/u$ since during moving on each hexagon $6r/u$ number of beacons are transmitted.

8.2.1 Comparison with existing schemes

Table 8.1: Coefficients of higher order term L^2/r in the expressions of different schemes including proposed scheme ($D_{Hexagon}$)

$D_{Hexagon}$	D_{Chia}	D_{Scan}	D_{DScan}	$D_{Hilbert}$	$D_{S-curves}$	$D_{Circles}$	D_{LMAT}
$\frac{1}{\sqrt{3}}\left(\frac{2k}{2k-1}\right)\left(\frac{2k}{2k-1}+\frac{1}{\sqrt{3}}\right)$	$\frac{k}{k-1}$	$\frac{k}{k-1}$	$\frac{k}{k-1}$	$\frac{k}{k-1}$	$\frac{\pi}{3}\left(\frac{k}{k-1}\right)$	$\frac{\pi}{2}\left(\frac{k}{k-1}\right)$	$\frac{2}{\sqrt{3}}$

Theoretical comparison with existing schemes [25, 34, 37, 59] in terms of path length of mobile anchor is presented in this section. Let L be the length of the sides of a square region and r be the communication range of sensors and anchor. To normalize all the expressions of path length given in [59], we take $X = r/k$ for some integer $k > 1$. We denote path length of path planning of mobile anchor proposed in [59] by D_{Chia}. Path lengths of mobile anchor in different schemes in [37] are denoted by D_{Scan}, D_{DScan} and $D_{Hilbert}$. Path lengths of mobile anchor in different schemes in [34] are denoted by $D_{Circles}$ and $D_{S-curves}$. D_{LMAT} is the path length of the scheme proposed by [25]. We denote the path length of mobile anchor of our proposed scheme by $D_{Hexagon}$. Expressions of path lengths of different schemes are given below.

$D_{Chia} = (L+2r)\left(\left\lceil\left(\frac{L+2r}{r-r/k}\right)\right\rceil+1\right)+(r-r/k)\left\lceil\left(\frac{L+2r}{r-r/k}\right)\right\rceil$

$D_{Scan} = \left\lceil\left(\frac{L}{r-r/k}+2\right)\right\rceil L$

$D_{DScan} = 2\left(\left\lceil\left(\frac{L-r}{2(r-r/k)}+2\right)\right\rceil L-r\right)$

$D_{Hilbert} = \left\lceil\left(\frac{L+r}{r-r/k}\right)\right\rceil^2 (r-r/k)$

$D_{S-curves} = \left[\left(\frac{L}{3(r-r/k)/2}+1\right)\frac{L}{2}\pi\right]+L+r\pi/2$

$D_{Circles} = N^2\pi(r-r/k)$+L, where $N = \frac{L/\sqrt{2}-r}{r-r/k}$

Expression of $D_{Circles}$ is modified in such a way that it can also cover the corner points of the rectangle.

According to [25],

$D_{LMAT} = \frac{2}{\sqrt{3}}L\left(\left\lceil\frac{L}{r}\right\rceil\right)+L+r\sqrt{3}$

The path length for our proposed scheme is

$D_{Hexagon} = \left\lceil\frac{L}{\sqrt{3}(2r-r/k)}\right\rceil\left\lceil\frac{2L}{3(2r-r/k)}\right\rceil 6r + L\left\lceil\frac{2L}{3(2r-r/k)}\right\rceil + 3r\left\lceil\frac{2L}{3(2r-r/k)}\right\rceil + L.$

In all the above expressions, the highest order term is L^2/r. So, we compare the coefficients of L^2/r as shown in Table 8.1 to decide minimality of path length theoretically. In D_{Chia}, D_{Scan}, D_{DScan} and $D_{Hilbert}$, the coefficient of higher order term L^2/r is equal to $\frac{k}{k-1}$. For $D_{S-curves}$, the coefficient of L^2/r is $\frac{\pi}{3}\left(\frac{k}{k-1}\right)$. The coefficient of L^2/r in $D_{Circles}$ is $\frac{\pi}{2}\left(\frac{k}{k-1}\right)$. The coefficient of L^2/r in $D_{Hexagon}$ is $\frac{1}{\sqrt{3}}\left(\frac{2k}{2k-1}\right)\left(\frac{2k}{2k-1}+\frac{1}{\sqrt{3}}\right)$. We show that coefficient of L^2/r in $D_{Hexagon}$ is lesser than all the above mentioned coefficients for all k. Among the existing path planning schemes *Circles* in [34] does best in terms of path length to cover a circular region. But for a square region, larger circles are needed to cover the corners of the square, which increases path length and makes *Circles* an inefficient strategy for covering a square. Since $\frac{\pi}{2}\left(\frac{k}{k-1}\right) > \frac{\pi}{3}\left(\frac{k}{k-1}\right) > \frac{k}{k-1}$ for all $k > 1$, so if we can show $\frac{k}{k-1} > \frac{1}{\sqrt{3}}\left(\frac{2k}{2k-1}\right)\left(\frac{2k}{2k-1}+\frac{1}{\sqrt{3}}\right)$ for all k, then we can claim the minimality of path length of our scheme as the coefficient of the highest order term L^2/r of our scheme is least among the aforesaid schemes. One can easily verify that $\frac{k}{k-1} > \frac{1}{\sqrt{3}}\left(\frac{2k}{2k-1}\right)\left(\frac{2k}{2k-1}+\frac{1}{\sqrt{3}}\right)$ for $2 \leq k \leq 9$. Again, for all $k \geq 10$, $\frac{1}{\sqrt{3}}\left(\frac{2k}{2k-1}\right)\left(\frac{2k}{2k-1}+\frac{1}{\sqrt{3}}\right) < 1$ but $\frac{k}{k-1} > 1$. Hence for any r, there exists L such that path length of $D_{Hexagon}$ is minimum. Considering $LMAT$ in [25], coefficient of L^2/r in $D_{Hexagon}$ beats D_{LMAT} for all $k \geq 5$. So, for any r, there exists L such that path length of $D_{Hexagon}$ is lesser compared to D_{LMAT}.

8.3 Simulation Results

MATLAB platform is used to study the performances of our proposed schemes. We evaluate path length of the proposed scheme for a bounded region for $X = r/20$ and compared with existing range based and range free schemes. The value of communication range $r = 10$ meter and square region with side length $L = 200$ meter. Results are shown in Table 8.2. We show the percentages of improvement of our scheme over various schemes compared to path length in Table 8.3 for $r = 10$ and $X = r/20$. Results show 7.35% to 27.74% improvement over different schemes. Values of average localization error of our scheme are shown in Table 8.4 varying communication ranges r and beacon distance u. We take $X = u$ in Table 8.4. Here also, localization error decreases as beacon distance decreases for any fixed communication range.

Path planning schemes in [25, 37] localize sensors using range-based methods. Hence

Table 8.2: Comparison of path length (in meter) of our scheme ($D_{Hexagon}$) with existing schemes

$D_{Hexagon}$	D_{Chia}	D_{Scan}	D_{DScan}	$D_{Hilbert}$	$D_{Circles}$	$D_{S-curves}$	D_{LMAT}
4271	5728	4610	4780	4620	5911	4939	4836

Table 8.3: Percentage (%) of improvement of our scheme in terms of path length compared to existing schemes

Existing schemes	D_{Chia}	D_{Scan}	D_{DScan}	$D_{Hilbert}$	$D_{Circles}$	$D_{S-curves}$	D_{LMAT}
% of improvement of our scheme compared to the existing schemes in terms of path length	25.43%	7.35%	10.64%	7.55%	27.74%	13.52%	13.22%

yields better accuracy than our proposed method as we use range-free method for localization. However we have better results in terms of path length. In [59], Chia-Ho-Ou et al. produces better localization accuracy with average error 0.5 meter when communication range is equal to 20 meter and beacon distance is 1 meter, whereas under same condition our average error is 1.6 meter. But our scheme outperforms in terms of path length compared to [59].

Table 8.4: Showing average error (in meter) for different communication range and beacon distance

Beacon distance → Communication range(↓)	$r/10$	$r/15$	$r/20$	$r/25$	$r/30$
10	1.59	1.17	0.78	0.57	0.46
15	2.75	1.58	1.22	0.98	0.85
20	2.93	1.95	1.61	1.17	0.89
25	4.28	2.47	1.61	1.19	0.99
30	4.94	2.65	1.72	1.36	1.11

8.4 Conclusion

With our proposed path planning strategy, it is possible to localize all sensors in a rectangular region with known boundary. We have compared path length of our proposed movement strategy for rectangular region theoretically with existing literature to show better performance. Simulation results show 7.35% to 27.74% improvement of our path planning strategy over existing strategies in terms of path length of mobile anchor for rectangular region. In future we will try to investigate path planning in presence of obstacles.

Chapter 9

Conclusion

At the beginning of the thesis we have proposed two deterministic range-based localization algorithms for static sensors in presence of NLOS signals using static anchors. The algorithm (FindPosition(ϕ, w)) finds position of a static sensor based on receiving two reflected signals from an anchor. If a sensor receives signals from different anchors, then communication among anchors are required. The proposed technique does not need to know the positions of those reflectors. The algorithm produces actual position of a sensor if there are no range measurement errors. In presence of measurement errors, the algorithm returns approximate position of the sensor. Simulation results show better accuracy of our scheme compared to existing works in presence of measurement errors. The strong point of our approach is that our algorithm works in a sparse network since only two reflected signals from an anchor are sufficient for finding position of a sensor. Another good aspect of our algorithm is that the positioning error does not increase significantly with significant increment of distance measurement error. The weak aspect of this approach is, however, that we have put restriction on NLOS signals. We have also considered a three dimensional space and got similar results for exact positioning of sensors. We have proved that with accurate range measurements, anchor can detect presence of misbehaving sensor under certain conditions. However, further studies are needed in this direction for detecting misbehaving sensors in presence of measurement errors. To generalize the above problem, we have proposed a localization algorithm (LocalizeSensor) considering multiple-bound signals. Our algorithm provides a circle within which the sensor is

bound to reside for each received unknown-bound signal. Theoretically we have shown that radius of this circle is lesser than the distance traveled by the signal. Hence our algorithm outperforms trilateration in terms of positional accuracy.

Two deterministic range-free localization algorithms (LWCD and LCD) for mobile sensors using static anchors have been proposed. In presence of obstacles we have modified above algorithms and proposed LWCDPO and LPO respectively. The algorithms work under irregular radio model. LWCD and LWCDPO assume that there is no change of direction of the mobile sensor during localization. We have given bounds on localization error of LWCD for a given communication range and beacon distance. LWCD is able to localize sensors within any predetermined error bound by fixing appropriate beacon distance for any given communication range. Using our technique a mobile sensor can further reduce localization error whenever it passes through the communication circle of different anchors by repeated calculation of the approximate line of movement. We have shown that the upper bound of the localization error of LWCDPO remains same as LCD. Simulation results show that in our approach, average error is very less than the maximum possible error and the algorithm outperforms over the existing approaches in terms of positional accuracy. LCD and LPO give a general solution where mobile sensor can change direction of movement within communication circle of an anchor. LPO uses two different signal strength of static anchors effectively to select appropriate beacon points in presence of obstacles. Better positioning accuracy is observed in simulation for LCD and LPO compared to existing works.

A mobile anchor is equivalent to many static anchors for localizing sensors in a network. Suitable movement strategies help reducing travel path and provide better accuracy if a good localization scheme can be used while following the path planning algorithm. A distributed range-free path planning algorithm (HexagonalLocalization) for mobile anchors is proposed to localize static sensors in a connected network. Proposed algorithm localizes all sensors using connectivity without any knowledge of the deployment area. Simulation results show improvement over existing works in terms of both path length and localization accuracy. Another movement strategy for mobile anchors is proposed to localize sensors in a rectangular region with known boundary. Path length of our proposed movement strategy is lesser compared to existing literatures. The basic structure of both

the proposed strategies is hexagonal movement. The hexagonal movement reduces the usual requirement of three beacon points for localization to two beacon points which helps to improve path length. Summary of the thesis work is represented in tabular form in the Table 9.1.

Table 9.1: Tabular representation of the thesis work

Algorithm	Anchor	Sensor	Type	Assumptions	Techniq-ue used	Error bound	Min. No. of signals/ beacon points
1	Static	Static	Range based	At most one reflection	AOA, TOA	No	One
2	Static	Static	Range based	Known upper bound on number of reflections	AOA, TOA, RSSI	No	One
3, 4	Static	Mobile	Range free	Direction unchanged during localization	Beacon point selection	Yes	Four
5, 6	Static	Mobile	Range free	Direction may change during localization	Beacon point selection	No	Two
7	Mobile	Static	Range free	Connected network	Beacon point on LRH	Yes	Two
Rectangular region	Mobile	Static	Range free	Known boundary	Beacon point on Hexagon	Yes	Two

In future we can think of a more practical approach towards multiple-bound NLOS problem by considering measurement errors. The mobile sensor localization problem can be extended by considering the case where mobile sensor changes direction after passing through a communication circle of some anchor and before entering in the communication circle of some other anchor. We have not considered presence of obstacle in any of the path planning problems which can be an important extension. Apart from these, we can look into anchor-free localization problems as well.

Bibliography

[1] Galstyan A., Krishnamachari B., Lerman K., and Pattem S. Distributed online localization in sensor networks using a moving target. In *Third International Symposium on Information Processing in Sensor Networks, 2004. IPSN 2004*, pages 61–70, 2004.

[2] Hady S. AbdelSalam and Stephan Olariu. Hexnet: Hexagon-based localization technique for wireless sensor networks. In *Seventh Annual IEEE International Conference on Pervasive Computing and Communications - Workshops (PerCom Workshops 2009), 9-13 March 2009, Galveston, TX, USA*, pages 1–6, 2009.

[3] Hady S. AbdelSalam, Stephan Olariu, and Syed R. Rizvi. Tiling-based localization scheme for sensor networks using a single beacon. In *Proceedings of the Global Communications Conference, 2008. GLOBECOM 2008, New Orleans, LA, USA, 30 November - 4 December 2008*, pages 790–794, 2008.

[4] Aylin Aksu and Prashant Krisnamurthy. Sub-area localization: A simple calibration free approach. In *Proc. of MSWIM'10*, 2010.

[5] Shafagh Alikhani, Thomas Kunz, and Marc St-Hilaire. iCCA-MAP versus MCL and dual MCL: Comparison of mobile node localization algorithms. In *ADHOC-NOW*, pages 163–176, 2010.

[6] Waleed Ammar, Ahmed ElDawy, and Moustafa Youssef. Secure localization in wireless sensor networks: A survey. *CoRR*, abs/1004.3164, 2010.

[7] Aline Baggio and Koen Langendoen. Monte-carlo localization for mobile wireless sensor networks. In *MSN*, pages 317–328, 2006.

[8] Kostas E. Bekris, Antonis A. Argyros, and Lydia E. Kavraki. Angle-based methods for mobile robot navigation: Reaching the entire plane. In *ICRA*, pages 2373–2378, 2004.

[9] Nirupama Bulusu, John S. Heidemann, and Deborah Estrin. Gps-less low-cost outdoor localization for very small devices. *IEEE Personal Commun.*, 7(5):28–34, 2000.

[10] Srdjan Capkun and Jean-Pierre Hubaux. Secure positioning of wireless devices with application to sensor networks. In *INFOCOM*, pages 1917–1928, 2005.

[11] Alberto Cerpa, Jeremy Elson, Deborah Estrin, Lewis Girod, Mic hael Hamilton, and Jerry Zhao. Habitat monitoring: application driver for wireless communications technology. *Computer Communication Review*, 31(2-Supplement):20–41, 2001.

[12] Yiu-Tong Chan, Wing-Yue Tsui, Hing-Cheung So, and Pak-Chung Ching. Time-of-arrival based localization under nlos conditions. *IEEE T. Vehicular Technology*, 55(1):17–24, 2006.

[13] C. T. Chang, C. Y. Chang, and C. Y. Lin. Anchor-guiding mechanism for beacon-assisted localization in wireless sensor networks. *IEEE SENSORS JOURNAL*, 12(5):1098–1111, 2012.

[14] Hongyang Chen, Gang Wang, Zizhuo Wang, Hing-Cheung So, and H Vincent Poor. Non-line-of-sight node localization based on semi definite programming in wireless sensor networks. *IEEE Transaction on Wireless Communication*, 11(1):108–116, 2012.

[15] X. Cheng, A. Thaeler, G. Xue, and D. Chen. TPS: A time-based positioning scheme for outdoor wireless sensor networks. In *INFOCOM*, 2004.

[16] Xiuzhen Cheng, Xiao Huang, and Ding-Zhu Du. *Ad-hoc wireless networking*. Springer Verlag, 2004.

[17] Chia-Ho-Ou. A localization scheme for wireless sensor networks using mobile anchors with directional antennas. *Sensors Journal, IEEE*, 11(7):1607–1616, 2011.

[18] Karthik Dantu, Mohammad H. Rahimi, Hardik Shah, Sandeep Babel, Amit Dhariwal, and Gaurav S. Sukhatme. Robomote: enabling mobility in sensor networks. In *IPSN*, pages 404–409, 2005.

[19] Suprakash Datta, Chris Klinowski, Masoomeh Rudafshani, and Shaker Khaleque. Distributed localization in static and mobile sensor networks. In *WiMob*, pages 69–76, 2006.

[20] Sylvie Delat, Partha Sarathi Mandal, Mariusz A. Rokicki, and Sbastien Tixeuil. Deterministic secure positioning in wireless sensor networks. *Theoretical Computer Science*, 412(35):4471 – 4481, 2011.

[21] Anirvan DuttaGupta, Arijit Bishnu, and Indranil Sengupta. Maximal breach in wireless sensor networks: Geometric characterization and algorithms. In Miroslaw Kutylowski, Jacek Cichon, and Przemyslaw Kubiak, editors, *Algorithmic Aspects of Wireless Sensor Networks, Third International Workshop, ALGOSENSORS 2007, Wroclaw, Poland, July 14, 2007, Revised Selected Papers*, volume 4837 of *Lecture Notes in Computer Science*, pages 126–137. Springer, 2007.

[22] Z. Ebrahimian and R. A Scholtz. Source localization using reflection omission in the near-field. In *IEEE-ACES Conf. on Applied Comput. Electromagnetics*, 2005.

[23] Jonathan Friedman, David Lee, Ilias Tsigkogiannis, Sophia Wong, Dennis Chao, David Levin, William J. Kaiser, and Mani B. Srivastava. RAGOBOT: A new platform for wireless mobile sensor networks. In *DCOSS*, pages 412–412, 2005.

[24] Richard Fuller and Xenofon D. Koutsoukos, editors. *Mobile Entity Localization and Tracking in GPS-less Environnments, Second International Workshop, MELT 2009, Orlando, FL, USA, September 30, 2009. Proceedings*, volume 5801 of *Lecture Notes in Computer Science*. Springer, 2009.

[25] Han G., Xu H., Jiang J., Shu L., Hara T., and Nishio S. Path planning using a mobile anchor node based on trilateration in wireless sensor networks. *Wireless Communications and Mobile Computing*, 13(14):1324–1336, 2013.

[26] Lewis Girod and Deborah Estrin. Robust range estimation using acoustic and multimodal sensing. In *IROS*, pages 1312–1320, 2001.

[27] Guangjie Han, Deokjai Choi, and Wontaek Lim. Reference node placement and selection algorithm based on trilateration for indoor sensor networks. *Wireless Communications and Mobile Computing*, 9(8):1017–1027, 2009.

[28] Guangjie Han, Huihui Xu, Trung Q. Duong, Jinfang Jiang, and Takahiro Hara. Localization algorithms of wireless sensor networks: a survey. *Telecommunication Systems*, 52(4):2419–2436, 2013.

[29] Guangjie Han, Chenyu Zhang, Jaime Lloret, Lei Shu, and Joel J. P. C. Rodrigues. A mobile anchor assisted localization algorithm based on regular hexagon in wireless sensor networks. *The Scientific World Journal*, 2014, 2014.

[30] Tian He, Chengdu Huang, Brian M. Blum, John A. Stankovic, and Tarek Abdelzaher. Range-free localization schemes for large scale sensor networks. In *Proc. of 9th Annual Int. Conf. on Mobile Computing and Networking*, MobiCom '03, pages 81–95, New York, USA, 2003. ACM.

[31] B. Hofmann-Wellenhof, H. Lichtenegger, and J. Collins. *Global Positioning System: Theory and Practice, 4th edition*. Springer Verlag, 1997.

[32] Chen-Chien Hsu, Hsin-Chuan Chen, and Chien-Yu Lai. An improved ultrasonic-based localization using reflection method. In *CAR*, pages 437–440, 2009.

[33] Lingxuan Hu and David Evans. Localization for mobile sensor networks. In *MOBICOM*, pages 45–57, 2004.

[34] Rui Huang and Gergely V. Záruba. Static path planning for mobile beacons to localize sensor networks. In *PerCom Workshops*, pages 323–330, 2007.

[35] S. Jauregui-Ortiz, M. Siller, and F. Ramos. Node localization in wsn using trigonometric figures. In *IEEE Topical Conf. on Wireless Sensors and Sensor Networks (WiSNet)*, pages 65 –68, jan. 2011.

[36] Kyunghwi Kim, Byunghyuk Jung, Wonjun Lee, and Ding-Zhu Du. Adaptive path planning for randomly deployed wireless sensor networks. *J. Inf. Sci. Eng.*, 27(3):1091–1106, 2011.

[37] Dimitrios Koutsonikolas, Saumitra M. Das, and Y. Charlie Hu. Path planning of mobile landmarks for localization in wireless sensor networks. *Computer Communications*, 30(13):2577–2592, 2007.

[38] Xing-Hong KUANG, Hui-He SHAO, and Rui FENG. A new distributed localization scheme for wireless sensor networks. *Acta Automatica Sinica*, 34(3):344 – 348, 2008.

[39] A. V. U. Phani Kumar, Adi Mallikarjuna Reddy V, and D. Janaki Ram. Distributed collaboration for event detection in wireless sensor networks. In *Proceedings of the 3rd International Workshop on Middleware for Pervasive and Ad-hoc Computing (MPAC 2005), held at the ACM/IFIP/USENIX 6th International Middleware Conference, November 28 - December 2, 2005, Grenoble, France*, pages 1–8, 2005.

[40] Branislav Kusy, Ákos Lédeczi, and Xenofon D. Koutsoukos. Tracking mobile nodes using RF doppler shifts. In *SenSys*, pages 29–42, 2007.

[41] Branislav Kusy, János Sallai, György Balogh, Ákos Lédeczi, Vladimir A. Protopopescu, Johnny Tolliver, Frank DeNap, and Morey Parang. Radio interferometric tracking of mobile wireless nodes. In *MobiSys*, pages 139–151, 2007.

[42] DAI Gui lan;ZHAO Chong-chong;QIU Yan;. A localization scheme based on sphere for wireless sensor network in 3d. *Chinese Journal of Electronics*, 36(7):1297, 2008.

[43] Julian Lategahn, Marcel Müller, and Christof Röhrig. TDoA and RSS based extended kalman filter for indoor person localization. In *Proceedings of the 78th IEEE Vehicular Technology Conference, VTC Fall 2013, Las Vegas, NV, USA, September 2-5, 2013*, pages 1–5, 2013.

[44] Loukas Lazos and Radha Poovendran. Hirloc: high-resolution robust localization for wireless sensor networks. *IEEE Journal on Selected Areas in Communications*, 24(2):233–246, 2006.

[45] HyungJune Lee, Martin Wicke, Branislav Kusy, and Leonidas Guibas. Localization of mobile users using trajectory matching. In *Proceedings of the first ACM international workshop on Mobile entity localization and tracking in GPS-less environments*, MELT '08, pages 123–128, New York, NY, USA, 2008. ACM.

[46] Sangho Lee, Eunchan Kim, Chungsan Kim, and Kiseon Kim. Localization with a mobile beacon based on geometric constraints in wireless sensor networks. *IEEE Transactions on Wireless Communications*, 8(12):5801–5805, 2009.

[47] Hongjun Li, Jianwen Wang, Xun Li, and Hongxu Ma. Real-time path planning of mobile anchor node in localization for wireless sensor networks. In *International Conference on Information and Automation, 2008. ICIA 2008.*, pages 384 – 389, 2008.

[48] Xu Li, Nathalie Mitton, Isabelle Simplot-Ryl, and David Simplot-Ryl. Dynamic beacon mobility scheduling for sensor localization. *IEEE Trans. Parallel Distrib. Syst.*, 23(8):1439–1452, 2012.

[49] C. H. Liu and D. J. Fang. Propagation. in antenna handbook: Theory, applications, and design. *Van Nostrand Reinhold*, Chapter 29:1–56, 1988.

[50] R.C. Luo, O. Chen, and S.H. Pan. Mobile user localization in wireless sensor network using grey prediction method. In *IECON*, pages 2689–2685, 2005.

[51] Honglei Miao, Kegen Yu, and M.J. Juntti. Positioning for NLOS propagation: Algorithm derivations and cramer-rao bounds. *Vehicular Technology, IEEE Transactions on*, 56(5):2568–2580, Sept 2007.

[52] Sichitiu M.L. and Ramadurai V. Localization of wireless sensor networks with a mobile beacon. In *IEEE International Conference on Mobile Ad-hoc and Sensor Systems, 2004*, pages 174–183, 2004.

[53] Bernd Neuwinger, Ulf Witkowski, and Ulrich Rückert. Ad-hoc communication and localization system for mobile robots. volume 5744/2009 of *Advances in Robotics*, pages 220–229. Springer-Verlag, 2009.

[54] Dragos Niculescu and B. R. Badrinath. Ad hoc positioning system (APS) using AOA. In *INFOCOM*, 2003.

[55] Dragos Niculescu and Badri Nath. DV based positioning in ad hoc networks. *Telecommunication Systems*, 22(1-4):267–280, 2003.

[56] Georg Oberholzer, Philipp Sommer, and Roger Wattenhofer. SpiderBat: Augmenting wireless sensor networks with distance and angle information. In *IPSN*, pages 211–222, 2011.

[57] Tomoaki Ogawa, Shuichi Yoshino, Masashi Shimizu, and Hirohito Suda. A new indoor location detection method adopting learning algorithms. In *PerCom*, pages 525–530, 2003.

[58] Chia-Ho Ou. Range-free node localization for mobile wireless sensor networks. In *ISWPC*, pages 535–539, 2008.

[59] Chia-Ho Ou. Path planning algorithm for mobile anchor-based localization in wireless sensor networks. *IEEE SENSORS JOURNAL*, 13(2):466–475, 2013.

[60] Chia-Ho Ou and Kuo-Feng Ssu. Sensor position determination with flying anchors in three-dimensional wireless sensor networks. *IEEE Trans. Mob. Comput.*, 7(9):1084–1097, 2008.

[61] Kaveh Pahlavan, Ferit O. Akgul, Mohammad Heidari, Ahmad Hatami, John M. Elwell, and Robert D. Tingley. Indoor geolocation in the absence of direct path. *IEEE Wireless Communications*, 13(6):50 –58, dec. 2006.

[62] Mayuresh M. Patil, Umesh Shaha, U. B. Desai, and S. N. Merchant. Localization in wireless sensor networks using three masters. *Proc. of IEEE Int. Conf. on Personal Wireless Commun. (ICPWC'05)*, pages 384–388, 2005.

[63] Nissanka B. Priyantha, Allen K.L. Miu, Hari Balakrishnan, and Seth Teller. The cricket compass for context-aware mobile applications. In *Proceedings of the 7th annual international conference on Mobile computing and networking*, MobiCom '01, pages 1–14, New York, NY, USA, 2001. ACM.

[64] Yihong Qi, Hisashi Kobayashi, and Hirohito Suda. Analysis of wireless geolocation in a non-line-of-sight environment. *IEEE Transactions on Wireless Communications*, 5(3):672–681, 2006.

[65] R. Racz, C. Schott, and S. Huber. Electronic compass sensor. In *Sensors, 2004. Proceedings of IEEE*, pages 1446–1449 vol.3, Oct 2004.

[66] Christof Röhrig and Marcel Müller. Indoor location tracking in non-line-of-sight environments using a IEEE 802.15.4a wireless network. In *2009 IEEE/RSJ International Conference on Intelligent Robots and Systems, October 11-15, 2009, St. Louis, MO, USA*, pages 552–557, 2009.

[67] Christof Röhrig and Marcel Müller. Localization of sensor nodes in a wireless sensor network using the nanoloc TRX transceiver. In *Proceedings of the 69th IEEE Vehicular Technology Conference, VTC Spring 2009, 26-29 April 2009, Hilton Diagonal Mar, Barcelona, Spain*, 2009.

[68] Chee Kiat Seow and Soon Yim Tan. Non-line-of-sight localization in multipath environments. *IEEE Trans. Mob. Comput.*, 7(5):647–660, 2008.

[69] Jang-Ping Sheu, Wei-Kai Hu, and Jen-Chiao Lin. Distributed localization scheme for mobile sensor networks. *IEEE Trans. Mob. Comput.*, 9(4):516–526, 2010.

[70] Chia-Yen Shih and Pedro Jos Marrn. COLA: Complexity-reduced trilateration approach for 3D localization in wireless sensor networks. SENSORCOMM '10, pages 24–32, Washington, USA, 2010.

[71] D. Singelee and B. Preneel. Location verification using secure distance bounding protocols. In *IEEE Int. Conf. on Mobile Adhoc and Sensor Systems Conference*, pages 7 pp. –840, nov. 2005.

[72] Koushik Sinha and Nabanita Das. Exact location identification in a mobile computing network. In *ICPP Workshops*, pages 551–558, 2000.

[73] Koushik Sinha and Atish DattaChowdhury. A distributed location identification algorithm for ad hoc networks using computational geometric methods. In *Proceed-*

ings of the 12th international conference on High Performance Computing, HiPC'05, pages 62–72, Berlin, Heidelberg, 2005. Springer-Verlag.

[74] Seshan Srirangarajan and Ahmed H. Tewfik. Localization in wireless sensor networks under non line-of-sight propagation. In *GLOBECOM*, page 5, 2005.

[75] Kuo-Feng Ssu, Chia-Ho Ou, and Hewijin Christine Jiau. Localization with mobile anchor points in wireless sensor networks. *IEEE T. Vehicular Technology*, 54(3):1187–1197, 2005.

[76] Sameer Tilak, Vinay Kolar, Nael B. Abu-Ghazaleh, and Kyoung-Don Kang. Dynamic localization protocols for mobile sensor networks. *CoRR*, cs.NI/0408042, 2004.

[77] Akira Uchiyama, Sae Fujii, Kumiko Maeda, Takaaki Umedu, Hirozumi Yamaguchi, and Teruo Higashino. UPL: opportunistic localization in urban districts. *IEEE Trans. Mob. Comput.*, 12(5):1009–1022, 2013.

[78] Andrija S. Velimirovic, Goran Lj. Djordjevic, Maja M. Velimirovic, and Milica D. Jovanovic. Fuzzy ring-overlapping range-free (FRORF) localization method for wireless sensor networks. *Computer Communications*, 35(13):1590 – 1600, 2012.

[79] Swaroop Venkatesh and R. Michael Buehrer. Nlos mitigation using linear programming in ultrawideband location-aware networks. *IEEE T. Vehicular Technology*, 56(5):3182–3198, 2007.

[80] Xin Wang, Zongxin Wang, and Bob O'Dea. A toa-based location algorithm reducing the errors due to non-line-of-sight (nlos) propagation. *IEEE T. Vehicular Technology*, 52(1):112–116, 2003.

[81] Yun Wang, Xiaodong Wang, Demin Wang, and Dharma P. Agrawal. Range-free localization using expected hop progress in wireless sensor networks. *IEEE Trans. Parallel Distrib. Syst.*, 20(10):1540–1552, 2009.

[82] Chin-Der Wann and Chih-Sheng Hsueh. Non-line of sight error mitigation in ultra-wideband ranging systems using biased kalman filtering. *Signal Processing Systems*, 64(3):389–400, 2011.

[83] Chin-Der Wann and Han-Yi Lin. Hybrid TOA/AOA estimation error test and non-line of sight identification in wireless location. *Wireless Communications and Mobile Computing*, 9(6):859–873, 2009.

[84] Bin Xiao, Hekang Chen, and Shuigeng Zhou. Distributed localization using a moving beacon in wireless sensor networks. *IEEE Trans. Parallel Distrib. Syst.*, 19(5):587–600, 2008.

[85] Bin Xu, Guodong Sun, Ran Yu, and Zheng Yang. High-accuracy tdoa-based localization without time synchronization. *IEEE Trans. Parallel Distrib. Syst.*, 24(8):1567–1576, 2013.

[86] Jun Xu, Maode Ma, and Choi Look Law. AOA cooperative position localization. In *GLOBECOM*, pages 3751–3755, 2008.

[87] Jiyoung Yi, Jahyoung Koo, and Hojung Cha. A localization technique for mobile sensor networks using archived anchor information. In *SECON*, pages 64–72, 2008.

[88] Ganggang Yu, Fengqi Yu, and Lei Feng. A localization algorithm using a mobile anchor node under wireless channel. In *ROBIO*, pages 1104–1108, 2007.

[89] Pei Zhang and Margaret Martonosi. LOCALE: Collaborative localization estimation for sparse mobile sensor networks. In *IPSN*, pages 195–206, 2008.

[90] Shigeng Zhang, Jiannong Cao, Lijun Chen, and Daoxu Chen. Accurate and energy-efficient range-free localization for mobile sensor networks. *IEEE Trans. Mob. Comput.*, 9(6):897–910, 2010.

[91] Weile Zhang, Qinye Yin, Hongyang Chen, Wenjie Wang, and Tomoaki Ohtsuki. Distributed angle estimation for wireless sensor network localization with multipath fading. In *ICC*, pages 1–6, 2011.

[92] Yanchao Zhang, Wei Liu, Yuguang Fang, and Dapeng Wu. Secure localization and authentication in ultra-wideband sensor networks. *IEEE Journal on Selected Areas in Communications*, 24(4):829–835, 2006.

Publication from the Contents of the Thesis

Papers published/Under review in International Journals:

[J1] Kaushik Mondal, Partha Sarathi Mandal and Bhabani P. Sinha, "Analysis of Multi-Bound Signals towards Localization: A Theoretical Approach", *Wireless Personal Communications*, (to appear), Jan 2015, (online available doi:10.1007/s11277-015-2379-1).

[J2] Kaushik Mondal, Partha Sarathi Mandal and Bhabani P. Sinha, "A Robust Deterministic Approach to sensor Localization in Presence of NLOS Signal", *Wireless Personal Communications*, 2015, *Under review.*

[J3] Kaushik Mondal and Partha Sarathi Mandal, "Deterministic Range-Free Mobile Sensor Localization using Static Anchors", *Ad Hoc Networks*, 2015, *Under review.*

[J4] Kaushik Mondal, Arindam Karmakar and Partha Sarathi Mandal, "Designing Path Planning Algorithms for Mobile Anchor towards Range-Free Localization", *Journal of parallel and Distributed Computing*, 2015, *Under review.*

Papers Published in International Conference Proceedings:

[C1] Kaushik Mondal, Arindam Karmakar and Partha Sarathi Mandal "Path Planning Algorithm for Mobile Anchor in Connected Sensor Networks" *11th International Conference on Distributed Computing and Internet Technologies (ICDCIT'15)*, (LNCS-8956), (Springer-Verlag), Bhubaneswar, India, pp. 193-198, Feb 5-8, 2015 *Accepted.*

[C2] Kaushik Mondal and Partha Sarathi Mandal "Range-Free Mobile sensor Localization using Static Anchor" in *Proc. of 8th International Conference on Wireless Algorithms, Systems, and Applications (WASA'13)*, (LNCS-7992), (Springer-Verlag), Zhangjiajie, China, pp. 269-284, Aug 7-10, 2013.

[C3] Kaushik Mondal, Arjun Talwar, Partha Sarathi Mandal and Bhabani P. Sinha, "Localization Based on Two Bounds Reflected Signals in Wireless Sensor Networks" in *Proc. of 9th International Conference on Distributed Computing and Internet Technologies (ICDCIT'13)*, (LNCS-7753), (Springer-Verlag), Bhubaneswar, India, pp. 334-346, Feb 5-8, 2013.

[C4] Kaushik Mondal, Partha Sarathi Mandal and Bhabani P. Sinha, "Localization in Presence of Multipath Effect in Wireless Sensor Networks" in *Proc. of 10th International Conference on Wired/Wireless Internet Communications (WWIC'12)*, (LNCS-7277), (Springer-Verlag), Island of Santorini, Greece, pp. 138-149, Jun 6-8, 2012.

[C5] Kaushik Mondal, Partha Sarathi Mandal and Bhabani P. Sinha, "Poster Abstract: Localization based on Reflected Signals in Wireless Sensor Networks" in *9th European Conference on Wireless Sensor Networks (EWSN'12)*, Trento, Italy, Feb 15-17, 2012.